Mafalda de Sande Ribeiro de Magalhães Cardoso

REMOVAL OF EMERGING ORGANIC CONTAMINANTS BY COMBINING NANOFILTRATION AND OZONATION: ONE OPTION FOR WATER REUSE

· U C ·

UNIVERSIDADE DE COIMBRA

Mafalda de Sande Ribeiro de Magalhães Cardoso

Removal of Emerging Organic Contaminants by combining Nanofiltration and Ozonation: one option for water reuse

Master Thesis in the scientific area of Chemical Engineering, supervised by Professor Dr. Licínio Ferreira and Dr. Rui Martins and submitted to the Department of Chemical Engineering, Faculty of Science and Technology, University of Coimbra

Supervisor(s):
Prof. Dr. Licínio Ferreira
Dr. Rui Martins

Host institutions:
Department of Chemical Engineering
Faculty of Sciences and Technology of the University of Coimbra
Group on Environment, Reaction, Separation and Thermodynamics (GERST)

Rua Sílvio Lima, Pólo II
3030-790 Coimbra, Portugal

Coimbra
2014

· U   C ·

UNIVERSIDADE DE COIMBRA

"Nariz no ar e vamos em frente."

"A sorte dá muito trabalho."

À minha Mãezinha e ao meu Papá
Nunca sequer sonharia chegar aqui sem vós.
Agradecer não é suficiente, mas, do fundo do meu coração, OBRIGADA.

Acknowledgements

First, I would like to acknowledge Prof. Dr. Licínio Ferreira, my supervisor, for the support, scientific opinions, guidance and for teaching me to trust my results. Also, I would like to acknowledge Dr. Rui Martins, my co-supervisor, for his patience, orientation on the Laboratory and for all the continuous explanations which have built on my scientific and academic growth. I must show my gratitude to all the people that, with their experience on different scientific fields, have contributed to this work: Prof. Dr. Rosa Quinta Ferreira; Prof. Dr. Maria Margarida Costa, Prof. Dr. José António Paixão, Prof. Dr. Sílvia Gramacho, Dr. Uladzimir Khomchanka, Dr. Maria João Bastos, Dr. Cátia Mendes, M. Sc. Sofia Fajardo, M. Sc. Daniela Lopes and Dr. André Rossi.

I would like to thank the board of the Department for their understanding of my continuous setting off the alarms late at night. I am grateful to the staff of the Department of Chemical Engineering – Mr. António Amado, Mrs. Dulce Pancas, Mr. José Santos and Miss Sandra Silva, for their constant availability and help with the Laboratory.

My Laboratory colleagues Cátia Gaspar, Helga Seca, Laura Cruz, Joana Andrade, Joana Marques, José Lobo, Raquel Ferreira and Roberto Barata for their companionship and help, which lead to a motivating and amusing working place, deserve a thank note. To Hugo Santos and Rodrigo Santos for all the shared thoughts, knowledge and lab skills and for the help on the Laboratory, thank you.

I must acknowledge my friends Alexandra Briosa, Ana Bento, Cátia Correia, Filipa Briosa, João Costa, Marta Moura, Marta Proença, Mário Castro, Miguel Cabrita, Nuno Mesquita, Rafael Filipe Milheiro, Ricardo Santos, Rui Póvoa, Rui Francisco, Sérgio Miranda and Sónia Mendes, for their visits to the Laboratory, for sharing my concerns and giving me amazing and empowering free time that allowed me to get stronger back to work. My loyal colleagues, some already graduated, deserve a special word: Ana Margarida Ferreira, Ana Rita Varelas, Anselmo Nunes, Dra. Cláudia Guilherme, Daniela Gomes, Diogo Figueiredo, Luciano Azevedo, João Sequeira, Margarida Fernandes, Marta Nunes, Patrícia Castro, Stacy Morgado and Tiago Nunes. I thank my Erasmus Fellows – Alice, Ana, Eline, Evgeniya, François, Frederico, Inês, Joni, Junior, Gamze, Gonçalo, Martin, Pablo, Paulo and Pierre, for taking me out of my comfort zone in such amazing ways. The Amazing Gospel singers – Amélia, Berta, Carina, Catarina, Joana, Nunos and Vasco – were tireless cheering me up and giving me essential moments out of the routine.

For being an amazing friend, psychologist, inspiration, worker, scientist (that truly understands the strange behaviour of bacteria) and professor, I must thank Ruben.

I am very grateful to the true Engineers and Managers (some without the deserved Diploma) that remarkably inspired my work: my Grandfather Alípio, my Grandfather

Abstract

The presence of emerging contaminants which are often persistent organic pollutants is an increasing problem in different types of water (even in drinking water supplies). Two of the most common emerging contaminants around the world are Active Pharmaceutical Ingredients such as Sulfamethoxazole (SMX), which maximum concentration detected in drinking water is 1.7 μg L^{-1}, and Diclofenac (DCF), which maximum concentration detected in surface water is 6.5 μg L^{-1}. These are molecules purposefully designed to bond with cellular receptors and elicit specific biological effects even in low concentrations. These compounds are not (fully) degraded in the common water treatment plants.

Nanofiltration and Ozonation were already proven to be efficient in what regards the removal of these individual emerging contaminants from water. Removals of both contaminants for both processes are around 100%.

Thus, the goal of this work is to study in which way the cumulative presence of different emerging compounds affects the efficiency of water treatment processes that have been proven to be effective on the removal of individual contaminants, considering potential synergetic effects. Besides, the analysis of the impact of different water matrices on the removal efficiencies is an important objective since these compounds are mostly found in secondary effluents from municipal wastewater treatment plants, natural water and drinking water.

This investigation was driven by:
- Environmental purposes, since the aquatic life has continuous exposure to these contaminants, which can trigger low dose effects;
- Public health issues like endocrine disrupting effects, resistance to antibiotics, renal effects, altered microbial community, bioaccumulation;
- Social motives, given that this is a growing concern for the society;
- Economic motives: eventual profit if the recovery of pollutants is possible (depending on the treatment used) and new market niche of mechanisms for these pollutants' removal on wastewater treatment plants, factories and drinking water facilities.

This work was divided into four main work stages which consisted on: (1) the characterization of the effluents/ materials used in the experiments (synthetic effluent, natural water effluent, membrane and catalysts); (2) the optimization of conditions for Nanofiltration; (3) the optimization of conditions for Ozonation; and (4) the Process integration.

Mainly for analytical purposes, it was decided to work with concentrations of 30 mg L^{-1} of both contaminants (SMX and DCF). The synthetic effluent was prepared with distilled water while the natural water effluent was prepared with filtered water from the river Mondego (Portugal).

The Nanofiltration batch experiments carried out in a flat-sheet laboratory-scale cross-flow membrane equipment permitted the analysis of the effects that are determinant on this specific membrane separation process. The membrane used was polyamide Trisep® TS-80 with a 150 g mol^{-1} molecular weight cut-off. Its permeability was 1.253 x 10^{-14} m. From the individual analysis of some membrane pores by AFM, it was possible to assume that the average membrane pore diameter would be around 50 nm.

DCF has higher retention due to its higher molecular weight and hydrophobicity (membrane is more hydrophilic with increasing pH). The membrane has negative zeta-potential, so these negative species are rejected by electrostatic repulsion. The change of the aqueous matrix has a significant negative impact on process efficiency perhaps due to the presence of Ca^{2+} ions. The best operation conditions determined for this treatment were pH = 7 and pressure drop of 7 bar. The pollutants were adsorbed on the membrane after 40 hours of operation. The interactions of the pollutants on the rejection mechanisms for the pH range 3 - 6 should be further investigated.

The batch Ozonation performed trials confirmed the previously stated fact that the ozone itself is enough for the SMX and DCF degradation. However, the presence of a catalyst can increase the Chemical Oxygen Demand degradation. The Ozonation's optimal conditions determined were the use of the catalyst Mn-Ce-O which has a specific area of 109 m^2 g^{-1} and an average diameter of pore o 0.0179 μm. Due to the reaction mechanism presented by this catalyst, the pH should not be buffered or adjusted. The aqueous matrix did not have influence on the process efficiency.

The process integration was done without the ozone's catalyst since its separation from the reaction media was difficult. The Ozonation carried on process integration was performed for 120 min on simple mode and with the Natural water effluent. Regarding the Nanofiltration, it was done using pH = 7 and pressure drop of 7 bar.

It was concluded regarding toxicity removal that the best sequence for Nanofiltration and Ozonation Process integration is Ozonation followed by Nanofiltration.

Resumo

A presença de contaminantes emergentes, que muitas vezes são poluentes orgânicos persistentes, é um problema crescente em diferentes tipos de água (mesmo no fornecimento de água para consumo humano). Dois dos contaminantes emergentes mais comuns em todo o mundo são Princípios Ativos como o Sulfametoxazol (SMX), cuja máxima concentração detetada em água para consumo foi 1.7 μg L^{-1} e o Diclofenac (DCF), cuja máxima concentração detetada em águas superficiais foi 6.5 μg L^{-1}.

Estas moléculas são propositadamente desenhadas para se ligar aos recetores celulares e desencadear efeitos biológicos específicos, mesmo quando presentes em concentrações baixas. Estes compostos não são (totalmente) degradados nas estações de tratamento de águas residuais.

Tanto a Nanofiltração como a Ozonólise se mostraram eficientes no que diz respeito à remoção destes contaminantes emergentes da água. As remoções dos dois contaminantes para os dois processos estão próximas dos 100%.

Assim, o objetivo deste trabalho é estudar a forma como a presença cumulativa de diferentes contaminantes emergentes afeta a eficiência de processos de tratamento de água que são eficazes na remoção dos contaminantes individualmente, considerando potenciais efeitos sinergéticos. Para além disso, a análise do impacte de diferentes matrizes aquosas nas eficiências de remoção é um objetivo importante, uma vez que estes compostos são maioritariamente encontrados em efluentes secundários de estações de tratamento de águas residuais, água natural e água para consumo humano.

Esta investigação foi impulsionada por:
- Propósitos ambientais, uma vez que a vida aquática tem exposição aos contaminantes, podendo desencadear efeitos de baixas doses;
- Problemas de saúde pública, como desregulação endócrina, resistência a antibióticos, efeitos renais, flora microbiana alterada e bioacumulação;
- Motivos sociais, uma vez que esta é uma preocupação crescente para a sociedade;
- Motivos económicos: possível lucro caso a recuperação dos poluentes seja possível (dependendo do tratamento usado) e um novo nicho de mercado respeitante a mecanismos para a remoção destes poluentes nas estações de águas residuais, em fábricas e em estações de tratamento de água.

Este trabalho foi composto por quatro grandes fases que consistiram em: (1) caracterização dos efluentes/ materiais usados nas experiências (efluente sintético, efluente de água natural, membrana e catalisadores); (2) otimização de condições de operação para a Nanofiltração; (3) otimização de condições de operação para a Ozonólise; e (4) Integração de processo.

Principalmente por questões analíticas, foi decidido trabalhar com concentrações de 30 mg L^{-1} para ambos os contaminantes (SMX e DCF). O efluente sintético foi preparado com

água destilada e o efluente de água natural foi preparado com água filtrada do rio Mondego (Portugal).

Os ensaios de Nanofiltração em descontínuo foram feitos num equipamento de filtro de folha de bancada em contracorrente. Estes permitiram a análise dos efeitos determinantes neste processo de separação por membrana específico. A membrana era de poliamida da marca Trisep ®, de nome TS-80 e com um *cut-off* de 150 g mol^{-1}. A sua permeabilidade era 1.253 x 10^{-14} m. Ds análise individual de alguns poros da membrana por AFM foi possível assumir que o diâmetro médio dos poros da membrana seria aproximadamente 50 nm.

O DCF tem uma maior retenção devido ao seu peso molecular maior e à sua hidrofobicidade (a membrana é mais hidrofílica com pH crescente). A membrana tem potencial-zeta negativo, pelo que estas espécies carregadas negativamente são rejeitadas por repulsão eletroestática. A mudaça da matriz aquosa tem um impacto negativo significante na eficiência doo processo talvez devido à presença de iões Ca^{2+}. As melhores condições operatórias determinadas para este tratamento foram pH = 7 e diferencial de pressão de 7 bar. Os poluentes ficaram adsorvidos na membrana após 40 horas de operação. As interações entre os poluentes nos mecanismos de rejeição para a gama de pH 3 − 6 deve ser investigada em posteriores desenvolvimentos do trabalho.

Os ensaios de Ozonólise descontínua desenvolvidos comprovaram o facto previamente constatado de que o ozono *per si* é suficiente para a degradação do SMX e do DCF. Porém, a presença de um catalisador pode aumentar a degradação da Carência Química de Oxigénio. As condições ótimas de Ozonólise determinadas foram o uso do catalisador Mn-Ce-O que tem uma área específica de 109 m^2 g^{-1} e um diâmetro médio de poros de 0.0179 µm. Devido ao mecanismo de reação demonstrado por este catalisador, o pH não deveria ser tamponado ou ajustado. A matriz aquosa não teve influência na eficiência do processo.

A integração do processo foi feita sem o catalisador na Ozonólise uma vez que a sua separação do meio reacional foi difícil. A Ozonólise no processo de integração foi feita durante 120 minutos, em modo simples e com o efluente de água natural. Relativamente à Nanofiltração, esta foi feita usando pH = 7 e uma queda de pressão de 7 bar.

Concluiu-se, tendo em conta a remoção da toxicidade, que a melhor sequência para a integração dos processos é fazer a Ozonólise e, seguidamente, a Nanofiltração.

Palavras-chave: Contaminantes emergentes; Farmacêuticos; Nanofiltração; Ozonólise; Sulfametoxazol; Diclofenac.

Table of contents

List of Figures

List of Tables

List of Abbreviations and Symbols

Abreviations

AFM – Atomic Force Microscopy

AOP – Advanced Oxidation Processes

APIs – Active Pharmaceutical Ingredients

BET – Brunaurer-Emmett-Teller

BOD – Biochemical Oxygen Demand

COD – Chemical Oxygen Demand

DCF – Diclofenac (CAS: 15307-86-5)

DNS – Dinitrosalicylic acid

EDCs – Endocrine disrupting chemicals

GC-MS – Gaseous Chromatography-Mass Spectroscopy

HPLC – High Performance Liquid Chromatography

LC-ESI-QTOF-MS – Liquid chromatographer-electrospray ionisation-quadrupole-time-of-fight mass spectrometer

MBR – Membrane bioreactor

MOPAC – Combined adsorption and catalytic OZ by Fe_2O_3/CeO_2 loaded activated carbon

MWCNTs – Multi-walled carbon nanotubes

MWCO – Molecular weight cut-off

ND – Not detected on HPLC analysis

NF – Nanofiltration

NSAIDs – Non-steroidal anti-inflammatory drug

OZ – Ozonation

PAC – Combined adsorption and catalytic Ozonation by commercial activated carbon

PhACs – Pharmaceutical active compounds

PPCPs – Pharmaceuticals and personal care products

ppm – parts per million

RO – Reverse Osmosis

rpm – rotations per minute

SMX – Sulfamethoxazole (CAS: 723-46-6)

TOC – Total Organic Carbon

TrOC – Trace organic contaminants

UV – Ultraviolet

UVA – Ultraviolet A

WWT – Wastewater treatment

Symbols

% C (w/w)	weight percentage of carbon
% H (w/w)	weight percentage of hydrogen
% N (w/w)	weight percentage of nitrogen
% S (w/w)	weight percentage of sulphur
$[DCF]_f$	DCF concentration in the feed (mg L^{-1})
$[DCF]_p$	DCF concentration in the permeate (mg L^{-1})
$[DCF]_t$	DCF concentration for a certain reaction time t (mg L^{-1})
$[DCF]_{t=0}$	DCF concentration in the beginning of the reaction (mg L^{-1})
$[SMX]_f$	SMX concentration in the feed (mg L^{-1})
$[SMX]_p$	SMX concentration in the permeate (mg L^{-1})
$[SMX]_t$	SMX concentration for a certain reaction time t (mg L^{-1})
$[SMX]_{t=0}$	SMX concentration in the beginning of the reaction (mg L^{-1})
C	solute concentration (mol L^{-1})
C_f	concentration in the feed (mol L^{-1})
$C_{O3,in}$	initial ozone concentration in the batch Ozonation reactor (g m^{-3})
$C_{O3,out}$	ozone concentration exiting the batch Ozonation reactor (g m^{-3})
COD_t	Chemical Oxygen Demand for a certain reaction time t (mg O_2 L^{-1})
$COD_{t=0}$	Chemical Oxygen Demand in the beginning of reaction (mg O_2 L^{-1})
COD_p	Chemical Oxygen Demand for the permeate (mg O_2 L^{-1})
$COD_{t=0}$	Chemical Oxygen Demand for the feed (mg O_2 L^{-1})
C_p	concentration in the permeate (mol L^{-1})
d_h	hydraulic diameter
$D_{salt,\infty}$	diffusion coefficient of Stokes-Einstein for the salt
EC_{20}	dose required to lower the response to 20% of the control population

EC_{50}	dose required to lower the response
i	van't Hoff factor (dissociation factor)
J_v	flux through the membrane (m^3 m^{-2} s^{-1})
$J_{v,NaCl}$	flux through the membrane with NaCl
$J_{v,NF}$	Nanofiltration flux through the membrane
$J_{v,RO}$	Reverse osmosis flux through the membrane
$k_{f,i}$	mass transfer coefficient for the solute i
$\log K_{ow}$	logarithm of the octanol-water partition coefficient
L_p	membrane permeability (m)
M	molar mass of the solute (g mol^{-1})
n	number of moles dissociated
OH·	hydroxyl radicals
pK_a	acid dissociation constant
R	universal gas constant (L atm mol^{-1} K^{-1} or J mol^{-1} K^{-1})
R%	rejection of pollutants on filtration process
Re	Reynolds number
Re_{dh}	Reynolds number based on the hydraulic diameter
R_m	membrane intrinsic resistance
Sc	Schmidt number
Sh	Sherwood number
T	temperature (ºC or K)
V	volume
ΔC	solute concentration variation
ΔP	pressure drop (Pa or bar)
$\Delta \pi$	osmotic pressure (Pa or bar)
η_0	fluid viscosity (Pa s^{-1} or bar s^{-1})
π_b	osmotic pressure in the bulk
π_b	osmotic pressure in the permeate
ρ	density

1. Introduction

1.1 Relevance and motivation

The emerging contaminants are an embryonic problem that can be considered increasingly a public health question. The concentrations of different contaminants found in groundwater, river waters and Waste Water Treatment (WWT) plants are alarming. These problems are increasing for big metropolis, where environmental problems get denser. Between the most problematic emerging contaminants are the pharmaceutical active compounds (PhACs).

Even though conventional biological processes used in WWT plants do not degrade these contaminants, there are alternative processes, namely Membrane Separation Processes, Advanced Oxidation Processes (AOP), among others. However, these processes are not fully optimized for such complexes matrixes – with lots of different contaminants in different proportions and relatively low concentrations of pollutants (order of magnitude of µg and ng) and other organic and inorganic compounds, that are found in current streams (Bolong *et al.*, 2009).

These problems stimulated the appearance of an innovating investigation niche that aims to successively study the effect of these treatments on more and more complex matrixes that resemble the real ones. Eventually, and depending on the kind of treatment process undertaken, these compounds could be recovered and reused for the manufacturing of medicine.

All things considered, these investigations are driven by environmental, social and economic motives, since the presence of organic contaminants harms the ecosystems, are a concern for the actual society and can be profitable on the recovery of pollutants or on their removal on WWT plants, factories, drinking water plants and so on (Snyder *et al.*, 2007).

1.2 Objectives of the study

Nanofiltration and Ozonation were already proven to be efficient in what regards the removal of individual emerging contaminants from water (**3. Literature Review**). Since those processes have been broadly studied for the individual compounds on the scope of this study, it is now relevant to explore the use of these techniques for solutions containing two or more emerging compounds. Thus, the initial goal of this work is to study in which way the cumulative presence of different emerging compounds affects the efficiency of water treatment processes that have been proven to be effective on the removal of individual contaminants. The final objective of this investigation is to study the symbiosis of the two processes in order to optimize the removal and degradation of the contaminants. This aims to

be an approach to the real waste water processes and streams, where different processes are used to treat the different contaminants presented.

To mitigate the effects that the chemical processes have on the environment and on public health is a duty for a Chemical Engineer. Hereafter, this work aims to be a contribution for the global improvement of water quality so the exposure of living organisms to emerging contaminants and their related disadvantages are reduced.

1.3   Thesis structure

This work is organized in six main chapters. The Introduction, the relevance and motivation and the objectives of the study are exposed firstly. On the second chapter, the theoretical concepts that are essential to comprehend and discuss the developed work are presented. These involve the water use and treatment, the emerging contaminants, and the two processes approached on this work – Nanofiltration and Ozonation. The Literature Review relative to Nanofiltration and Ozonation is presented on chapter 3. The most important materials used, including chemicals and reagents are indicated on chapter 4. This chapter also includes the description of the experimental procedures performed in all the trials, as well as the explanation of the analytical methods used for the membrane, the catalysts and the liquid samples. The fifth chapter has the Results of the trials that were performed on the Nanofiltration and the Ozonation equipment that are commented and discussed along their presentation. The Results and Discussion chapter finished with a section where the efforts done towards the Process Integration, which is the main goal of this work, are described and discussed. After each main chapter, a number of conclusions are retained and finally in the sixth chapter the conclusions are presented. Here the most important remarks are mentioned and some recommendations for future research are given.

2. Theoretical background

This chapter aims to present some pertinent information regarding the water use, the emerging contaminants and some general concepts on WWT processes. Moreover, some theoretical concepts underlying Nanofiltration and Ozonation, techniques that are used on this work, are presented.

2.1 The water use and the emerging contaminants

The environmental issues are a dire concern nowadays for diverse motives and, therefore, sustainability is referred on multiple fields as the need to develop in a way that will not compromise the progress of future generations. The water resources have major importance on these distresses, since just 3% of the water on Earth is potable.

The so called endocrine disrupting chemicals (EDCs) are synthetic chemicals (surfactants, pesticides, pharmaceuticals, personal care products, phthalates, among others) or natural substances (like hormones or caffeine) that are introduced in the environment anthropogenically. They were found in drinking water, WWT plants, effluents, surface water, seawater, groundwater, soil, sediment and fish. The water pollution by these agents is a worrying issue, since they can have endocrine-disrupting effects on living organisms, which means that several functions can be changed on the endocrine system, having adverse effects on human health and its progeny. The increasing problems on human reproduction such as decreasing male fertility, birth defects and cancer can be caused by the exposure to these chemicals. Therefore, the presence of these emerging contaminants in different types of water is a growing concern, mostly because persistent organic pollutants are an increasing problem in drinking water supplies (Nikolaou *et al.*, 2006). These are also known by trace organic contaminants (TrOC) due to their usual low concentrations.

In 1999, the concept pharmaceuticals and personal care products (PPCPs) started being mentioned on an environmental health perspective and by 2007 more than 100 of these had been identified in aqueous samples (including drinking water). This group of contaminants include, among other products, prescription, veterinary and over-the-counter therapeutic drugs, diagnostic agents and biopharmaceuticals. These were in water from the moment the humans started using them, but just the technological advance allowed the detection and quantification of these chemicals, as well as accessing their effects on humans and environment. The continuous human activities, the production of residues from pharmaceutical industries and hospitals, the use illicit drugs, the use of veterinary drugs and the intense agribusiness make this be an emerging problem (**Figure 1**). Among the most common pharmaceuticals found in the environment are: anti-inflammatory drugs, analgesics,

antibiotics, steroids and related hormones, cancer therapeutics (very present on the leachate from cemeteries) and lipid regulators.
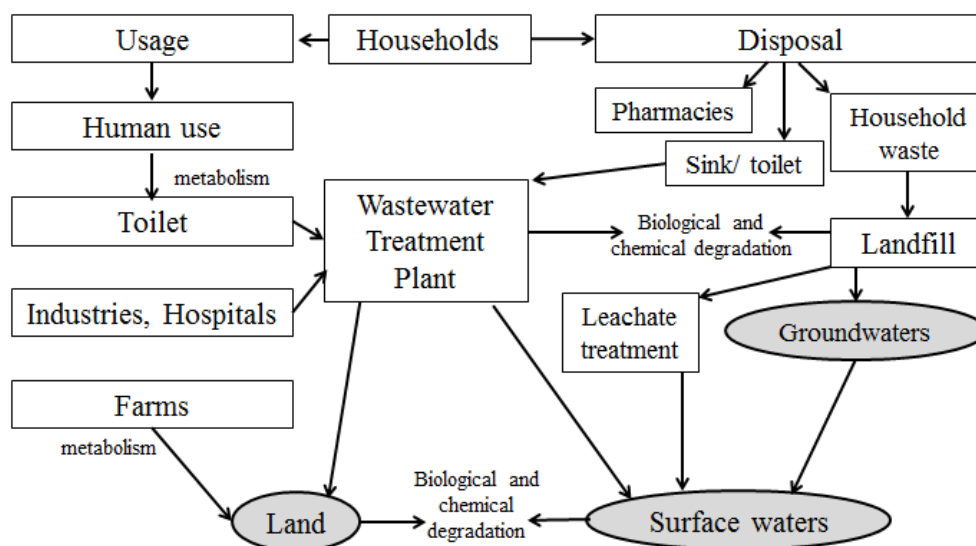
Figure 1 – Sources and fate of PhACs (adapted from Nikolaou *et al*., 2007).

Although the pharmaceutical active compounds (PhACs) are not regulated in drinking water or wastewater directives worldwide, the increasing release of these emerging contaminants is worrying and reported all around the world by several authors. The fact that they easily get dissolved in water and do not evaporate at normal temperatures and pressures, makes the PhACs be significantly present in soil and aquatic environments. Two common emerging contaminants found in different aqueous media are Sulfamethoxazole (SMX), which is an antibiotic, and Diclofenac (DCF), which is a non-steroidal anti-inflammatory and analgesic (**Table 1**) (Richardson *et al.*, 2005).

Table 1 – Concentrations of DCF and SMX found in different aqueous media (collected from Quintanilla, 2010; Madureira *et al.*, 2010; Nikolaou *et al.*, 2007; Vieno *et al.*, 2014 and Gracia-Lor *et al.*, 2012).

	SMX	DCF
Drinking water	1.7 µg L^{-1} (maximum for Europe) 0.04 µg L^{-1} (maximum for Holland)	6 ng L^{-1} (Germany)
WWT plants	0.45µg L^{-1} influent, 0.05µg L^{-1} effluent (Spain) 101 ng L^{-1} (Italy) 4664 ng L^{-1} (Croatia) 12 ng L^{-1} (UK)	0.53 µg L^{-1} influent, 0.34 µg L^{-1} effluent (Spain) 2 µg L^{-1} influent, 1 µg L^{-1} effluent (Germany)
Surface/ river water	26.0 ng L^{-1} (France) 2.39 ng L^{-1} (Italy) 9 ngL^{-1} (Croatia) 53.3 ng L^{-1} (Douro River, Portugal) 93.3 ng L^{-1} (Germany) 1 ng L^{-1} (UK) 0.09 µg L^{-1} (Netherlands)	6.5 µg L^{-1} (Germany) 1.2 µg L^{-1} (Europe)
Groundwater	13.5 – 28.7 (median 121.5) ng L^{-1} (Spain)	60.2 – 219 (median 121.5) ng L^{-1} (Spain) 18.7 ng L^{-1} (Spain)

It is important to refer the season influence on some types of medicine. The antibiotics as SMX, for instance, have higher levels in spring and autumn, which can be explained by higher administration on certain seasons (Seifrtová *et al.* 2007).

The majority of maximum concentrations found in water have an order of magnitude thousand times smaller than the levels that can cause acute toxicity. The fact that the concentrations in drinking water are low does not betoken that these pollutants could have significant effects on human health. However, the PhACs molecules are purposefully designed to bond with cellular receptors and elicit specific biological effects even in low concentration. It is concerning that aquatic life has continuous exposures, which can lead to possible low dose effects.

The presence of SMX in water can promote problems regarding resistance to antibiotics and resistance among bacterial pathogens that lead to altered microbial community structure in the nature consequently disturbing the top of the food chain (Daughton and Ternes, 1999). It is important to understand the behaviour of the molecule itself and its behaviour in water (**Figure 2**) to take an action over this pollutant. As the pH decreases, neutral SMX species appear in detriment to negatively charge species that are present for higher pH (specially over pK_a 5.6). When the pH is lower than the other pK_a of SMX (1.8), it can acquire positive charge (Simon *et al.*, 2011).

On the **Table 2** further information on SMX is presented.
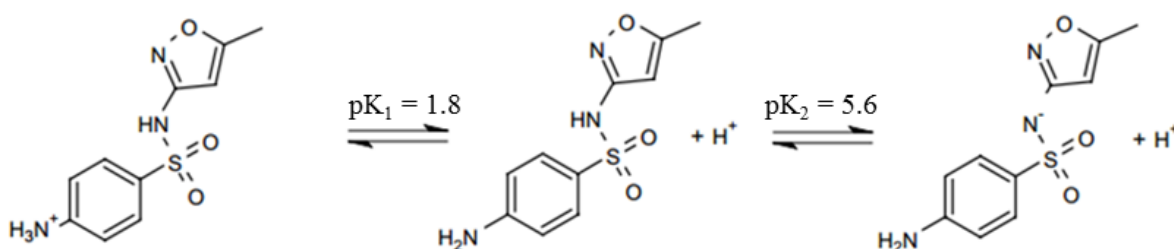
DCF is a worrying medicine in water due to its renal effects, according to Richardson *et al.* (2005). Its molecular structure is represented on the **Figure 3**.
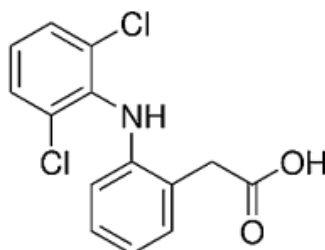
Figure 3 – DCF molecular structure.

This pharmaceutical is one of the least biodegradable anti-inflammatories. This compound is a non-steroidal anti-inflammatory drug (NSAID) which is an important group of pharmaceuticals that are the most frequent in WWT plants. Since it is an over-the-counter

drug in some places, it was the most frequently detected drug in the European water cycle. Diclofenac consumption rate is considerable: 2613 µg capita^{-1}day^{-1}(Germany), 2124 µg capita^{-1}day^{-1}(Spain) and 2104 µg capita^{-1}day^{-1}(Austria). The log K_{ow} reflects the likelihood of the compound to complex or sorb with organic carbon. According to Connell (1991), since the DCF log K_{ow} (4.51) lays between 3 and 6, it has the potential to bioaccumulate in the tissues of organisms. It is mentioned as a possible cause of endocrine deregulation and extinction of some organisms (Sari, S. *et al.*, 2014). Relevant information about DCF is presented on the **Table 2**.

Table 2 – **Important physicochemical properties of SMX and DCF for this study (Radjenović *et al.*, 2008, Verliefde *et al.*, 2008 and Nghiem and Simon, 2007).**

	SMX	DCF
Molecular weight (g mol^{-1})	253.277	296.148
Equivalent width (nm)	0.526	0.78
Classification	HL-ionic	Negative
pK$_a$	1.8; 5.81	4.18; - 2.25
log K$_{ow}$	0.659	4.51

A global improvement of water quality in order to diminish the exposure of living organisms to emerging contaminants and their related disadvantages is imperative.

2.2   Wastewater treatment processes

Indeed, one of the forthcoming problematic issues on the water treatment is the emerging contaminants threat, among which pharmaceuticals play an important role. Since the drugs are not entirely absorbed by the targeted living organisms, they end up being excreted and passed into WWT plants.

On sewage treatment plants there are normally several stages of treatment that basically consist on physicochemical treatment and biological treatment performed by microorganisms (bacteria). The conventional pH range in wastewater treatment processes is 6.5 – 7.5, which is imposed by the use of microorganisms.

Pharmaceuticals are often very toxic and resistant to conventional chemical and biological treatment. Heberer (2002) reports that some PhACs (DCF, for example) are not completely degraded in the WWT plants and are discharged to the receiving waters. However, Seifrtová *et al.* (2007) reported that, during a season of a WWT plant, 36.3 to 92.3% of the antibiotics was removed, having greater efficiency during summer. The effectiveness of the removal of the pollutants depends mainly on the type of chemical, its seasonality, the climate and the individual sewage treatment facilities. Tran *et al.* (2009) indicates a biological degradation constant of DCF for nitrification cultures of 0.31 – 0.52 g^{-1}d^{-1}, while the

conventional activated sludge reactor and the membrane bioreactor have a degradation value under 0.1 g^{-1} d^{-1}, which both indicate only partial biodegradation (Joss *et al.*, 2006).

The conventional sewage systems are not equipped for the removal of PhACs (and PPCPs generally), since these unregulated pollutants need specifically engineered treatment for their removal. Therefore, such substances can enter the water supply from various sources and are not effectively removed by conventional water treatment processes.

Since these treatments are not enough to efficiently eliminate all the pollutants on the effluents, new techniques, such as Membrane Separation Processes and Advanced Oxidation Processes (AOP) start to be studied and applied in order to promote the maximal removal of PhACs.

The Membrane Separation Processes employ a membrane, which is a separation barrier between two phases which selectively transfers mass between them. The membranes can be biological or synthetic, symmetric (porous or not) and asymmetric. The following processes include separations that need increasing pressure drop as driving-force: microfiltration, which uses microporous membranes; ultrafiltration, where asymmetric membranes are used; reverse osmosis, where asymmetric membranes with a dense film are used. Other membrane processes work with different driving forces: dialysis and pervaporation with a concentration gradient; gaseous permeation with a concentration and pressure gradient and electro-dialysis with a potential gradient. Generally the feed has a certain solute concentration and it is divided into the permeate, with lower concentration, and the retentate, with higher concentration than the feed. The Nanofiltration is additionally exploited on the **section 2.3**.

The AOP aim to mineralize completely (forming CO_2 and water) or partially organic compounds by the formation of hydroxyl radicals (OH·) which are very oxidative, reactive and have low selectivity to different compounds. These attack the chemical bonds of the organic compounds breaking them, thus oxidising the compounds *in situ*. If this process is taken to the very end, the chemical molecules present in water are mineralized to carbon dioxide and water. (Rosal *et al.*, 2010).The AOP can employ: ozone (O_3, with an oxidative potential of 2.42 V), hydrogen peroxide (H_2O_2, oxidative potential of 1.78 V) and UV light. Among the AOP are processes that use these components alone or consist on hybrid methodologies, for example Fenton oxidation, which uses a combination of hydrogen peroxide and an iron catalyst as oxidation agents and Ozonation (OZ), which is presented on **section 2.4** (Cheremisinoff, 2002).

After a WWT, there are several parameters that should be evaluated before its discharge to the reception media. The concentration of the pollutant (in this case, SMX and DCF) is a crucial parameter and can be measured by Gaseous Chromatography-Mass Spectroscopy (GC-MS), High Performance Liquid Chromatography (HPLC) or hybrid HPLC techniques (Nikolaou *et al.*, 2007). Nowadays there are no regulations in Europe that indicate the limit concentrations for the discharge wastewaters containing SMX and DCF (and generally PhACs, PCPs and EDCs) or for drinking water. Nevertheless, some pollutants are regulated on the United States (but not the ones on the scope of this study). However, since this is an

emerging issue, the Water Framework Directive 2000/60/EC delineates a strategy to deal with the chemical pollution of aqueous streams. This includes listing the 33 priority substances of concern. On 2006 the definition of environmental quality standards was proposed to ensure high level of milieu protection. There are countries in which excellent water quality programs have been implemented (example: Holland). Nowadays exists REACH (EC 1907/2006) that regulates, records, evaluates and authorizes chemicals of greater concern on a perspective to control them later (Quintanilla, 2010).

The Chemical Oxygen Demand (COD), which indicates the mass of oxygen necessary to degrade the organic matter present in a solution, is also a very important parameter. It can be accessed through an analysis (dichromate method) that involves a chemical reaction that is the following:

$$C_nH_aO_bN_c + d\ Cr_2O_7^{2-} + (8d + c)\ H^+ \rightarrow n\ CO_2 + \frac{a+8d-3c}{2}\ H_2O + c\ NH_4^+ + 2dCr^{3+} \quad (2.1).$$
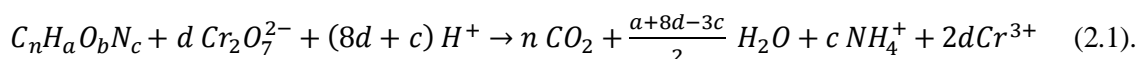
Where $d = 2n/3 + a/6 - b/3 - c/2$. Taking into account the molecular formula of SMX ($C_{10}H_{11}O_3N_3S$) and DCF ($C_{14}H_{11}O_2NCl_2$), it is necessary to take into account possible inorganic interferences due to the chloride presence ($6Cl^- + Cr_2O_7^{2-} + 14\ H^+ \rightarrow 3\ Cl_2 + 2Cr^{3+} + 7H_2O$). However, they can be eliminated by the addition of mercury sulphate ($Hg^{2+} + Cl^- \leftrightarrows HgCl_2$).

By the chemical reaction (2.1), it is possible to determine the theoretical COD of the PhACs on the scope of this study. Considering an aqueous solution containing 30 mg L^{-1} of each component, the COD is: 35.31 mg O_2 L^{-1} for SMX and 30.20 mg O_2 L^{-1} for DCF. The European Directive 91/271/EEC (and, consequently, the Portuguese law with the decree-law 152/97), indicates that the urban wastewaters discharges should fulfil the COD requirements of being under 125 mg O_2 L^{-1}. Alternative parameters to COD are Total Organic Carbon (TOC), which indicates the amount of carbon in an organic compound, and Biochemical Oxygen Demand (BOD), which shows the amount of dissolved oxygen needed so that aerobic biological organisms can degrade the organic material in water.

Another important parameter is the toxicology of the sample. This can be measured with the use of luminous bacteria. The dose (concentration) required to lower the response (luminescence) to 20% and 50% of the control population (no toxic substance added) is the EC_{20} and EC_{50}, respectively The higher the EC_{50}, the more toxic substance it is needed to add to the bacteria to make them loose response (i. e. the less toxic is the substance).

The scientific research on wastewater treatment usually starts with a simulated effluent for different motives: the reduction of the variables that could increase the complexity of the experiments (for example, compounds present in the aqueous matrix); the simplification of the result's analysis; the sensibility of the analytical techniques (in this case they were not sensible enough to detect similar concentrations to the ones found in the environment); among others. However, at the end, it aims to be applied to real effluent with different properties and multiple pollutants to treat. Therefore, this work consists in a step forward the real effluent, - since it combines two pollutants.

2.3   Nanofiltration

The Nanofiltration permits the separation of small organic compounds with sizes between 1 and 8 nm. This process employs asymmetric flat membranes which are composed by an active layer (homogeneous and with a thickness range from 0.1 to 0.5 μm) and a porous layer (with a thickness from 50 to 150 μm) which has a porosity gradient on the perpendicular direction of its surface (Mulder, 1996).

The flux that goes through the membrane is the volume per area and time, $J_v (m^3 m^{-2} s^{-1})$, and can be given by:

$$J_v = \frac{L_p}{\eta_0} (\Delta P - \Delta \pi) \qquad (2.2)$$

where L_p is the membrane permeability (m), η_0 is the fluid viscosity $(Pa\ s^{-1})$ that is a function of the temperature, ΔP is the pressure drop (Pa) and $\Delta \pi$ is the osmotic pressure (Pa). This model considers that the bulk concentration of the feed is equal to the concentration next to the membrane, which is not fairly true due to the membrane concentration polarization (phenomena that consists on the accumulation of solutes rejected by the membrane nearby which adds resistance to the mass transference). However, this model is valid for cases in which the concentration polarization is not negligible, being $\Delta \pi$ calculated with the membrane's concentration on the feed's side. In some cases in which the solute has low concentration, $\Delta \pi$ (given by $R\ T\ \Delta C\ n/M$, where R is the universal gas constant, T is the temperature, ΔC is the solute concentration variation, n is the number of mol dissociated and M is the molar mass of the solute) can be neglected.

The permeability L_p is the inverse of the membrane intrinsic resistance, R_m, which is normally a fraction of all the resistances felt on the membrane (which include the gel layer, the adsorption and the concentration polarization resistance).

The fouling of the membrane consists on the deposition of elements of the feed on the membrane's surface and can interfere on its behaviour, namely the reduction of the flux through it. This phenomenon can happen due to adsorption of material on the surface (gel layer) and to the blocking of its pores (clogging).

According to Sutzkover (2000), the mass transfer coefficient, $k_{f,i}$, for a certain solute (as an example, for sodium chloride, $k_{f,NaCl}$) can be obtained experimentally through the measurement of the flux with water, J_{v,H_2O}, and aqueous solutions of sodium chloride, $J_{v,NaCl}$:

$$k_{f,NaCl} = \frac{J_{v,NaCl}}{ln\left[\frac{\Delta P}{\pi_b - \pi_p}\left(1 - \frac{J_{v,NaCl}}{J_{v,H_2O}}\right)\right]} \qquad (2.3).$$

where $\pi_b = i\ C_f\ R\ T$ and $\pi_p = i\ C_p\ R\ T$, being i the van't Hoff factor (dissociation factor), C_f the concentration in $mol\ L^{-1}$ of the salt in the feed, C_p the concentration in $mol\ L^{-1}$ of the salt on the permeate, R the product between the gas constant and T the temperature in Kelvin.

There are several correlations that can be used to predict the mass transfer coefficient. For example:

- Grobber correlation (Schäfer $et\ al.$, 2005): $Sh = 0.664\ Re_{dh}^{0.5}\ Sc^{0.33}\ (d_h/L)^{0.5}$ (2.4);

- Geraldes correlation (Geraldes and Afonso, 2008): $Sh = 0.142\,Re^{0.46}Sc^{0.37}$ (2.5);
- Lévêque correlation (Cheryan, 1998): $Sh = 1.86\,Re_{d_h}^{0.33}(d_h/L)^{0.33}$ (2.6).

where d_h is the hydraulic diameter, L the channel length, Re_{dh} the Reynolds number based on the hydraulic diameter (given by $Re_{dh} = \rho\,u\,d_h/\eta_0$), Re the Reynolds number (given by $Re_{dh} = \rho\,u\,h/\eta_0$) and Sc is the Schmidt number (given by $Sc = \eta_0/\rho\,D_{salt,\infty}$). The Sherwood number, Sh, applied to this case, is equal to:

$$Sh = \frac{k_{f,NaCl}\,d_h}{D_{salt,\infty}}$$ (2.7).

The molecular weight cut-off (MWCO) of the membrane is the lowest molecular weight at which there is a retention of 90% of the solute by the membrane.

The retention based on COD measurements is given by:

$$Retention\ (COD) = 1 - \frac{COD_p}{COD_f}$$ (2.8).

where COD_p and COD_f are the COD values for permeate and feed, respectively.

The selectivity of a the membrane regarding a certain compound is commonly given by the apparent rejection coefficient, R, which is given by:

$$R = 1 - \frac{c_p}{c_f}$$ (2.9).

The retention of a certain compound (ex: SMX) taking into account the concentration of the pollutant (ex: $[SMX]$) is calculated according to the following:

$$SMX\ Retention = 1 - \frac{[SMX]_p}{[SMX]_f}$$ (2.10)

where $[SMX]_p$ and $[SMX]_f$ are the concentrations of SMX on the permeate and the feed, respectively.

The global retention takes into account the concentration of SMX and DCF on the permeate and on the feed:

$$Global\ Retention = 1 - \frac{[SMX]_p + [DCF]_p}{[SMX]_f + [DCF]_f}$$ (2.11).

Other parameters which are important do characterize the membrane are the porosity (ration between the pores' volume and the total membrane's volume), the pores' diameter and the superficial charge (the membrane has some molecular groups which confer it charge when the membrane is in the aqueous media). These parameters interfere on the separation process that is affected by several mechanisms:

- Steric hindrance or size exclusion, which influences the rejection of uncharged trace organics. The rejection of these compounds increases linearly with the molecular weight and the molecular width and is related with de MWCO.
- Electrostatic repulsion, which is important do separate charged solutes and can be explained by the repulsive force between negatively charged molecules and negatively charged membrane surfaces. This repulsion is ruled by the Donnan effect which increases with the concentration of species on the feed. However, if the

Donnan equilibrium is attained (the charge of the membrane is neutralized by the opposite charge of the ions in solution), the size exclusion prevails.

- Adsorptive interactions, which happens to hydrophobic compounds. The sites are accessible to the molecules' adsorption due to the pressurize advective flow characteristic on the dynamic filtration processes. (Quintanilla, 2010)

For this motive, the speciation (protonation) of trace organics is important and the pH and the ionic strength affect the separation processes.

2.4   Ozonation

The oxidative power of ozone makes it react with organic and inorganic compounds to generate other simpler compounds, being effective degrading complex organic molecules and decreasing COD. For a batch process, the percent COD degradation given at the time t of the Ozonation reaction is a function of the COD at that reaction time, COD_t, and the COD in the beginning of the reaction, $COD_{t=0}$:

$$Degradation\ (COD)_t = 1 - \frac{COD_t}{COD_{t=0}} \qquad (2.12).$$

The Ozonation process can be a direct or indirect oxidation. On the first one, the ozone directly attacks the molecules, while on the last the pollutants are attacked by hydroxyl radicals formed when the ozone decomposes.

The degradation of a certain compound (ex: SMX) for a certain time of a batch Ozonation reaction, t, taking into account the concentration of the pollutant (ex: $[SMX]$)is calculated according to the following:

$$SMX\ Degradation\ _t = 1 - \frac{[SMX]_t}{[SMX]_{t=0}} \qquad (2.13).$$

The global degradation takes into account the concentration of SMX and DCF for the initial time ($t = 0$) and for a certain time, t, and is calculated by:

$$Global\ Degradation_t = 1 - \frac{[SMX]_t + [DCF]_t}{[SMX]_{t=0} + [DCF]_{t=0}} \qquad (2.14).$$

The use of catalysts can improve the global degradation of specific pollutants or of the organic matter (measured by the COD). There are several types of catalysts. The catalysts' structure can be characterized according to their pores size: microporous (pores diameter smaller than 2 nm), in which movement is done by activated diffusion; mesoporous (pores between 2 and 50 nm), in which movement is done by Knudsen diffusion and macroporous (pores larger than 50 nm), in which the flow is made by bulk diffusion.

It is important to ensure that the Ozonation reaction occurs on a chemical regime that can be attained by the powdering of the catalyst and the continuous mixing of the reactor on a considerable speed. Under these conditions the reaction occurs is a slurry reactor.

Saturated carboxylic acids are intermediates found in single and catalytic-promoted Ozonation of SMX. These compounds rapidly disappear from water as a result of direct ozone reactions.

There are three reactional mechanisms through which the ozone action can be improved by a solid catalyst:

- The ozone gets to the catalyst and the reaction of the formation of hydroxyl radicals occurs on its surface. Posteriorly these react with the dissolved organic matter degrading it;
- Both the ozone and the organic matter are adsorbed on the catalyst and they react while adsorbed there;
- The ozone molecule reacts in the catalyst to form reactive adsorbed oxygen species that will degrade non-adsorbed organic matter.

When unsaturated compounds are being degraded, because of the reaction in which ozone breaks the double carbon bonds or the aromatic ring, hydrogen peroxide is formed. It can also be formed due the ozone decomposition on the catalyst (Beltrán *et al.*, 2004). It is also possible to add hydrogen peroxide. The quantity to add should take into account the overall stoichiometry of the O_3 reaction with H_2O_2 to avoid the excess of this compound and the creation of hydroxyl scavengers (H_2O_2/O_3 molar ratio under 0.5) (Ormad, P. *et al.* 1997).

Ozone has a great potential for wastewater treatment processes despite some operational problems. The main disadvantages of the Ozonation are the toxicity, corrosion and instability of ozone. It has to be produced in situ and their generators have generally low efficiency, what makes the energy costs increase.

3.   Literature Review

Since the TrOC are an emerging problem on water treatment, lots of compounds that range from pesticides to PPCPs have been studied. Taking into account the subject of this work, on this chapter, the techniques being used on the removal of SMX or DCF are exposed. Since Nanofiltration and Ozonation were done and have been broadly used to achieve this objective, most of the results presented are related with these techniques.

The **Table 3** comprises a summary of the Membrane Separation processes for SMX retention. Simon *et al.* (2009) refers retentions of almost 100% of the pollutant with both Reverse Osmosis (RO) and Nanofiltration (NF) processes. The retention of pollutants in function of pH for Nanofiltration membranes resembles a sigmoidal function increasing with pH with inflection point close to the pK_a of SMX. Chang *et al.* (2012) reports that the calcium ions create fouling reducing the flux trought the membrane.

Table 3 – Review of the literature regarding Membrane Separation Processes of aqueous solutions containing SMX.

Ref.	Objectives	Technology	Operating conditions	Conclusions
Simon *et al.*, 2009	Evaluate the effects of membrane degradation on the removal of SMX by NF/RO	Laboratory-scale membrane filtration test unit with a rectangular stainless steel crossflow cell. Membranes used: NF 90, TFC-SR2 and NF270 BW30 (RO)	20 mM NaCl, 1 mM NaHCO$_3$, 1 mM CaCl$_2$. Crossflow velocity = 30.4 cm s^{-1}, T = 20.0°. Rejection (R%) evaluated as a function of pH with virgin membrane and after being exposed to 2000 and 500 mg L^{-1}.	NF90 and BW30 are the most resilient to chlorine exposure because of their small pores. The rejection diminishes with increasing chlorine exposure. The R% is almost 100% regardless the pH and the chlorine exposure for NF90 and BW30. The RO membrane has better results. Behaviour of R% in function of pH for TFC-SR2 and NF270 resembles a sigmoidal function (increasing with pH) with inflection point close to the pK_a of SMX. Membrane polyamide active skin layer changed roughness after chlorine exposure. The exposure can loosen or tighten the pore size of the membrane.
Radjenović *et al.*, 2008	Evaluation of the rejection of SMX in NF and RO	Drinking Water Treamtment Plant. RO treatment that can take a feed of 486 m^3 h^{-1} with 356.4 m^3 h^{-1} flow of permeate (recovery of 73%). It consists on 40 + 20 membrane modules, each one with 6 BW30 LE440 membranes. NF can take a feed of 360 m^3 h^{-1} giving 234 m^3 h^{-1} of permeate (recovery of 65%). Composed by 31 + 15 membrane modules, each with 6 NF90-400 membranes.	Feed: groundwater; [SMX] = 13.5 – 28.7 ng L^{-1} (median: 21 ng L^{-1}) J$_{v,NF}$= 22.9 L m^{-3} h^{-1}; J$_{v,RO}$= 22.5 L m^{-3} h^{-1}; pH = 5.6 – 6.1; T = 17°C. %R measured on waste water.	The NF permeate had [SMX] = < 2– 4.8 ng L^{-1} (median < 2 ng L^{-1}), while the RO permeate had [SMX] < 2 ng L^{-1}. Therefore, it is possible to conclude that RO is slightly more efficient than NF for SMX removal.
Chang *et al.*, 2012	Identify the rejection mechanisms of SMX on fouled membranes.	Cross-flow module. Membranes: NF270 (polyamide thin-film) and NTR7450 (composite structure with active layer on top of polysulfone support).	[SMX] = 500 µg L^{-1}. Flux evaluation for fouled membranes with humic acid and calcium (Ca^{2+}). Rejection as a function of pH (4, 6, 8, 10).	Complete blocking and cake-layer formation of membranes with humic acid. With Ca^{2+} the flux decreases due to pore blocking. Fouling decreased the rejection of SMX (large compound) because of concentration polarization. Size exclusion is more dominant for NF270, while electrostatic repulsion has a role for NTR7450.

On the **Table 4** is a synthesis of the Membrane Separation Processes used to remove DCF. Vergili (2013) indicates that the presence of DCF on water makes the flux trough the membrane decrease due to adsorption and fouling. Verliefde *et al.* (2008) reports a 99% rejection of DCF dissolved in surface water from a WWT plant at pH=7.

Table 4 – Review of the literature regarding Membrane Separation Processes of aqueous solutions containing DCF.

	Objectives	Technology	Operating conditions	Conclusions
Vergili, 2013	Application of NF for the removal of DCF from drinking water sources	Laboratory-scale NF membrane system with cross-flow operation mode. Flat-sheet membrane FM NP010 with 80 cm^2 made of polyethersulfone.	Feed 1: Water collected from Drinking Water Treatment Plant with no PhACs (carbamazepine, DCF and ibuprofen were under the limit of detection of 0.005 ng L^{-1}), [DCF] = 0.025, 0.05 and 0.1 ng L^{-1}. Feed 2: carbamazepine + DCF + ibuprofen (0.05 ng L^{-1}). ΔP = 12 bar; pH = 8; T = 25°C; Quotient between initial volume of feed and final volume of concentrate = 1.25. J_v, Fouling, Concentration polarization (flux recovery minus relative flux) and R% were measured.	J_v decreases 25.5 – 27% with raw water, while it decreases 37.2 – 40.8% with water spiked with DCF due to fouling or adsorption on the membrane. The higher concentration of DCF, the more the flux decreases. The concentration polarization is 2.2 - 3.6 higher with DCF than with raw water (the bigger the [DCF], the higher). R% ≈ 93 for Feed 1 (regardless the [DCF]) R% DCF = 76% for Feed 2.
Verliefde *et al.*, 2008	Study the role of electrostatic interactions (mono and divalent cations) on the rejection of DCF in aqueous solutions	Bench-scale membrane system, flat-sheet membranes Trisep TS80 and Desal HL were used.	Feed 1: Mili-Q water + CaCl$_2$ (5 or 10 mM); pH = 7. Feed 2: Surface water from WWT plant. pH = 7. Range of pH: 3 – 10. %R and pH effect were tested.	The higher the concentration of Ca$^+$ (Feed 1), the lower the rejection is for both membranes (10 mM reduces R% in maximum 3%). DCF had 99% rejection with surface water (Feed 2) and TS-80. The pH (on a range 3 – 11) does not have a significant effect on the rejection of DCF by TS-80. However, Desal HL, just gives high retentions (97%) for a pH range from 7 to 9. The Feed 2 water provides a higher %R in two percent than the Feed 1.
Radjenović *et al.*, 2008	Evaluation of the rejection of DCF in NF and RO	Drinking Water Treamtment Plant implemented technology. RO treatment that can take a feed of 486 m^3 h^{-1} with 356.4 m^3 h^{-1} flow of permeate (recovery of 73%). It consists on 40 + 20 membrane modules, each one with 6 BW30 LE440 membranes. NF can take a feed of 360 m^3 h^{-1} giving 234 m^3 h^{-1} of permeate (recovery of 65%). Composed by 31 + 15 membrane modules, each with 6 NF90-400 membranes.	Feed: groundwater; [DCF] = 60.2 – 219 ng L^{-1} (median: 121.5 ng L^{-1}) $J_{v,NF}$ = 22.9 L m^{-3} h^{-1}; $J_{v,RO}$ = 22.5 L m^{-3} h^{-1}; pH = 5.6 – 6.1; T = 17°C. %R measured on waste water.	Since the both the NF permeate had [DCF] < 18.7 ng L^{-1}, it is possible to conclude both processes were very effective with removals of 100%.

On the **Table 5** several AOP processes are described for the SMX degradation in aqueous solutions. Beltrán *et al.* (2009) reports a complete removal of SMX after 6 minutes, regardless the presence or absence of catalyst. However, the catalysts are interessant for the removal of TOC. Degradation pathways of SMX include: hydroxylation of the benzene ring; oxidation of the amine group at the benzene ring; oxidation of the methyl group at the isoxazole ring; oxidation of the double bond C=C at the isoxazole ring and S–N bond cleavage. Some of these stages create toxic substances on the early moments of the Ozonation reaction that can persist after the Ozonation reaction time (Gómez-Ramos *et al.*, 2011).

	Objectives	Technology	Operating conditions	Conclusions
Akhtar *et al.* (2011)	Study the effect of combined adsorption and catalytic OZ for removal of SMX using $Fe_2O_3/CeO2$ loaded activated carbon. Compare the performance of simple OZ, PAC (combined adsorption and catalytic OZ by commercial activated carbon) and MOPAC (combined adsorption and catalytic OZ by Fe_2O_3/CeO_2 loaded activated carbon).	OZ glass reactor; V = 250 mL.	Oxygen/ ozone mixture 1.0 L/min; $C_{O3,in}$= 48 mg L^{-1}; T = 26±1℃; t = 20 min; adjusted pH = 5±1. Kinetic experiments: [SMX] = 100 mg L^{-1}; two catalysts; pH_0 = 3 or 7.5; TOC removal: [SMX] = 100 mg L^{-1}; two catalysts; pH_0 = 5 ± 1; t = 15 min. Ozone consumption efficiency: [SMX] = 200 ppm L^{-1}; ozone through blank, PAC/O_3 and MOPAC/O_3; pH_0 = 4.5 – 5; t = 5 min.	PAC uptakes more TOC than MOPAC. Adsorbed SMX increases a with initial [SMX] and T. Optimal conditions: adsorbent dosage of 2 g L^{-1}, initial pH = 6.5 and t = 50 min. GC-MS detected SMX after simple OZ and PAC, but not after MOPAC. MOPAC was better for low pH values but for pH = 7.5 the catalyst effect was minimal. Better consumption of O_3 for MOPAC.
Beltrán *et al.* (2009)	Analysis of catalysts to improve the abatement of SMX and the resulting organic carbon in water during OZ.	Using granular activated carbon: Tubular glass reactor (300 mm long, 50 mm diameter) in series with a packed bed column (30 mm long, 30 mm diamter). Using powered perovskite catalysts: cylindrical glass vessel with magnetic agitation, air diffuser and sampling port; V=300 cm^3. Catalysts: Hydraffin P110, Darco 12−20, GMI 2000, $LaTi_{0.15}Co_{0.85}O_3$, Al_2O_3 and Al_2O_3/Co.	T = 20℃; $C_{O3,in}$= 20 mg L^{-1}. pH buffering with NaH_2PO_4 and Na_2HPO_4. Tests of different catalysts: [SMX] = 30 mg L^{-1}; pH=7. TOC evolution: [TOC] = 15 mg L^{-1}; pH = 7; different catalysts; absorbance measurements (254 nm) to detect aromatics. pH effect: pH = 2, 5, 7 and 9; simple OZ and different catalysts tested, TOC measured. Different pre-OZ times.	Complete removal of SMX after 6 min. Catalysts do not make significant difference except on first 3 minutes due to higher reaction rates. Hydrogen peroxide and saturated carboxylic acids (pyruvic and oxalic acids) detected (first increase and then decrease as a result of direct ozone reactions); aromatics decreasing along time. For the removal of TOC, catalysts are recommended, since they stimulate the hydroxyl radical oxidation eliminating saturated carboxylic acids. Low pH has negative effect on perovskite catalysts due to metal leaching. Decreasing pH increases TOC removal rate on activated carbon (more hydroxyl radicals on the catalyst's surface).
Gonçalves *et al.* (2013)	OZ of SMX promoted by multi-walled carbon nanotubes (MWCNTs)	Laboratory scale reactor (V = 1 L). MWCNTs prepared from Nanocyl 3100 with diameter 9.5 average and 95% carbon purity.	[SMX] = 50 ppm in ultrapure water; pH = 4.8 (natural); ~ 143 mg L^{-1} MWCNT; Flow rate = 150 cm^3 min^{-1}; $C_{O3,in}$ = 50 g cm^{-3}; stirring at 200 rpm.	Complete SMX conversion after 30 min. MWCNTs increase mineralization. MWCNTs should be basic or neutral, so the highest mineralization occurs for MWCNT-HNO_3_N_2_900 because it has basic properties with no surface groups containing oxygen. Successive use leads to catalyst deactivation.
Gómez-Ramos *et al.* (2011)	Study of the chemical and toxicological evolution of the SMX under ozone treatment in water solution.	Semi-batch reactor with porous glass disk for ozone bubbling and mixed by four blade impeller; V = 5 L. Analysis by Liquid chromatographer-electrospray ionisation-quadrupole-time-of-flight mass spectrometer (LC-ESI-QTOF-MS).	[SMX] = 0.150 mM; pH = 2 and 8; T = 25℃; 1000 rpm. Fast kinetic regime of OZ, that optimizes ozone consumption. Some trials involved hydrogen peroxide. Samples collected. Catalase used to remove hydrogen peroxide from samples. LC-ESI-QTOF-MS for products identification. Toxicity evaluation for *D. magna* and *P. subcapitata*.	Removal of SMX under 0.2 mM under conditions that allow the radical formation: pH = 8 with and without peroxide. Several main transformation products identified (that originated other products after): $C_4H_2N_2O$ (99.0554 g mol^{-1}), $C_{10}H_{14}N_3O_5S$ (288.0654 g mol^{-1}), $C_{10}H_{10}N_3O_5S$ (288.0334 g mol^{-1}), $C_{10}H_{10}N_3O_5S$ (288.0039 g mol^{-1}), $C_{10}H_{12}N_3O_4S$ (270.0541 g mol^{-1}), $C_{10}H_{10}N_3O_5S$ (284.0340 g mol^{-1}). Degradation pathways include: hydroxylation of the benzene ring; oxidation of the amine group at the benzene ring; oxidation of the methyl group at the isoxazole ring; oxidation of the double bond C=C at the isoxazole ring and S–N bond cleavage. Formation of toxic by-products during the early stages of reaction when there was still SMX. Persistence of residual toxicity for *P. subcapitata* after SMX total depletion.
Beltrán *et al.* (2012)	Direct photolysis (UVA), adsorption (TiO₂), OZ (O₃), Photoozonation (O₃+UVA), photocatalytic oxidation (UVA+TiO₂+O₂), catalytic OZ (O₃+TiO₂) and photocatalytic OZ (O₃+UVA+TiO₂) of SMX in water.	Cylindrical reactor in a box with four 15 W black lights (UVA). V = 1 L with mechanical agitation. Inlets for measuring temperature, feeding the gas (oxygen or ozone−oxygen) and sampling. Outlet for non absorbing gas.	[SMX] = 25,33 mg/L (0,1 mM) T = 20℃; pH_0 = 7; gas flow rate 30 L h^{-1}; $C_{O3,in}$ = 10 mg L^{-1}. [TiO_2] = 0.5 g L^{-1}. Photon flux in the photoreactor = 5.08 x 10^5 Einstein min^{-1}.	Processes involving ozone have very high removals (99.7%) and reduce [SMX] to 100 μg L^{-1} (under detection limit) after 15 min. Rate constant of direct ozone reaction is 4.15 x 10^5 M^{-1} s^{-1}. UVA+TiO_2+O_2 permit some removal but reaction rates are lower. Increasing efficiency on TOC removal: UVA+TiO_2+O_2 ≈ O_3, O_3+UVA ≈ O_3+TiO_2. Black light or TiO_2 accelerate the refractory compounds degradation.

15

On the **Table 6** are presented summaries of AOP techniques used on DCF aqueous solutions. Vogna *et al.* (2004) report that both simple Ozonation and UV/H$_2$O$_2$ are efficient degrading DCF. However, while the first converts all chlorine into chroride ions, the second just converts 52%. Pocostales *et al.* (2011) reports that, as in the SMX degradation, the catalysts do not accelerate the DCF removal, but are important for COD degradation.

Table 6 – Review of the literature regarding AOP applied to aqueous DCF solutions.

	Objectives	Technology	Operating conditions	Conclusions
Vogna *et al.* (2004)	Study of the advanced oxidation of DCF with UV/H$_2$O$_2$ and ozone	Semi-batch glass reactor; continuous feed; ozone introduced through porous sparger.	[DCF] = 1 x 10^{-3} M; pH = 7 (adjusted); T = 25°C; C$_{O3,in}$ = 36 L h^{-1}. Kinetic constant evaluated for different pH. Simple OZ and UV/H$_2$O$_2$ tested.	Both systems (O$_3$ and UV/H$_2$O$_2$) are efficient in DCF degradation. For t = 30 min: OZ converts all chlorine into chloride ions with degree of mineralization of 32%; UV/H$_2$O$_2$ converts just 52% of chlorine and has a degree of mineralization of 39%. Reactions follow similar pathways that lead to hydroxilated intermediates and C-N cleavage products. Oxidative ring cleavage leads to carboxylic acid fragments. Kinetic constant of DCF OZ for pH range of 5 – 6, of 1.76 x 10^{-4} and 1.85 x 10^{-4} M^{-1} s^{-1}.
Pocostales *et al.* (2011)	Catalytic OZ promoted by alumina-based catalysts for the removal of DCF from water	Gas-liquid reactor (300 mm long, 50 mm diameter); porous plate; bottom feed of O$_3$ and O$_2$. Fixed-bed reactor with 5 g of catalyst. OZ with different catalysts (Co$_3$O$_4$/Al$_2$O$_3$, γ-Al$_2$O$_3$).	[DCF] = 30 mg L^{-1} in ultrapure water; pH = 5,7; T = 20°C; C$_{O3,in}$ = 500 mg h^{-1}; catalyst mass (if applied) = 5g. Comparison of catalysts' performance, buffered and not buffered solution. Domestic secondary effluent tested.	OZ rapidly removes DCF and the presence of catalysts does not accelerate removal, however increase mineralization. Catalyst Co$_3$O$_4$/Al2O3 stable and reusable for 4 experiments. Co$_3$O$_4$/Al$_2$O$_3$ helps on the reaction rate of COD removal. Catalysts chemisorpt and decompose ozone into free radicals and adsorbe some compounds that react easily with ozone.
Aguinaco, A. (2012)	Study the influence of variables on photocatalytic OZ to remove the pharmaceutical DCF from water.	Cylindrical borosilicate glass photo-reactor (0.45 m height, 0.08 m inside diameter); ozone–oxygen mixture continuously bubbled through diffuser (on the bottom); high-pressure mercury lamp irradiation (3 x 10^5 Enstein s^{-1}); magnetic stirring. OZ with TiO$_2$ catalyst and UVA (O$_3$/UVA/TiO$_2$) Oxidation with with TiO$_2$ catalyst and UVA (O$_2$/UVA/TiO$_2$).	Standart conditions: pH = 7; T = 20°C; Gas flow rate = 30 L h^{-1}; TiO$_2$ = 1.5 g L^{-1}; [DCF] = 10^{-4} M. Effect of inlet O$_3$ concentration: different inlet ozone gas concentration (0 to 30 mg L^{-1}). Effect of [DCF]: [DCF] = 30, 50, 80 mg L^{-1}. Effect of [TiO$_2$]: [TiO$_2$] = 0; 0.5; 1.5; 2.5 mg L^{-1}. Ultra-pure water effect. Ozone consumption and ecotoxicity evaluated.	Increasing O$_3$ inlet to 20 mg L^{-1} augments yield (further increase indifferent). The higher [DCF], the fastest reaction rates. Optimum concentration of TiO$_2$ between 1.5 and 2.5 g L^{-1}. Photocatalytic OZ consumes the less ozone per mg of TOC consumed. O$_3$/UVA/TiO$_2$ and O$_2$/UVA/TiO$_2$ lead to the lowest ecotoxicity compared to other AOP (oxidising/radiation). Influence of the water matrix was not observed in the DCF removal rate respect to the ultrapure water medium.
Beltrán *et al.* (2012)	Direct photolysis (UVA), adsorption (TiO$_2$), OZ (O$_3$), photocatalytic oxidation (UVA+TiO$_2$+O2), catalytic OZ (O$_3$+TiO) and photocatalytic OZ (O$_3$+UVA+TiO$_2$) of DCF in water.	Cylindrical reactor in a box with four 15 W black lights. V = 1 L with mechanical agitation. Inlets for measuring temperature, feeding the gas (oxygen or ozone–oxygen) and sampling. Outlet for non absorbing gas.	[DCF] = 25.33 mg/L (0,1 mM) T = 20°C; pH$_0$ = 7, gas flow rate 30 L h^{-1}, C$_{O3,in}$ = 10 mg L^{-1}. [TiO$_2$] = 0.5 g L^{-1}. Photon flux in the photoreactor = 5.08 x 10^5 Einstein min^{-1}.	Processes involving ozone have very high removals (99.7%) and reduce [DCF] to 100 µg L^{-1} (under detection limit) after 7 min. Rate constant of direct ozone reaction is 10^6 M^{-1} s^{-1}. Increasing efficiency on TOC removal: UVA+TiO$_2$+O$_2$, O$_3$, O$_3$+UVA ≈ O$_3$+TiO$_2$. For initial concentrations < 50 µg L^{-1} competition between direct OZ and hydroxyl radical reactions.

Some previous work (Luong N. Nguyen *et al.*, 2013) refers the integration of membrane bioreactor (MBR) with UV oxidation or NF or RO as a way to considerably improve the removal of TrOC. While the MBR process acts as a remover of the hydrophobic and readily biodegradable TrOC, the complementing techniques have good performance removing on

hydrophilic and biologically persistent contaminants. The MBR was laboratory-scale and was composed by a glass reactor and a hollow membrane module (PVDF) that was submerged. It was seeded with activated sludge from a WWT plant and air was supplied during the operation of 196 days. The UV oxidation system consisted on a reactor and a low-pressure mercury lamp and operated for two hours. The total UV energy output emitted at 254 nm was 83 W during 7.5 min of operation. The crossflow membrane laboratory-scale filtration system was operated with flat sheet membranes NF270 (NF) and BW30 (RO). The approximate removal efficiency of this integration attempts were available for DCF: MBR itself has 17%; UV oxidation itself has 95%; hybrid MBR-UV has 96%; hybrid MBR-NF 270 has 97% and hybrid MBR-RO has 99%.

There were not found studies in which the simultaneous removal of SMX and DCF by AOP or Membrane Separation Processes was performed.

4. Materials and Methods

In this chapter all the materials and methods that were used during the development of the scientific activities in the scope of this study are presented. Several reagents were used, as well as membranes for the Nanofiltration and catalysts for the Ozonation. All the experimental procedures carried out, including the analytical techniques, are also described in this chapter.

4.1 Chemicals and Materials

The origin, preparation and utilisation of the most relevant chemicals and materials are described in the following sections.

4.1.1 Chemicals and Reagents

The two main reagents performing this research are the Active Pharmaceutical Ingredients (APIs) that were used to simulate a wastewater containing emerging contaminants: Sulfamethoxazole (SMX) and Diclofenac (DCF) (**Table 7**). Both compounds were stored on a fridge at the approximate temperature of 5ºC.

Table 7 – Relevant properties and data of the active pharmaceutical ingredients on the scope of this study (Active Pharmaceutical Ingredients Database, 2011).

Properties	Sulfamethoxazole (SMX)	Diclofenac (DCF)
Molecular weight	253.27764 g mol^{-1}	296.148 g mol^{-1}
Molecular formula	$C_{10}H_{11}N_3O_3S$	$C_{14}H_{11}Cl_2NO_2$
CAS-Number	723-46-6	15307-85-5
Medical use	Antibiotic	Non-steroidal anti-inflammatory and analgesic
Manufacturer	Alfa Aesar (J66565)	Acros Organic (445250100)

There were several chemical reagents that were used as auxiliary on the experiments, from which the more important are on **Table 8**.

Table 8 – List of important chemicals used.

Name (Chemical Formula)	Characteristics	CAS-Number	Manufacturer (Product Code)
Sodium chloride (NaCl)	Refined and centrifuged	7647-14-5	José M. Vaz Pereira, S.A. (2826)
Sodium hydroxide (NaOH)	Microbeads	1310-73-2	Cmd Chemicals
Sulphuric acid (H_2SO_4)	96%	7664-93-9	Panreac (211058.1214)
Hydrogen peroxide (H_2O_2)	33% w/v	7722-84-1	Panreac (211077.1214)
Sodium phosphate dibasic (Na_2HPO_4)	99,95% trace metals basic	7558-79-4	Sigma-Aldrich (255793)
Sodium phosphate monobasic monohydrate (NaH_2PO_4)	ACS reagent, ≥98%	10049-21-5	Sigma-Aldrich (S9638)
Ortho-Phosphoric acid	85%	7664-38-2	Fluka (79620)
Oxygen (O_2)	Pressurized, >99,9%	7782-44-7	Praxair

The solutions were prepared with distilled water from the equipment Autostill 4000X.

The more important reagents which were used to perform the analytical techniques are designated along with their description (chapter **4.3 Analytical methods**).

4.1.2 Membrane

The membrane used on the Nanofiltration equipment was a TS-80 manufactured by TriSep®, which has 140 cm^2 of filtration area.The choice of this membrane took into account previous studies in which membranes with similar properties proved to be effective on the contaminants removal (Quintanilla, 2010).

The membrane is a polyamide-urea composite, so polyamide is its main material of construction. Its MWCO is 150 g mol^{-1}.

The working pH of this membrane should be between 2 and 11 (Sterlitech Corporation, 2013) to avoid its damage. This membrane has decreasing (and negative) zeta potential with increasing pH, as shown on **Figure 4**.
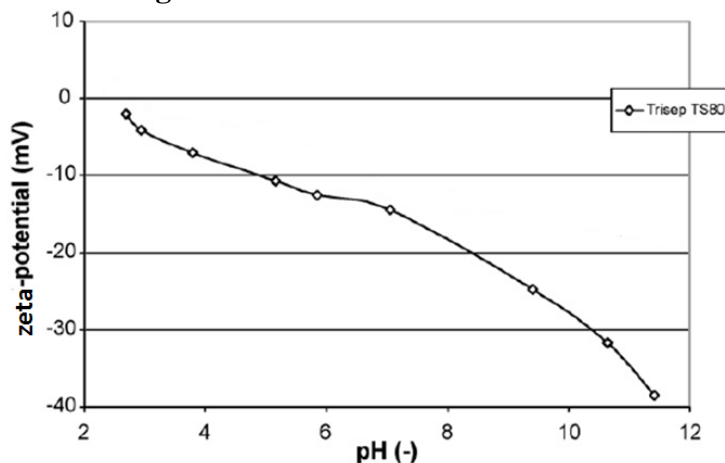
Figure 4 – Zeta potential representation of the TS-80 membrane as a function of the pH of the feed water (adapted from Verliefde *et al*., 2008).

4.1.3 Catalysts

Two different catalysts were used during some of the Ozonation trials: Mn-Ce-O and N-150. The choice of these catalysts lies on the fact that both of them can increase the biodegradability of a simulated phenolic wastewater (Martins and Quinta-Ferreira, 2011). Therefore, the efficiency of both materials for the abatement of the above mentioned APIs can be foreseen. Before being employed, they were processed in different manners.

Catalyst Mn-Ce-O

The Mn-Ce-O is a laboratory-made catalyst prepared by the co-precipitation of the nitrate precursors with a molar ration between Mn/Ce of 70/30. Before use, it was firstly calcined at 300 ºC during 2 h and afterwards powdered to ensure that a chemical regime was kept on the reactor.

Catalyst N-150

The N-150 is a commercial catalyst that has Fe-Mn-O in its composition; according to the manufacturer information, it consists of Fe_2O_3 (60%) and MnO_x (30%) (weight percentages). It was acquired from Clariant Catalysts (Japan) and was received in cylindrical pellets. It was powdered before its use to ensure that a chemical regime was kept on the reactor.

4.2   Experimental Procedures

In this section, the way the Nanofiltration and Ozonation were operated is briefly described. The feed for most of the trials had certain characteristics which are detailed on **Table 9**. The initial trials were performed using the synthetic effluent (prepared with distilled water and 30 mg L^{-1} of each of the pollutants), while the experiments involved in the integration of the processes were done with the effect of the matrix was analysed and for that the pollutants were dissolved in natural water (coming from Mondego river).

Table 9 – Characteristics of the effluent used in most of the experiments.

	Synthetic effluent	Natural water effluent
Dissolution media	Distilled water	Filtered water from river Mondego
Sulfametoxazole concentration (mg L^{-1})	30	30
Diclofenac concentration (mg L^{-1})	30	30
pH	5.5 ± 1	6.9 ± 1
COD (mg L^{-1})	80 ± 10	85 ± 10

The COD values for the synthetic effluent are expectable considering the theoretical COD values calculated considering an aqueous solution containing 30 mg L^{-1} of each component (35.31 mg O_2 L^{-1} for SMX and 30.20 mg O_2 L^{-1} for DCF). The Natural water effluent, as expectable, has higher COD due to the presence of organic matter on the river stream.

The complete dissolution of the compounds in the dissolution media was achieved by using ultrasound equipment UltrasonicsMedi III, JP SELECTA®.

All the weighting was done with a Radwag AS 220/C/2 lab scale.

4.2.1 Nanofiltration

The Nanofiltration experiments were carried out in a flat-sheet laboratory-scale (SEPA CF II, Osmonics), crossflow membrane filtration equipment. Besides the membrane module, there is a reservoir, a diaphragm pump, valves and sensors (**Figure 5**).

The process was operated in batch mode, since the retentate and the permeate returned to the feed reservoir. The feed reservoir temperature was approximately at 20°C and

contained at least 2.5 L. The layout of the equipment in the laboratory is presented in the **Figure 6**.
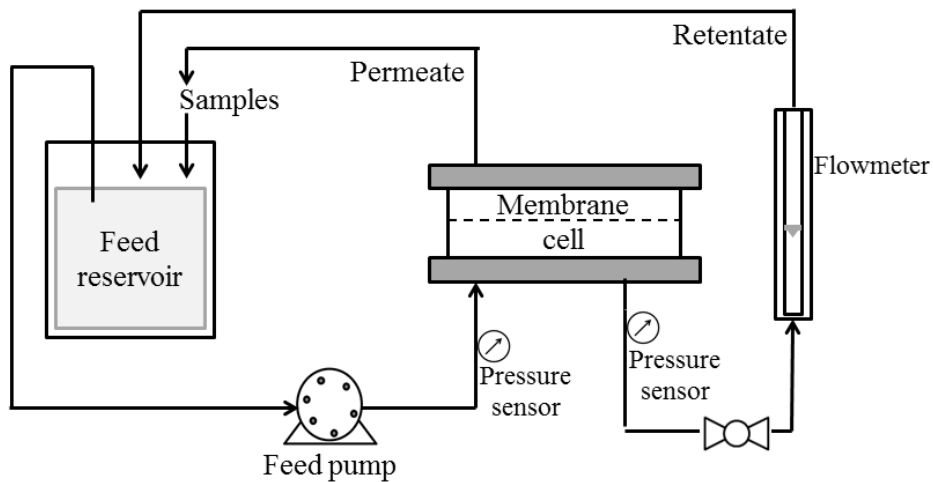
Figure 5 – Experimental scheme of Nanofiltration equipment.
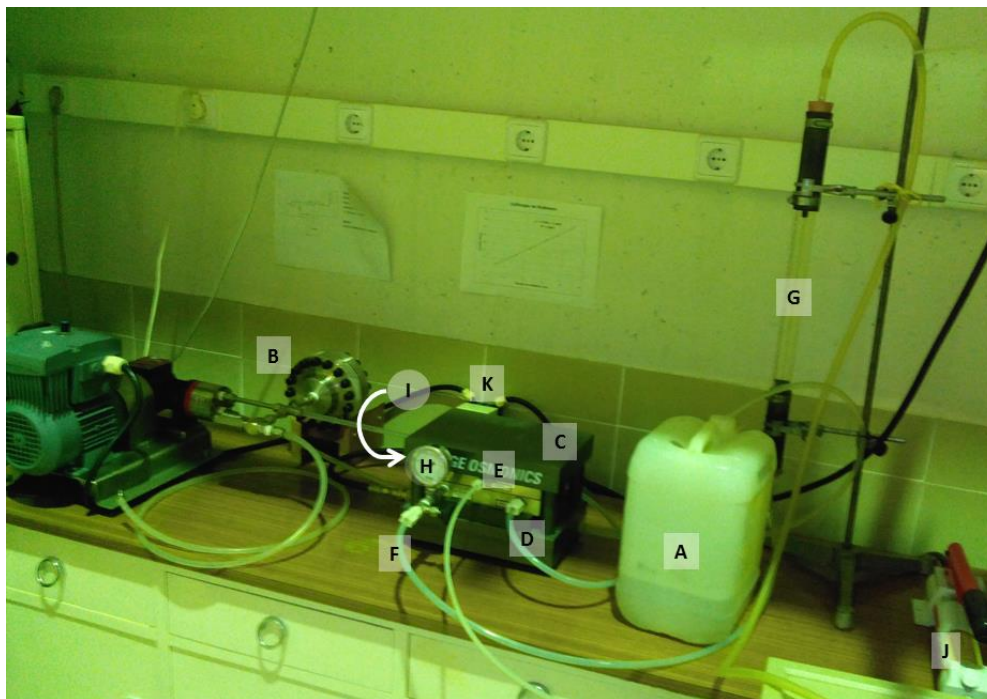
Figure 6 – Layout of the Nanofiltration equipment in the laboratory.
A – feed reservoir; B – feed pump; C – membrane cell; D – feed inlet; E – permeate outlet; F – retentate outlet; G – flowmeter for the retentate; H – pressure sensor for the retentate; I – concentrate valve control; J – hydraulic pump to pressurize the membrane; K – power supply for feed pump.

Several trials were done using the Nanofiltration equipment with different objectives. The data collected during the trial itself was complemented with data coming from analysis (examples: **COD**, **HPLC**) that are exploited on the chapter **4.3 Analytical Methods**.

In order to characterize the membrane, the experiments presented on **Table 10** were performed. These experiments involved the filtration of distilled water, aqueous solutions of sodium chloride (NaCl) and xylose at different pressure drops.

Table 10 – Experiments performed with the aim of characterizing the membrane.

Aim of experience	Conditions	Studied variables	Code
Determination of membrane permeability	Distilled water ΔP= 3, 4, 6, 8, 12, 16, 18 bar	J_v (m^3 m^{-2} s^{-1}) vs ΔP	N1
Determination of mass transfer coefficient for NaCl	C_{NaCl}=0,1M ΔP=10 bar	$J_{v,NaCl}$(m^3 m^{-2} s^{-1}) vs t C_p vs t Retention% vs t	N2A
Determination of steady state achievement time	C_{NaCl}=0,1M ΔP=18 bar	$J_{v,NaCl}$ (m^3 m^{-2} s^{-1}) vs t C_p vs t Retention% vs t	N2B
Determination of the pores' diameter	C_{xylose}=127 mg L^{-1} ΔP= 3, 4, 6, 8, 12, 16, 18 bar	C_p vs ΔP (attempt) Retention% vs ΔP (attempt)	N3

The experiments developed to access the effect of the initial pH of the solution containing emerging contaminants are presented on **Table 11**. The effect of the feed's pH on the retention of the contaminants and permeate flux was studied as a function of the applied pressure. The range of pH used took into account the characteristics of the membrane, trying to avoid its damage (the pH used should be between 2 and 11). On these experiments, aqueous solutions containing 30 mg L^{-1} of SMX and 30 mg L^{-1} of DCF with different pH were used in the Nanofiltration equipment. The pH was adjusted with concentrated hydrochloric acid (HCl) and sodium hydroxide (NaOH) aqueous solutions. After every trial, the membrane was washed and the permeate flux with distilled water was evaluated to make sure the membrane did not have fouling. Distilled water was used to wash the membrane between the experiments and 15 minutes passed before every sample of permeate was taken, in order to stabilize the system.

Table 11 – Experiments performed with the aim of the analysis of the initial pH of the filtrated solution.

Conditions	Studied variables	Code
SMX 30 mg L^{-1} + DCF 30 mg L^{-1} ΔP= 3, 4, 5, 7, 10, 14, 18 bar pH = 5.5 (natural)	J_v (m^3 m^{-2} s^{-1}) vs ΔP COD vs ΔP Retention% (COD) vs ΔP HPLC vs ΔP Retention% (HPLC) vs ΔP	N5A1
SMX 30 mg L^{-1} + DCF 30 mg L^{-1} ΔP= 10 bar pH = 4.0 (HCl)	J_v (m^3 m^{-2} s^{-1}) vs ΔP COD vs ΔP Retention% (COD) vs ΔP HPLC vs ΔP Retention% (HPLC) vs ΔP	N5B1
SMX 30 mg L^{-1} + DCF 30 mg L^{-1} ΔP= 3, 4, 5, 7, 10, 14, 18 bar pH = 3.1 (HCl)	J_v (m^3 m^{-2} s^{-1}) vs ΔP COD vs ΔP Retention% (COD) vs ΔP HPLC vs ΔP Retention% (HPLC) vs ΔP	N5C1
SMX 30 mg L^{-1} + DCF 30 mg L^{-1} ΔP= 10 bar pH = 7.2 (NaOH)	J_v (m^3 m^{-2} s^{-1}) vs ΔP COD vs ΔP Retention% (COD) vs ΔP HPLC vs ΔP Retention% (HPLC) vs ΔP	N5D1
SMX 30 mg L^{-1} + DCF 30 mg L^{-1} ΔP = 3, 4, 5, 7, 10, 14, 18 bar pH = 10.0 (NaOH)	J_v (m^3 m^{-2} s^{-1}) vs ΔP COD vs ΔP Retention% (COD) vs ΔP HPLC vs ΔP Retention% (HPLC) vs ΔP	N5E1
SMX 30 mg L^{-1} + DCF 30 mg L^{-1} ΔP= 10 bar pH = 3.1; 4.0; 5.9; 6.9; 8.0; 8.9; 9.6.	J_v (m^3 m^{-2} s^{-1}) vs ΔP COD vs ΔP Retention% (COD) vs ΔP HPLC vs ΔP Retention% (HPLC) vs ΔP	N5F1

Another experience was performed to evaluate the effect of the Natural Water on the Nanofiltration process. On this experience 30 mg L^{-1} of SMX and 30 mg L^{-1} of DCF were dissolved in filtered water from the river. The equipment was operated in a range of pressure drops – ΔP = 3, 4, 5, 7, 10, 14, 18 bar – and the pH was adjusted to 7.

There were also some experiments that aimed to evaluate the membrane fouling (**Table I.1, Appendix I**).

In what concerns the process integration, two Nanofiltration trials were done: one before Ozonation, which permeate would be used on Ozonation, and another in which the feed used was the product of the single Ozonation of the raw effluents. As it was already referred, the experiments involved in the integration of the process started with the filtered water from the river that was used as a dissolution media for 30 mg L^{-1} of SMX and 30 mg L^{-1} of DCF. It was decided that the Nanofiltration would be done with pH = 7, since it is a normal pH for wastewater treatment processes and showed interesting results on the previous trials. Therefore, the pH was adjusted to 7 before all the trials (after Ozonation and before Ozonation). For each trial, a range of pressure drops was tested (ΔP = 3, 4, 5, 7, 10, 14, 18 bar). On the trial that preceded Ozonation, the permeate that was afterwards subjected to Ozonation, was collected under the pressure drop of 7 bar, since it had shown good results on the previous trials.

4.2.2 Ozonation

To perform the Ozonation a batch reactor of 500 mL was used. The ozone was produced *in situ* by an Ozone generator (802N, BMT) that was fed by pure oxygen (99,9%) supplied by Praxair. There was a gas ozone measurer (BMT 963 vent, BMT) which determined the ozone concentration produced by the ozone generator. This concentration was the same entering the reactor, which is designated by $C_{O3,in}$. It was also possible to measure the ozone exiting the reactor ($C_{O3,out}$) by changing the positions in a valve system. To ensure chemical regime into the reactor, it was agitated at the approximate speed of 300 rpm with the help of a magnetic stirrer (Agimatic-N, P Selecta®). The experimental scheme is presented in **Figure 7,** while the layout of the equipment in the laboratory is presented in the **Figure 8**.
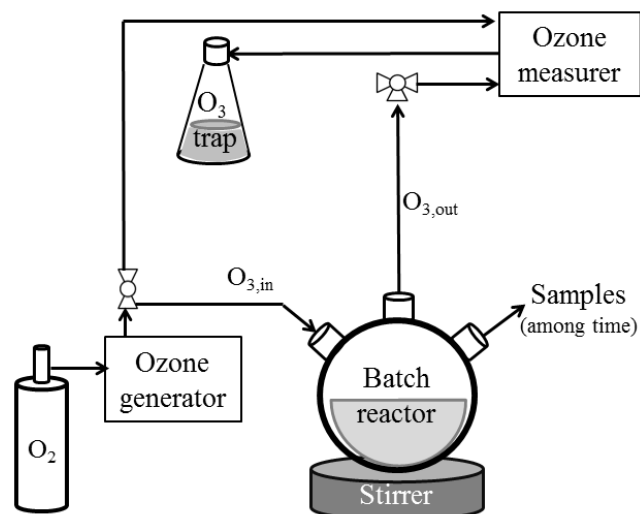
Figure 7 – Schematic representation of the Ozonation equipment.
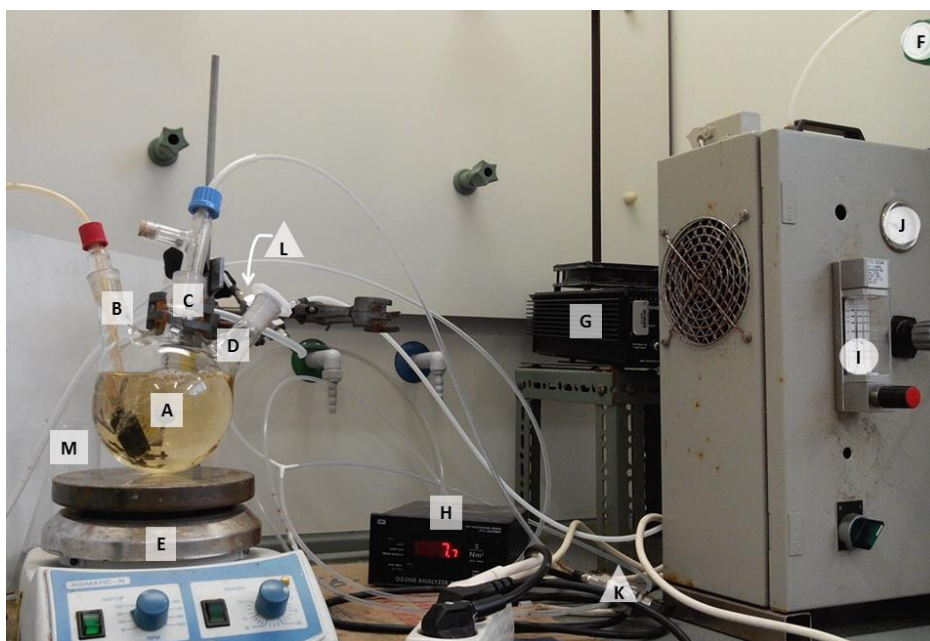
Figure 8 – Layout of the Ozonation equipment in the laboratory.
A – batch reactor; B – ozone inlet with air diffusor stone; C – ozone outlet; D – orifice for sample collection; E – stirring plate; F – oxygen supply; G – ozone generator; H – ozone measurer; I – flowmeter for gas supply; J – manometer for gas supply; K and L – valves; M – ozone trap.

Several trials were done in the Ozonation equipment in order to find out which reaction conditions would be the most effective (**Table 12**). The data and samples collected during the trial itself were complemented with data coming from the analysis of the samples, as **pH**, **Spectroscopy UV-Vis** (for hydrogen peroxide concentration, $[H_2O_2]$, determination), **COD** and **HPLC**. The procedures underlying these analyses are detailed on the chapter **4.3 Analytical Methods**.

Table 12 – Experiments performed with Ozonation before process integration.

Gas flow (L min^{-1})	C_{O3in} (g m^{-3})	pH	Catalyst	Catalyst concentration (g L^{-1})	[H_2O_2] g L^{-1}	Code
0.2	~10	7 (buffered)	None	0	0	O1
0.2	~10	7 (buffered)	N-150	1	0	O2
0.2	~10	7 (buffered)	Mn-Ce-O	1	0	O3
0.2	~10	pH_0=7	N-150	1	0	O4
0.2	~10	pH_0=7	Mn-Ce-O	1	0	O5
0.2	~10	~7 (adjusted manually with NaOH)	Mn-Ce-O	1	0	O6
0.2	~10	7 (buffered)	None	0	12 injections of 8.6µl of a solution with 82.5 g L^{-1}	O7
0.2	~10	7 (buffered)	Mn-Ce-O	1	12 injections of 8.6µl of a solution with 82.5 g L^{-1}	O8

In all the trials in which **Table 12** indicates that the pH was buffered, this parameter was set at 7 with 1.44 g L^{-1} of disodium phosphate (Na_2HPO_4) and 0.24 g L^{-1} of monosodium phosphate (NaH_2PO_4). The pH was, afterwards, adjusted to be around 7 with phosphoric acid (H_3PO_4) to be within the conventional range of pH in wastewater treatment processes (6.5 - 7.5).

During the experiments, different variables were controlled, according to the reactions' characteristics (**Table II.1, Appendix II**).

When the trials involved a catalyst, the reaction media (and, consequently, the collected samples) had suspended catalyst. Therefore, each sample collected was centrifuged in falcon plastic tubes using the centrifuge Nahita 2655. Afterwards, the samples were filtered and the remaining solid was dried in an oven from Memmert for further analysis.

An additional trial was performed to evaluate the effect of the Natural Water on the Ozonation. On this experience 30 mg L^{-1} of SMX and 30 mg L^{-1} of DCF were dissolved in filtered water from the river and submitted to simple Ozonation. The gas flow was kept constant at the value 0.2 L min^{-1} and the initial ozone concentration, $C_{O3,in}$, was around 10 g m^{-3}.

In what concerns the process integration, it would be expectable to make the Ozonation with the experimental conditions that showed the best results. However, it was decided that the Ozonation would be without catalyst. This decision took into account that the powdered catalyst could interfere in the Nanofiltration process with which Ozonation was being integrated. The pH was never buffered or altered taking into account the same reason. On all trials the gas flow was kept constant at the value 0.2 L min^{-1}. The $C_{O3,in}$ was kept around 10 g m^{-3}. As it was already referred, the experiments involved in the integration of the process

were performed with natural water (filtered water from the river was used as a dissolution media for 30 mg L^{-1} of SMX and 30 mg L^{-1} of DCF).

When the sequence Ozonation – Nanofiltration was being tested, it was necessary to perform six Ozonation trials before Nanofiltration, in order to have enough feed volume for this equipment. Regarding the Nanofiltration – Ozonation sequence, 500 mL of Nanofiltration permeate was collected for ideal conditions and it was subjected to Ozonation under the above described conditions.

4.3   Analytical Methods

Several analytical techniques were fulfilled in order to either characterize the materials involved in Nanofiltration and Ozonation either to find out details about liquid samples that resulted from these two processes.

4.3.1 Membrane and catalysts

On this chapter, four different methods are presented, from which one (**AFM**) was used on the Nanofiltration's membrane and the remaining three (**BET**, **Mercury porosimetry** and **Elemental analysis**) were applied to characterize the catalysts used in Ozonation.

AFM

Atomic Force Microscopy (AFM) analysis was applied to compare the virgin and used membranes using a nanometric tip which evaluated the surface's topography. Due to the characteristics of the Nanofiltration membrane, since polyamide is a soft material, the method used was semicontact with a NSG10 tip. The radiant frequency was 285 kHz. The sample was placed in a sapphire holder. The equipment was placed over an anti-vibrational table (Accurion).

A 5 µm x 5 µm and a 1 µm x 1 µm surface topography were done for both the virgin and used membrane (~ 40 hours of operation). The roughness was also evaluated using the AFM software for both samples. Moreover, the porosity was evaluated for the virgin membrane.

BET

Brunaurer-Emmett-Teller (BET) method aims to describe the physical adsorption of gas molecules to a solid surface. This technique can be used to measure the specific surface area and to draw BET adsorption and desorption isotherms of the catalyst. This determination was performed using nitrogen (-196 ºC) with an accelerated surface area and porosimetry analyser (ASAP 2000, Micromeritics) (Brunauer *et al.*, 1938).

Mercury porosimetry

The Mercury (Hg) porosimetry consists on the intrusion of mercury (which is a non-wetting liquid) into a material with a porosimeter at high pressure. Using the Poresizer 9320 (Micromeritics), it was possible to determine the catalyst pore size distribution and porosity. To exemplify, the pore size is obtained by comparing the external pressure that is applied to the liquid to force it into the pores of the material with the force of the surface tension of the liquid that is opposite.

Elemental Analysis

The elemental analysis, when quantitative, allows one to know the weight percentage of a certain element which is in a sample. This analysis was done to the catalysts before and after the Ozonation reactions and enabled to know the mass percentage of nitrogen (N), carbon (C), hydrogen (H) and sulphur (S) in each sample.

This determination was performed with a Fisons Instruments EA 1108 1108 CHNS-O.

4.3.2 Liquid samples

Several analytical techniques were used to analyse the liquid samples that were generated during the experiments. It is necessary to highlight the **COD** and the **HPLC**, since these techniques were broadly employed and applied to the majority of the samples.

COD

Chemical Oxygen Demand (COD) can be determined by the Potassium dichromate method. In this procedure the potassium dichromate ($K_2Cr_2O_7$) is used as an oxidizer of the organic matter under acidic conditions (sulphuric acid) and with a catalyst (silver sulphate). To perform the analysis, it is necessary to use: (1) potassium dichromate solution (digestion solution) for the range 5-100 mg L^{-1}, which contains 4 x 10^{-3} M of potassium dichromate, 25 g L-1 of mercury (II) sulphate ($HgSO_4$) and 125 g L^{-1} of sulphuric acid (H_2SO_4); and (2) acidic solution, which is a silver sulphate ($AgSO_4$) solution of 10 g L^{-1} in sulphuric acid.

For each solution to be analysed two vials were prepared containing each 2.5 mL of sample, 1.5 mL of the digestion solution and 3.5 mL of acidic solution. For each trial, two blanck vials containing 2.5 mL of distilled water instead of the sample were prepared according to the same procedure. Each tube was slightly agitated and placed at a thermo-reactor (Eco 25 from VELP Scientifica) at 150ºC for 120 minutes. Later on, the absorbance of at 445 nm was measured using a Photolab S6 photometer from WTW. For each pair of vials the values were compared and if they were uneven the measurements were repeated.

The amount of Cr^{3+} which is measured in the end of the experiment is and indirect indicator of the organic contents on the sample. On this specific procedure (due to the low

range of COD of the samples), the dichromate that is consumed from experience to experience is measured.

The procedure is described by ISO 6060 which is adequate for concentrations between 30 and 700 mg/L, but preferably from 300 to 600 mg/L. For lower concentrations of solute, compared to the ones normally used, it is necessary to make a new calibration curve.

A calibration curve was prepared by the determination of the absorbance corresponding to samples with known COD that were under this procedure (**Appendix III – COD – Calibration curve**).

It is important to refer that the COD measurement is affected by the presence of hydrogen peroxide on the liquid samples. Therefore, on the trials in which this reagent was used, some droplets of a 100 mg L^{-1} solution of catalase from bovine liver (Sigma Life Science, Sigma-Aldrich, C9322-1G) was added to the all the samples, including the distilled water (guaranteeing that the catalase concentration was equal in all the samples). Furthermore, 0-100 ppm H_2O_2 Test Strips (Indigo Instruments) were used to ensure there was no remaining hydrogen peroxide on the samples.

HPLC

The High Performance Liquid Chromatography (HPLC) method allows one to know which compounds are present on an aqueous solution and their corresponding quantity. In this method the components of a mixture are separated using a pressurized eluent that drags the sample through a column filled with an adsorbent material. Since each component of the sample interacts in a different manner with the solid, those will be separated while they flow out the column.

The equipment used is composed by an auto-sampler, a high pressure pump, an UV detector and a degasser from KNAUER and a C18 chromatographic column with a stove from Scansci. The detector is connected to a computer where the software Borwin is used to process the data. The HPLC conditions were optimized in order to detect both contaminants on the scope of this study (SMX and DCF) in the same analysis. After several steps of optimization (described on **Appendix III – HPLC – Eluent optimization**), it was settled that the mobile phase would be acetonitrile and water at a 40:60 volume ratio, acidified at pH 3 by the addition of phosphoric, the UV detector should be settled for a 270 nm wavelength (Dantas *et al.*, 2008), the set-point temperature of column should be 50ºC and the retention time should be 30 min.

Under these conditions, a calibration curve for SMX and DCF was built by analysing the peak areas with solutions containing known concentrations of both compounds (**Figure III.2**). The peak areas of the graphics built in Borwin were always calculated by using the internal function "Search Peaks" that the program provides. More information regarding the HPLC graphics is presented on **Appendix III (HPLC – Eluent optimization)**. This method has a limit of detection of 0.3 mg L^{-1}.

There were also several attempts to detect xylose with the HPLC, but it was not possible.

The acetonitrile from Chem-Lab used for the preparation of the eluent had HPLC grade (more than 99.9% purity) and the ortho-phosphoric acid from Fluka was 85%. The solution was always prepared with distilled water.

Spectroscopy UV-Vis

This colorimetric method was used on an attempt to detect the concentration of different compounds in aqueous solutions. Four methodologies for samples' preparation were used for the UV-Vis analysis: (1) direct analysis of the sample; (2) Dinitrosalicylic acid (DNS) method; (3) DNS modified method and (4) hydrogen peroxide concentration. It is important to refer that different cells, quartz and plastic, were used for UV and visible spectrum, respectively.

The first three methods were used as an attempt to determinate the xylose concentration in aqueous solutions. These methods are effective to determinate glucose concentrations, but they showed not to be effective for xylose. Their description can be found on **Appendix III – Spectroscopy UV-Vis**. Finally, the fourth method was used effectively to determine the hydrogen peroxide concentration on samples coming from Ozonation reactions. An ammonium metavanadate (6.2 $mmolL^{-1}$) and sulphuric acid (0.058 mol L^{-1}) solution was prepared. After, the absorption at 450 nm of 1 mL of sample and 1mL of the solution was measured (Nogueira *et al.*, 2005).

The analyses were performed using a T50 Spectrophotometer from PG Instruments Limited.

Atomic Absorption Spectroscopy

The Atomic Absorption Spectroscopy was used to analyse liquid samples from the reaction media of catalytic Ozonation in order to quantify the amount of active metal leached during the process. Having as basic principle the fact that free atoms in stable state can absorb light in a certain and unique wavelength, this method enables to detect and quantify certain chemical elements of interest. The analyses were carried on in a spectrometer Perkin-Elmer3300.

Luminescent bacteria test

This method is used to determine the toxicity of the effluent in order to decide its impact on the ecosystems. *Vibrio fischeri* is a very sensible marine bacteria that normally emits light. When subjected to the effluent, if it is toxic, the microorganism light emission capacity will be diminished. Therefore, the toxicity can be measured based on the difference on the luminescence before and after the bacteria being in contact with the pollutant mixture. This method was used to determine the EC_{20} and, when possible, the EC_{50} of some samples.

The experimental procedure underlying this technique is described on ISO 11348 – Part 2, since liquid-dried bacteria (lyophilized) were used. To use this method, the bacteria are unfrozen and introduced in a commercial glycose solution. Basically, several dilutions of the potentially toxic sample are made with a 2% NaCl solution and the different resulting solutions are added to the bacteria in the culture media. The pH of the sample is previously adjusted to the range 6.5 – 7 to ensure the measurement is not affected by its value. The luminescence for each mixture is measured in comparison to the same parameter for the bacteria in the culture media itself.

To perform this procedure, a LUMISTherm and a LUMIStox with the software LUMIStox 300 (version 4.00) from Hach-LANGE were used. The 2% NaCl solution to use in the dilutions was prepared from a standard solution of 7.5% (LUMIStox). The luminous bacteria kit used was LCK 480.

Conductivity

The conductivity was measured by the equipment Hanna Instruments 2550, using the conductivity cell HI 76312, which has platinum and is a 4-ring potentiometric probe (2 current electrodes and 2 voltage electrodes) with a temperature sensor. Known concentration NaCl solutions were prepared to trace a calibration curve for this equipment.

pH

The equipment Crison micro pH 2002 in conjunction with a glass electrode was used for pH measurements. The pH was also measured by the equipment Hanna Instruments 2550, using the pH cell HI 10430, which has a single ceramic junction and a pH and temperature sensor. The calibration of both equipment was frequently done using the buffer solutions from Scharlau SO2070 for pH = 7 and SO2040 for pH = 4.

5. Results and Discussion

On this chapter, some results of the executed experiments are complemented with the results of the analytical techniques performed in order to discuss and justify them scientifically.

5.1   Nanofiltration

The Nanofiltration experiments were performed in three different stages. First, some experiments were done in order to characterize the membrane. Then, some trials involving the two emerging contaminants in the scope of this study (SMX and DCF) were carried out. Along with these two stages, the fouling caused in the membrane was analysed.

5.1.1 Membrane characterization

To better understand the results obtained in further activities, it was important to wage some time on characterizing the membrane. Three different parameters are crucial to comprehend membrane processes: the membrane permeability, the mass transfer coefficient and the membrane pore size.

Determination of membrane permeability

To assess the membrane permeability, the permeate mass flow (m^3 s^{-1}) was measured at various pressure differences with the help of a chronometer and a beaker. Taking into consideration the flowrate of 9.60 mL s^{-1} given by the rotameter, and the membrane area, 140 cm^2, it was possible to calculate the flux, $J_v(m^3 m^{-2} s^{-1})$. To calculate the membrane permeability, L_p, the equation 2.2 was fitted to the experimental data using the least squares method (**Figure 9**). The water viscosity was considered to be 1.0 x 10^{-8} bar s due to the water temperature (20ºC) registered *in loco* (Kestin *et al.*, 1978) and the effect of osmotic pressure, $\Delta\pi$, was neglected. Therefore, starting from equation (2.2), comes:

$$J_v = \frac{L_p}{\eta_0}(\Delta P - \Delta \pi) \quad \Rightarrow \quad J_v = \frac{L_p}{\eta_0}\Delta P \xrightarrow{\text{slope } (m) \text{ from regression}} m = \frac{L_p}{\eta_0} \quad \Rightarrow \quad L_p = m\,\eta_0$$
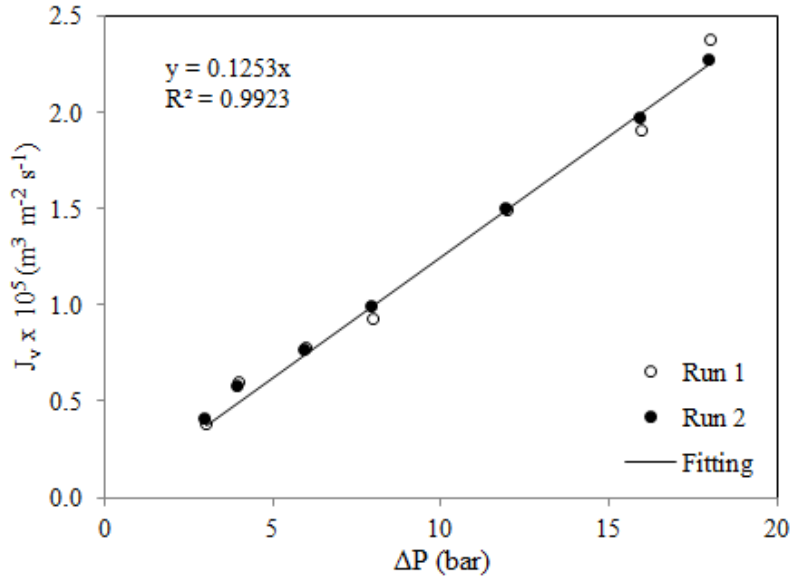
Figure 9 – Linear regression between flux (J_v) and pressure drop (ΔP) for two runs.

From the **Figure 9**, the results obtained for two runs result on the following regression, which gives the membrane permeability of $1.253 \times 10^{-14} \pm 5 \times 10^{-17}\ m$:

$$J_v = 1.253 \times 10^{-6}\ \Delta P \Rightarrow L_p = m\ \eta_0 \Leftrightarrow L_p = 1.253 \times 10^{-14}\ m.$$

This has the same order of magnitude for a desalination NF membrane (Desal 5K) of $1.253 \times 10^{-14}\ m$ (Gomes *et al.* 2010).

Mass transfer measurement

By operating with a sodium chloride (NaCl) solution and measuring the permeate flux, $J_{v,NaCl}$, and concentration of this salt when applying different pressures, it was possible to determine the mass transfer coefficient for this solute, $k_{f,NaCl}$. For this purpose, the steady-state values of flux and concentration of NaCl for $\Delta P = 10$ and 18 bar were used. Since it was not possible to obtain constant values on the steady-state, a flux value that can be considered steady (for every run, after 15 min) was used. The values of permeate flux for distilled water, J_{v,H_2O}, were obtained from the previous experiences.

The equation 2.3 was applied to determine the coefficient:

$$k_f = \frac{J_{v,NaCl}}{ln\left[\frac{\Delta P}{\pi_b - \pi_p}\left(1 - \frac{J_{v,NaCl}}{J_{v,H_2O}}\right)\right]} \tag{2.3}$$

resulting in a $k_{f,NaCl}$ of arround $2.85 \times 10^5\ m^3 m^{-2}\ s^{-1}$ (**Table 13**).

Table 13 – Data used to calculate the mass transfer coefficient.

ΔP (bar)	Salt Flux, $J_{v,NaCl}$ x 10^6 (m^3 m^{-2} s^{-1})	Water Flux, $J_{v,H2O}$ x 10^6 (m^3 m^{-2} s^{-1})	C_f (M)	C_p (M)	Osmotic pressure under bulk conditions, π_b (bar)	Osmotic pressure on the permeate, π_p (bar)	%Retention	Mass transfer coefficient, $k_{f,NaCl}$ x 10^{-5} (m^3 m^{-2} s^{-1})
10	.9.2	12.5	0.077	0.037	3.682	1.767	69.8%	2.749
18	17.7	22.6	0.076	0.030	3.639	1.422	65.2%	2.942
						Average mass transfer coefficient, $k_{f,NaCl}$ x 10^5		2.845

$RT = 0.08206 \ x \ 293 = 24.04358 \ L \ atm \ mol^{-1}$
$i = 2$

The mass transfer coefficient found for this membrane has the same order of magnitude of other values found in the literature for similar membranes: $k_{f,NaCl}(\Delta P = 10 \ bar) = 6.26 \times 10^{-5} \ m^3 m^{-2} \ s^{-1}$ for NF 90 and $k_{f,NaCl}(\Delta P = 20 \ bar) = 1.63 \times 10^{-5} \ m^3 m^{-2} \ s^{-1}$ for Desal 5 DK (Nghiem, 2005). The motive of the difference between the values lies in the fact that the membrane used is TS-80, which has different properties than the above mentioned membranes.

From the correlations that can be used to predict the mass transfer coefficient, three were considered: Grobber, Geraldes and Lévêque (equations 2.4, 2.5 and 2.6, respectively).

Being the Sherwood number, Sh, applied to this case, equal to:

$$Sh = \frac{k_{f,NaCl} \ d_h}{D_{salt,\infty}} \quad (2.7) \quad \Rightarrow \quad k_{f,NaCl} = \frac{D_{salt,\infty} \ Sh}{d_h}$$

it was possible to calculate the mass transfer coefficient for the salt using the three different correlations. The Geraldes correlation, given by $Sh = 0.142 \ Re^{0.46} Sc^{0.37}$, is the closer estimation to the average experimental values obtained: $k_{f,NaCl,Geraldes} = 1.74 \times 10^{-5} m^3 \ m^{-2} \ s^{-1}$ has a relative error of $1.10 \times 10^{-5} \ m^3 m^{-2} \ s^{-1}$.

Estimation of membrane pore size

The pore size of the membrane could be determined by operating the Nanofiltration equipment with a feed solution containing 127 mg L^{-1} of xylose. It would be possible to determine the pore size by analysing the effect of the pressure drop on the permeate concentration of xylose. To make this calculations it would be necessary to make iterative calculations with known values of the concentration of the permeate, C_p; the concentration of the feed, C_f; the radius of the solute, r_s, and the Stokes-Einstein coefficient, D_∞.

There were several attempts to evaluate the xylose concentration on the permeate. The method had to be sensible enough to make it possible to determine small differences between the concentrations of the solutions obtained under different pressure drops. All the methods used are described on the scope of the Analytical Methods (**4.2.2 Liquid Samples**). Several of the techniques tried were not effective to detect xylose: direct analysis of the sample on UV spectrum; direct analysis of the sample on Visible spectrum; HPLC of solutions;

dinitrosalicylic acid (DNS) method (that also involved UV-Vis analysis) and DNS modified method (that also involved UV-Vis analysis).

The COD was also attempted and, even though the presence of xylose was detected, the method was not sensible enough to create a concentration profile that would permit the application of the iterative method, since all the values determined were very close and did not have statistic tendency.

A last technique was supposed to be tried, which consisted in the derivatisation of the glycose and its identification with Gaseous Chromatography-Mass Spectroscopy (GS-MS) (Frias *et al.*, 2014). However, due to time and logistics limitations, it was not possible to perform it.

During the AFM analysis of the virgin membrane it was possible to observe some of its pores and use the software to obtain an approximate diameter (**Figure 10**).
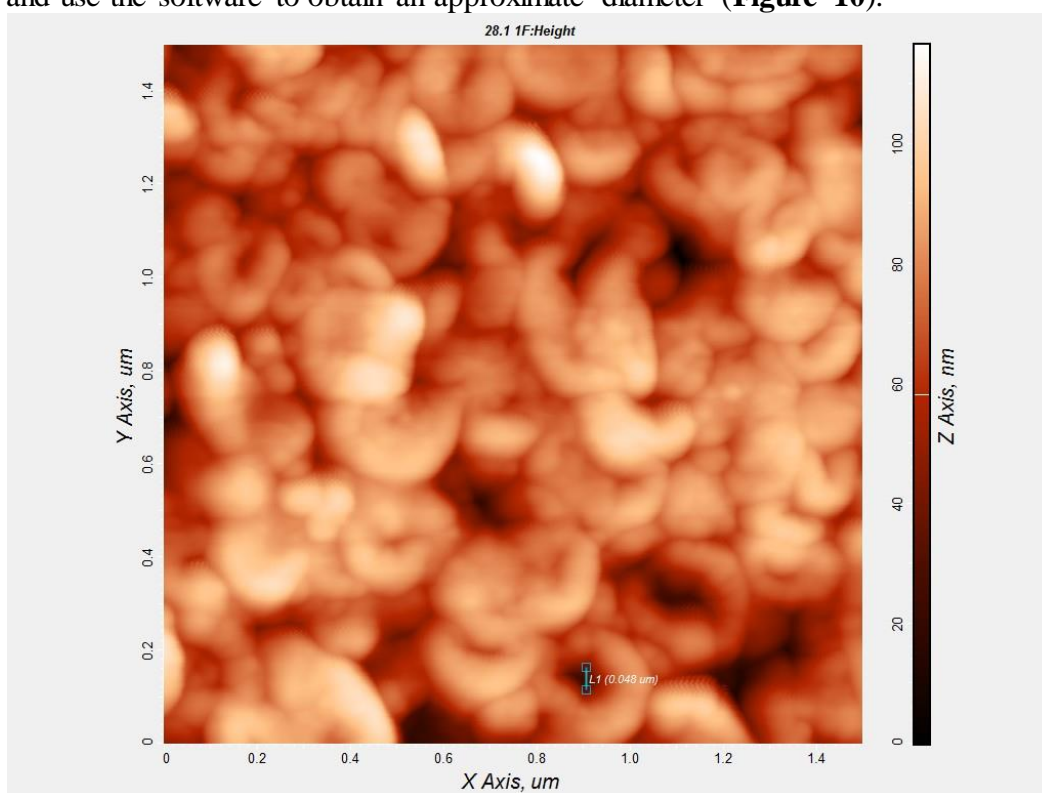

Figure 10 – AFM capture of the virgin membrane showing a 0.048 μm (48 nm) pore.

From the individual analysis of some pores, it was possible to assume that the average membrane pore diameter would be around 50 nm.

5.1.2 Nanofiltration of solutions containing emerging contaminants

Preliminary experiments performed on this equipment point out that the steady-state is achieved 15 min after operating under the same conditions (see **Figure 17**). Therefore, the permeate samples for analysis were taken after this stabilization period.

The Nanofiltration showed to be effective in the removal of SMX and DCF. The general effect of the Nanofiltration process can be observed on the **Figure 11**, in which the chromatograms obtained by HPLC of the feed (left) and of the permeate (right) are shown.

For both contaminants (SMX and DCF), the area of the concentration peaks diminishes after the filtration. This indicates that, when the aqueous solutions was filtered, a part of the contaminants was retained by the membrane, which resulted in a permeate with a smaller concentration of both contaminants (reduction from approximately 30 mg L^{-1} of each contaminant to 3 mg L^{-1} of SMX and 0.1 mg L^{-1} of DCF).

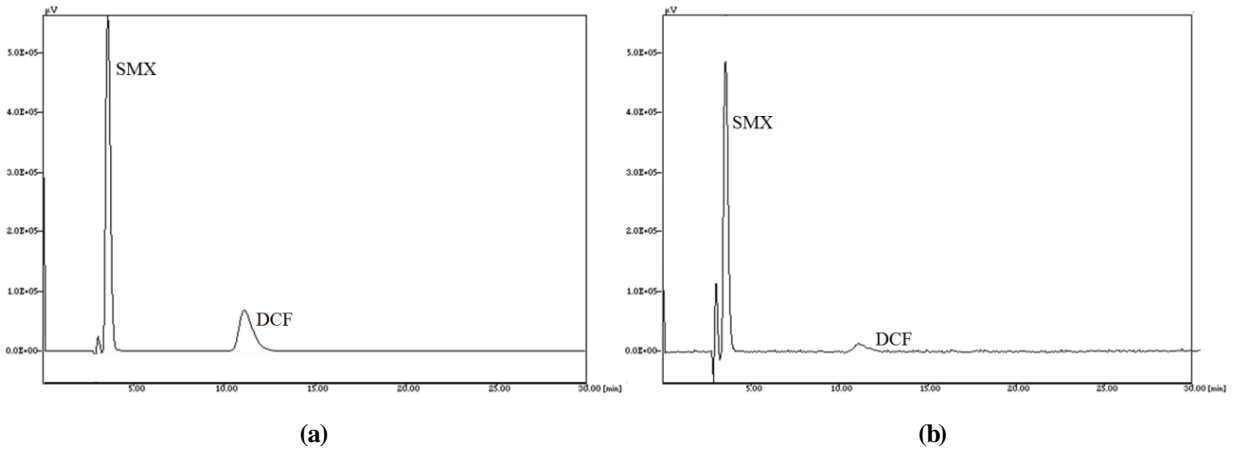| (a) | (b) |

Figure 11 – HPLC corresponding to the feed (a) and of the permeate (b) of a Nanofiltration process under pressure drop of 10 bar at natural pH (5.5).

Effect of initial pH

On this section, the effect of the feed's pH on the rejection of contaminants and permeate flux was studied as a function of applied pressure. On these experiments, aqueous solutions containing 30 mg L^{-1} of SMX and 30 mg L^{-1} of DCF with different pH values were used in the Nanofiltration process. Firstly, the effect of the pressure drop at different solution pH was analysed. Afterwards, the effect of the pH at constant pressure drop was studied.

The **Figure 12** shows the effect of the applied pressure on the global retention of the pollutants measured through the COD. The results for the natural pH of the solution (approximately 5.5), for an acidic pH and for a basic pH are presented.

The retention based on COD measurements is given by:

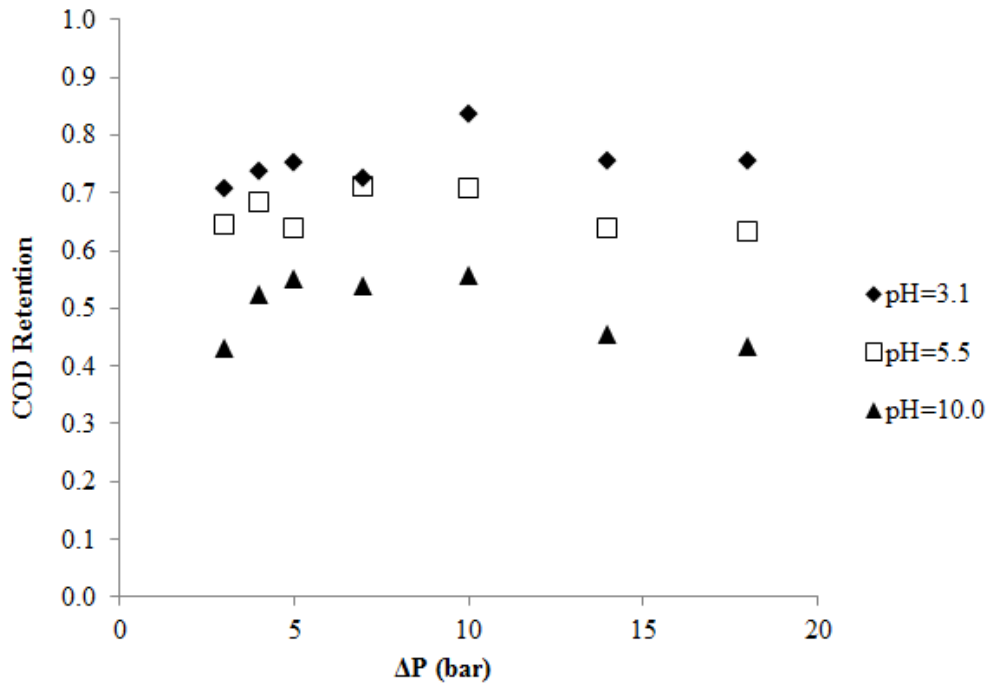$$Retention\ (COD) = 1 - \frac{COD_p}{COD_f} \qquad (2.8).$$

Figure 12 – Effect of the applied pressure on the global retention of the pollutants (COD) for different pH values.

This Figure shows that the retention of the pollutants is higher for lower pH. Moreover, it is possible to conclude that the pressure drop that allows a better retention is 10 bar.

The **Figure 12** can be complemented with the **Figure 13** in which the HPLC data are used to determine the retention for each pollutant and combined to present the global retention for the three different pH presented above (3.1, 5.5, 10.0).

The retention of a certain compound (ex: SMX) taking into account the concentration of the pollutant (ex: $[SMX]$) calculated by HPLC analysis is calculated according to the following (based on equation 2.10):

$$SMX\ Retention\ (HPLC) = 1 - \frac{[SMX]_p}{[SMX]_f} \qquad (5.1).$$

The global retention takes into account the concentration of SMX and DCF on the permeate and on the feed calculated by HPLC (based on equation 2.11):

$$Global\ Retention\ (HPLC) = 1 - \frac{[SMX]_p + [DCF]_p}{[SMX]_f + [DCF]_f} \qquad (5.2).$$
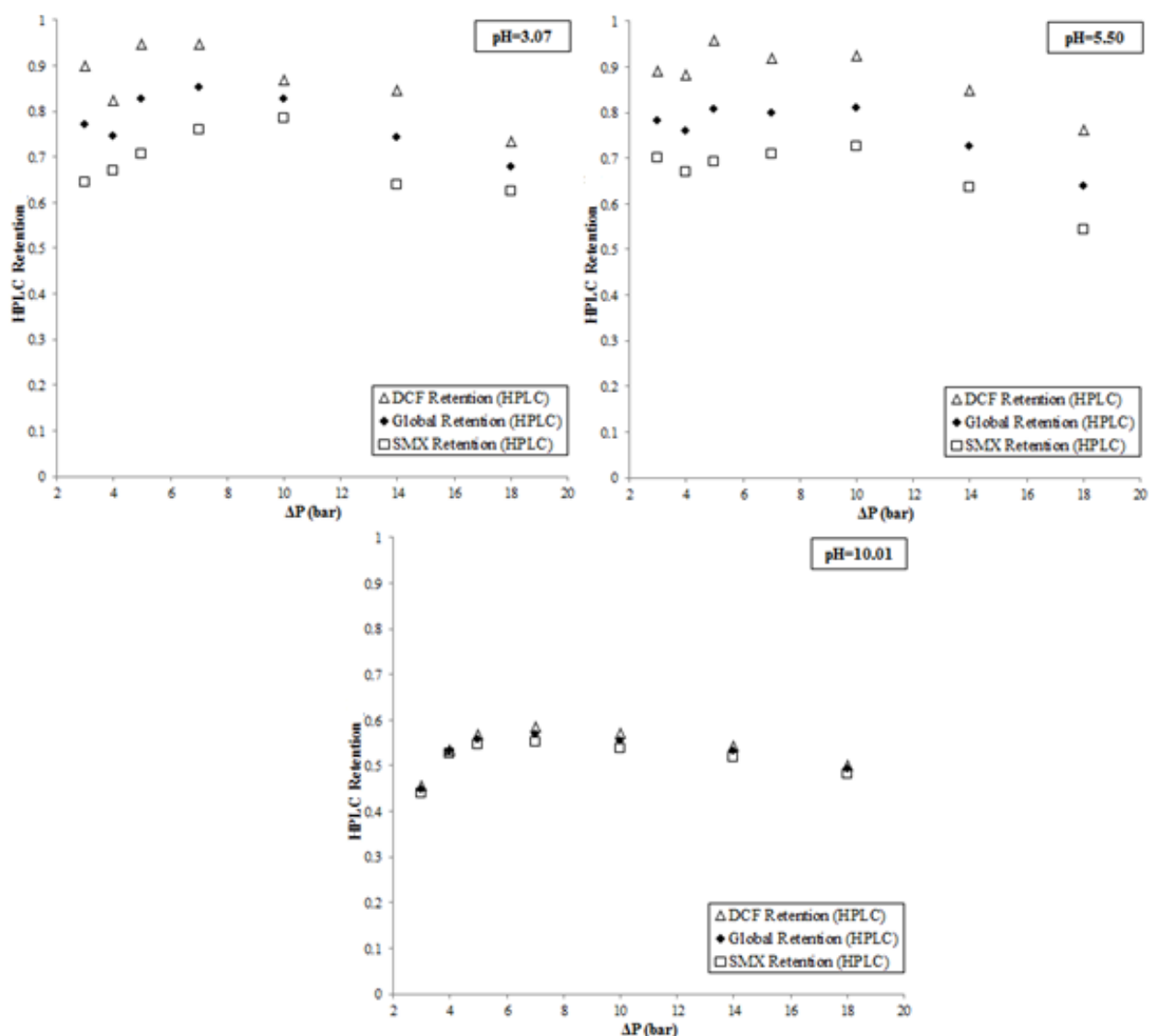
Figure 13 – Effect of the applied pressure on the partial and global retention of the pollutants for pH=3.07, pH=5.50 and pH=10.01.

This Figure indicates that the optimum pressure drop for the rejection of the pollutants should be between 5 and 10 bar.

Considering that the molar masses of the SMX and DCF are 253.277 and 296.148 g mol^{-1}, respectively, and that the MWCO of the membrane is 150 g mol^{-1}, it was expectable to observe a higher retention for DCF.

The **Figure 14** shows the effect of pressure and pH on the flux of permeate.
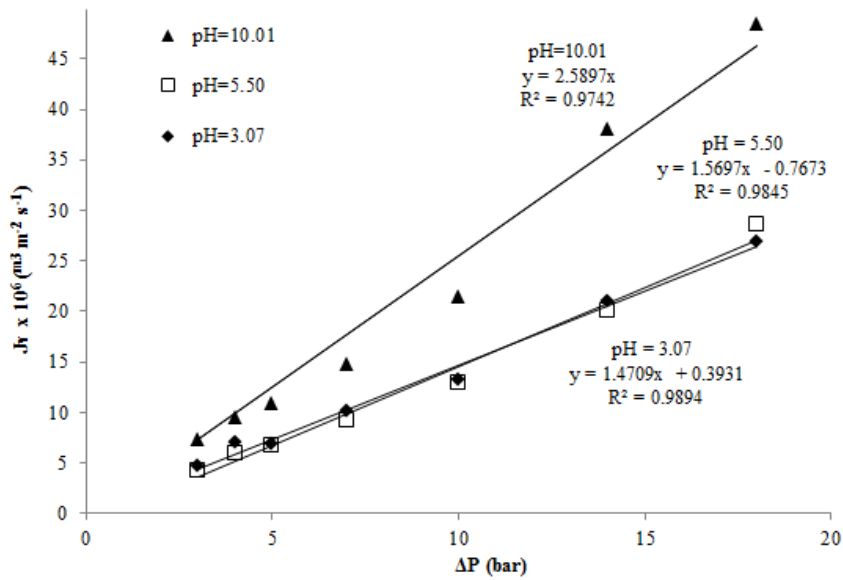
Figure 14 – Effect of pressure and pH on the flux of permeate.

It is expectable that the flux increases linearly with the pressure drop, since

$$J_v = \frac{L_p}{\eta_0}(\Delta P - \Delta \pi) \qquad (2.2).$$

The membrane has negative zeta-potential and with a higher pH, the flux augments. The flux behaviour observed in the **Figure 14** can be explained by the change of the surface chemistry of the membrane when the solution pH is varied. The skin layer of the membrane tested (TS-80) is mostly made of polyamide material which possesses dissociable carboxylic and amine groups. At high pH values, the carboxylic group dissociates fully and the surface gains its strongest negative charge. These conditions favour the interactions with water molecules and make the surface more hydrophilic resulting that more water molecules are permeated through the membrane.

The **Table 14** shows the effect of the pH on the global retention of contaminants (assessed by COD) and on the flux for a constant applied pressure (10 bar).

Table 14 – Effect of the pH on the COD retention and on the permeate flux for a $\Delta P = 10$ bar.

pH	Permeate Flux J_v x 10^6 (m^3 m^{-2} s^{-1})	COD Retention (%)
3.07	13.54	83.60%
4.04	15.58	65.98%
5.50	13.24	70.61%
6.72	23.01	42.20%
10.01	21.80	55.67%

For a constant pressure drop ($\Delta P = 10$ bar), a pH scanning was done and the individual and global rejection were calculated with the results of HPLC analysis (**Figure 15**).
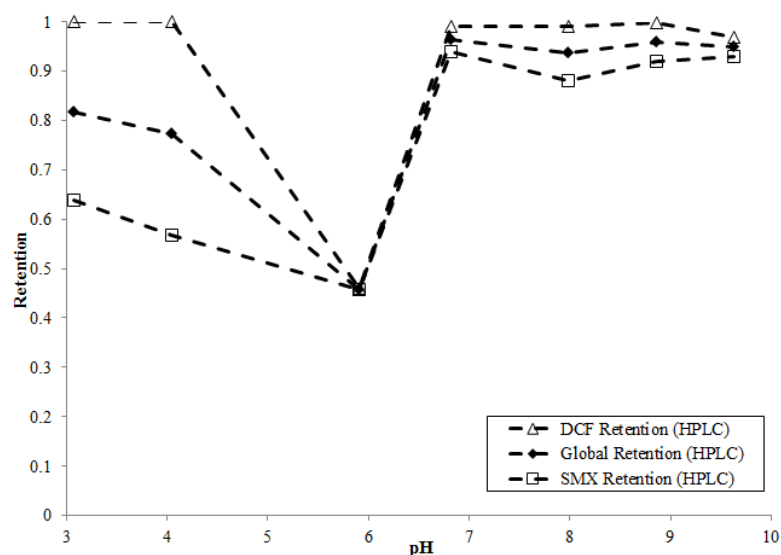
Figure 15 – Partial and global retention calculated with HPLC tests as a function of pH.

Once more, it is proven that the DCF has a higher retention due to the previously referred MWCO.

The best retention values are reached for pH values above 7. However, operating at low pH leads also to satisfactory results. The fractionation of SMX and DCF mixtures by Nanofiltration is dependent on the pH of the solution which determines the charge density of the membrane surface with negative zeta potential throughout the pH range tested. In other words, the membrane charge interferes on the rejection mechanisms.

The speciation of the contaminants in aqueous solution should also be taken into account in this analysis. Simon *et al.* (2011) reports that, when the pH matches the second pK_a of SMX (5.6), it exists in both neutrally and negatively charged forms with the same fraction. As the pH increases until pH = 8, the fraction of negatively charged species increases up to 100%. When the pH decreases under 5.6, mostly neutral forms exist. Considering its log K_{ow}, SMX can be said to be hydrophilic, which means that its adsorption to the membrane and fouling can be neglected. In what concerns de DCF, it has pK_a of 4.18 (and - 2.25) and under a pH = 8, it is negatively charged. It is moderately hydrophobic on its neutral form, but it is ionized, so the hydrophobicity is lower (Vergili, 2013). Therefore, and taking **Figure 15** into account, we can assume that SMX and DCF follow similar behaviours through the range of pH studied.

The behaviour of the retention from pH = 6 resembles a sigmoidal function as related in other studies (Belona and Drewes, 2005; Nghiem and Hawkes, 2007 and Nghiem *et al.*, 2005), being the inflection point around pH = 6 which is similar to the pK_a of SMX and DCF. Some deviations from the pK_a to the inflection point observed on **Figure 15** can occur since the membrane pores are very small, which make the pH on the pores slightly different than the pH on the bulk solution. There is often a negative proton retention observed in acidic solution, which can justify why the inflection point exists (Nghiem *et al.*, 2005).

Since the membrane has negative zeta potential (is negatively charged) at high pH and the molar fraction of the negative species is progressively bigger with increasing pH, it is comprehensible that the retention of the pollutants increases with increasing pH (on the range 6.0 – 10) due to charge repulsion (Simon *et al.*, 2011).

The polarity of the compounds determined by the log K_{ow} is also important, since the membrane has hydrophilic behaviour for higher pH (and hydrophobic behaviour for lower pH). SMX has log K_{ow} of 0.659, which means it is polar (and hydrophilic). On the other hand, DCF has a log K_{ow} of 4.51 (and hydrophobic). This data also justifies the higher retention of DCF. The influence of the molecule polarity on the retention is very significant for polar compounds with cylindrical shape such as SMX.

Regarding the range from pH 3 to 6, it is possible to say the predominant effect is the Donnan exclusion, since the membrane is looser (due to several hours of operation). Since the H^+ are more mobile and permeable than the other ions, they are fixed in the membrane (Nghiem *et al.*, 2005). Considering the individual behaviour of SMX and DCF in solution, it was expectable that their rejection dropped with the decreasing pH due to the presence of neutral or positively charged species that have opposite charge as the membrane (even though the zeta potential of the membrane increases with pH). However, the retentions observed for these pollutants are higher. This can be explained by the competitive behaviour of SMX and DCF on the Nanofiltration process. The simultaneous separation of both contaminants was not previously studied and the causes of these higher retentions should be further investigated.

In conclusion, multiple effects can be observed on the graphic shown on **Figure 15**: a dominant charge repulsion mechanism and polarity for pH over 6 and Donnan exclusion for pH under 6.

Effect of a Natural water Matrix

The effect of Natural water was also studied in order to verify the impact of the matrix over the removal of the pollutants. For this purpose a solution with 30 mg L^{-1} of SMX and 30 mg L^{-1} of DCF on natural water (filtered water from the river) was prepared and its pH was adjusted to 7. The Nanofiltration equipment was operated in a range of pressure drops – ΔP = 3, 4, 5, 7, 10, 14, 18 bar – and at pH 7, taking into account the previous optimization done and the approach to the normal pH for WWT processes. On the **Figure 16** stands the retention of pollutants calculated as a function of pressure drop based on COD and concentration (HPLC) measurements.
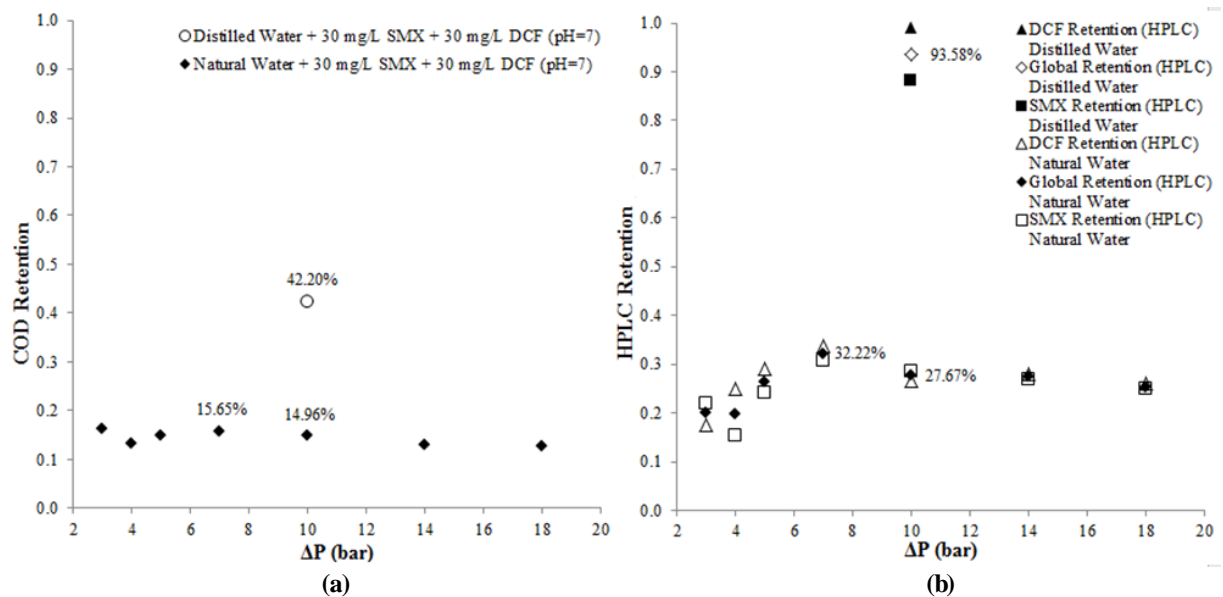
Figure 16 – Retention of pollutants as a function of pressure drop based on (a) COD and (b) concentration (HPLC) measurements for trial with distilled water (pH = 7 and ΔP = 10 ar) natural water (pH = 7, range of ΔP).

From the analysis of **Figure 16** it is possible to conclude that the change of the aqueous matrix (from distilled to natural water) has a significant negative impact on the efficiency of the Nanofiltration process. Regarding the COD removal, it is reduced, considering the same pressure drop (ΔP = 10 bar), to less than half. On the HPLC, a relatively small percentage of the pollutants is retained on the membrane. This can be justified by the presence of other compounds on the river water, which can interfere on the separation process. For example, Verliefde *et al.* (2008) reports that the presence of calcium ions (Ca^{2+}) reduces the rejection of the membrane TS-80 for DCF. The water in the central region of Portugal (where river Mondego stands) has significant hardness with a presence of calcium over 300 mg L^{-1} $CaCO_3$ (Entidade Reguladora dos Serviços de Águas e Resíduos, 2011). Therefore, this behaviour is justifiable.

The **Figure 16** also indicates that the best removal of pollutants is attained for a pressure drop of 7 bar.

5.1.3 Analysis of the membrane fouling

On this section the study of the membrane's fouling is presented. For this purpose, two trials, in which the flux through the membrane was measured over time, were done. The experiments were performed with a new membrane and, firstly, distilled water was used, following a trial with an aqueous solution containing 30 mg L^{-1} of SMX and 30 mg L^{-1} of DCF. The results of both trials are presented on the **Figure 17**.
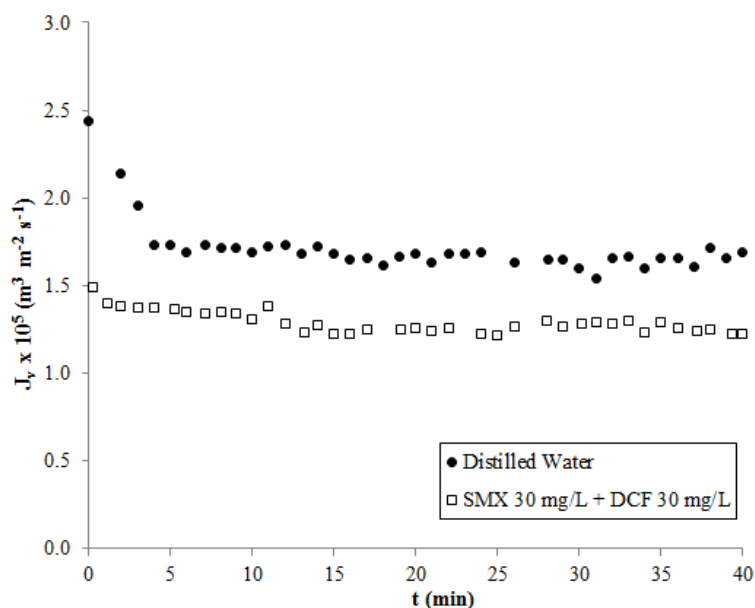
Figure 17 – Analysis of the membrane's fouling using distilled water and an aqueous solution containing SMX and DCF.

This figure shows that the water with the pollutants presents significantly more fouling than the distilled water. Even though the system with the pollutants takes more time to achieve a steady state, it is reasonable to assume that, after 15 minutes, the system stabilizes.

The flux is reduced in 26.97% for distilled water and 30.68% for water containing the pollutants.

The membrane permeability for the solution containing 30 mg L^{-1} was evaluated through the adjustment of a linear regression to the data of flux versus pressure drop. The membrane permeability was $1.503 \times 10^{-15}\ m$ which contrasts with the membrane permeability of water of $1.253 \times 10^{-14} \pm 5 \times 10^{-17}\ m$.

Atomic Force Microscopy (AFM) analysis is a very useful tool in what concerns the analysis of the effects of the operating conditions on the internal porosity of the membrane. It is possible to see, on **Figure 18**, the comparison between the topographic images of a fresh and a used membrane. These two images are corrected to the same average, which means that the same colour represents the same topographic height in the two images.
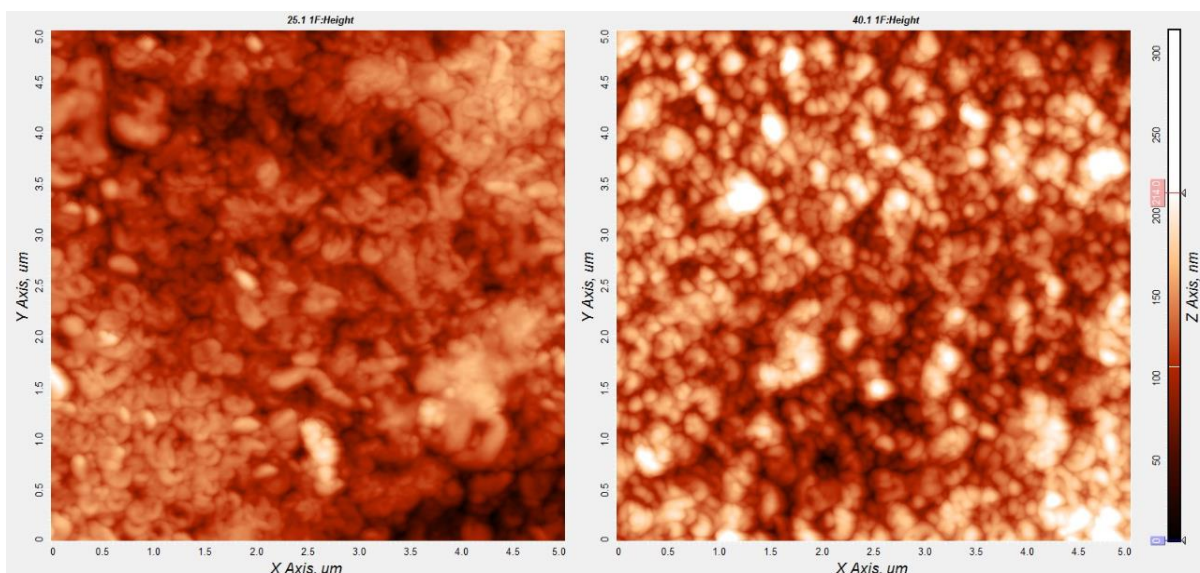
Figure 18 – 5 µm x 5 µm surface topography images with corrected average for a virgin membrane (on the left) and a membrane that was used for approximately 40 hours (right).

It is possible to conclude that the used membrane has adsorbed material on it, since the zed quota is higher for a corrected image with the same average. After 40 hours of operation with the simulated effluent, it is reasonable to assume that the pollutants SMX and DCF are adsorbed at the surface of the membrane.

The average roughness for the virgin membrane calculated based on a 5 µm x 5 µm surface topography image is 22.068 nm, while for the membrane used for 40 hours is 27.22 nm. These results corroborate that the used membrane has adsorbed material on it.

5.2   Ozonation

For the perfect understanding of the catalytic Ozonation trials it was important to characterize the catalyst used. Some trials involving the SMX and DCF dissolved in distilled water and natural water were done in order to access the effects of different variables on the performance of the batch Ozonation in what concerns the reduction of the concentration of the pollutants and the COD removal. As it is described along this chapter, the sequence of the experiments was performed taking into account one optimization path.

5.2.1 Catalyst characterization

As it was already described on **4.3 Analytical Methods**, three different techniques were applied to characterize the catalysts used in Ozonation: **BET**, **Mercury porosimetry** (**Table 15**) and **Elemental analysis**.

Table 15 – Synthesis of the results obtained from the techniques BET and Mercury porosimetry applied to the catalysts Mn-Ce-O and N-150 (adapted from Martins and Quinta-Ferreira, 2011).

Method	Parameter	Catalyst Mn-Ce-O	Catalyst N-150
BET	Catalyst's specific area ($m^2\ g^{-1}$)	109	-
Mercury porosimetry	Type of structure	Mesoporous/ macroporous	Mesoporous/ macroporous
	Average diameter of pores (range of pore size distribution) (μm)	0.0179	0.0167 (0.01 - 0.1)

The average diameter of the pore of the catalyst N-150 is slightly under the average for the other catalyst.

All the data collected through these analyses will be useful to interpret the results obtained on the catalysed Ozonation trials.

5.2.2 Ozonation of solutions containing emerging contaminants

Several Ozonation trials were performed in order to access the effect of variables with the final goal of choosing the most favourable conditions for the Ozonation of solutions containing the two emerging contaminants in use with concentrations of 30 mg L^{-1}.
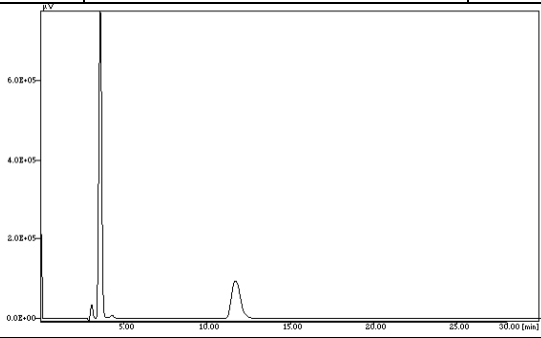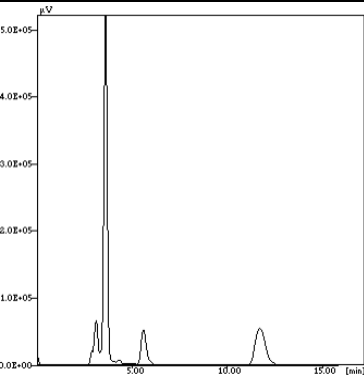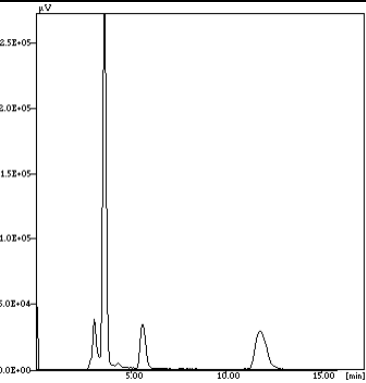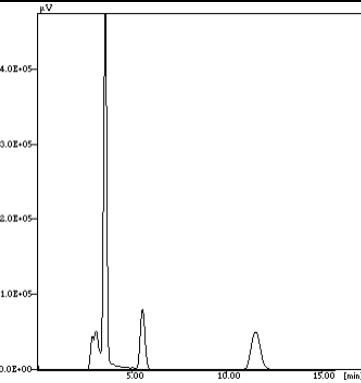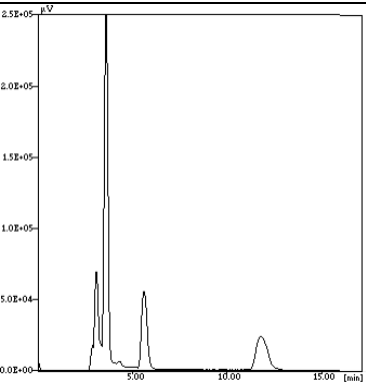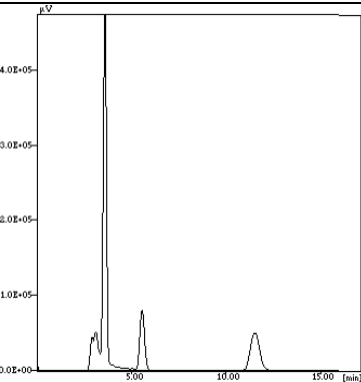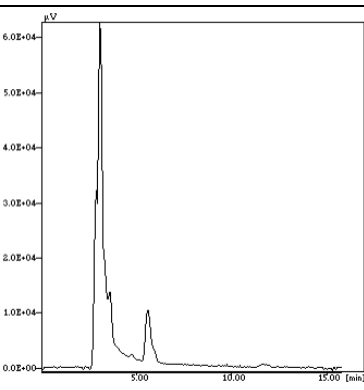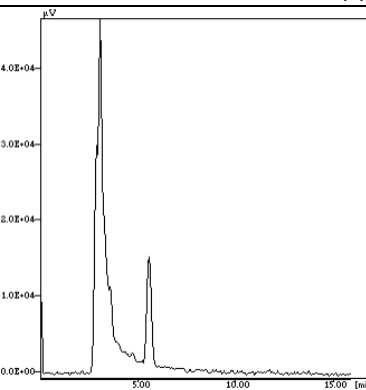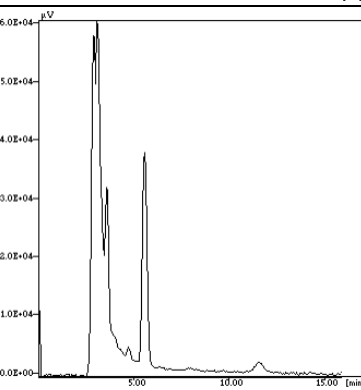
Catalyst effect

To access the catalyst effect, three of the trials that were done can be compared: simple Ozonation and catalytic Ozonation using Mn-Ce-O and N-150. On all trials the gas flow was kept constant at the value 0.2 L min^{-1}, the pH was buffered to be 7 and the initial ozone concentration, $C_{O3,in}$, was around 10 g m^{-3}. Both catalysts were powdered before use and the batch reactor was agitated at 300 rpm to ensure chemical regime. The catalysts concentration was 1 g L^{-1}.

HPLC analysis was done to solutions collected during the reactions performed to determine the concentration of the parent compounds along the treatment time. On the **Table 16** is the sequence of HPLC signal graphics for different reaction times for the simple and catalysed reactions.

Table 16 – HPLC signal graphics along the trials of simple Ozonation (OZ), Ozonation with catalyst Mn-Ce-O and with catalyst N-150.
For t = 6, 10, 45 and 60 min the graphic presented just until retention time of 15 min. Note that the μV scale is different between the images.

t (min)	Simple OZ	OZ w/ Catalyst Mn-Ce-O	OZ with Catalyst N-150
0			
6			
10	Not available		
45			

Table 16 (continued)

This sequence illustrates the Ozonation process, since the pollutants SMX and DCF (with a retention time of approximately 3.5 and 11.5 min, respectively) have higher concentration (bigger peak area) on the beginning of the process and that area decreases along time (note that the µV scale is different in the images). For better understanding of the HPLC analysis presented on this table, the **Appendix III – HPLC - Calibration curve** can be analysed.

From this table, it is possible to conclude that an intermediate product from the pollutants' degradation through the oxidation by ozone was detected in the HPLC. This product has a retention time of approximately 5.5 min, while SMX and DCF have retention times around 3.5 and 11.5 min, respectively. It appears straight after the Ozonation starts and its concentration augments until around 45 minutes of reaction and afterwards starts decreasing. By the 60 min of reaction, the intermediate peak is already decreasing, since other products (which peaks are not detected because their concentrations are too small) are being formed. Since the injection of possible SMX and DCF intermediates under the same HPLC conditions was not done on this work or on previous studies, it was not possible to identify the unknown intermediate present on the secondary peak. Previous works use techniques such as Gas chromatography–mass spectrometry (GC-MS) or liquid chromatography-electrospray ionisation-quadrupole-time-of-flight mass spectrometry (LC-QqTOF-MS/MS) to identify the Ozonation intermediates. These technologies could be a powerful tool on future steps of this investigation.

On the **Figure 19** stands the time evolution of the areas of the HPLC peaks for SMX, DCF and the unknown intermediate on a catalysed Ozonation (Mn-Ce-O). This image corroborate the HPLC images shown on **Table 16** and the comments regarding the unknown intermediate concentration (first increasing, after decreasing) that were done apropos.
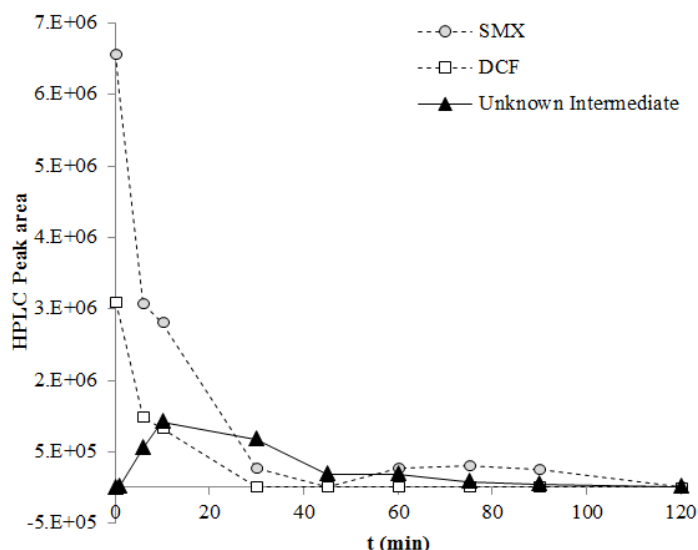
Figure 19 – HPLC peak area for SMX, DCF and unknown intermediate along the reaction time of Ozonation catalysed by Mn-Ce-O.

The concentration values of the compounds were obtained using the calibration curve on the HPLC values for the three trials. It is clear for all the trials that there is a decreasing concentration profile of both contaminants as exemplified for the Ozonation trial catalysed by Mn-Ce-O on **Figure 20**.
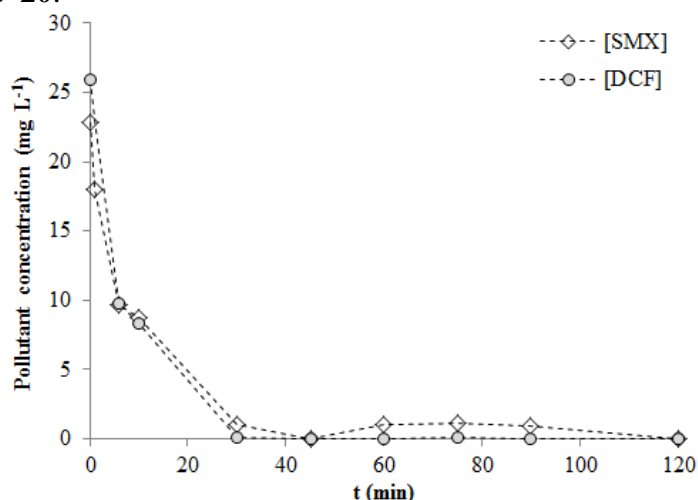
Figure 20 – Concentration profile of pollutants for Ozonation catalysed by Mn-Ce-O (buffered).

To make the results clearer, the degradation percentage of the compounds along time can be calculated. The degradation of a certain compound (ex: SMX) for a certain time, t, taking into account the concentration of the pollutant (ex: $[SMX]$) calculated by HPLC analysis is calculated according to the following (based on equation 2.13):

$$SMX\ Degradation\ (HPLC)_t = 1 - \frac{[SMX]_t}{[SMX]_{t=0}} \tag{5.3}$$

The global degradation takes into account the concentration of SMX and DCF for the initial time ($t = 0$) calculated by HPLC. For a certain time, t, and is calculated by an equation based on 2.14:

$$Global\ Degradation\ (HPLC)_t = 1 - \frac{[SMX]_t + [DCF]_t}{[SMX]_{t=0} + [DCF]_{t=0}} \tag{5.4}$$

On the **Figure 21** the degradation percentage of the compounds based on the HPLC concentration values is exposed.
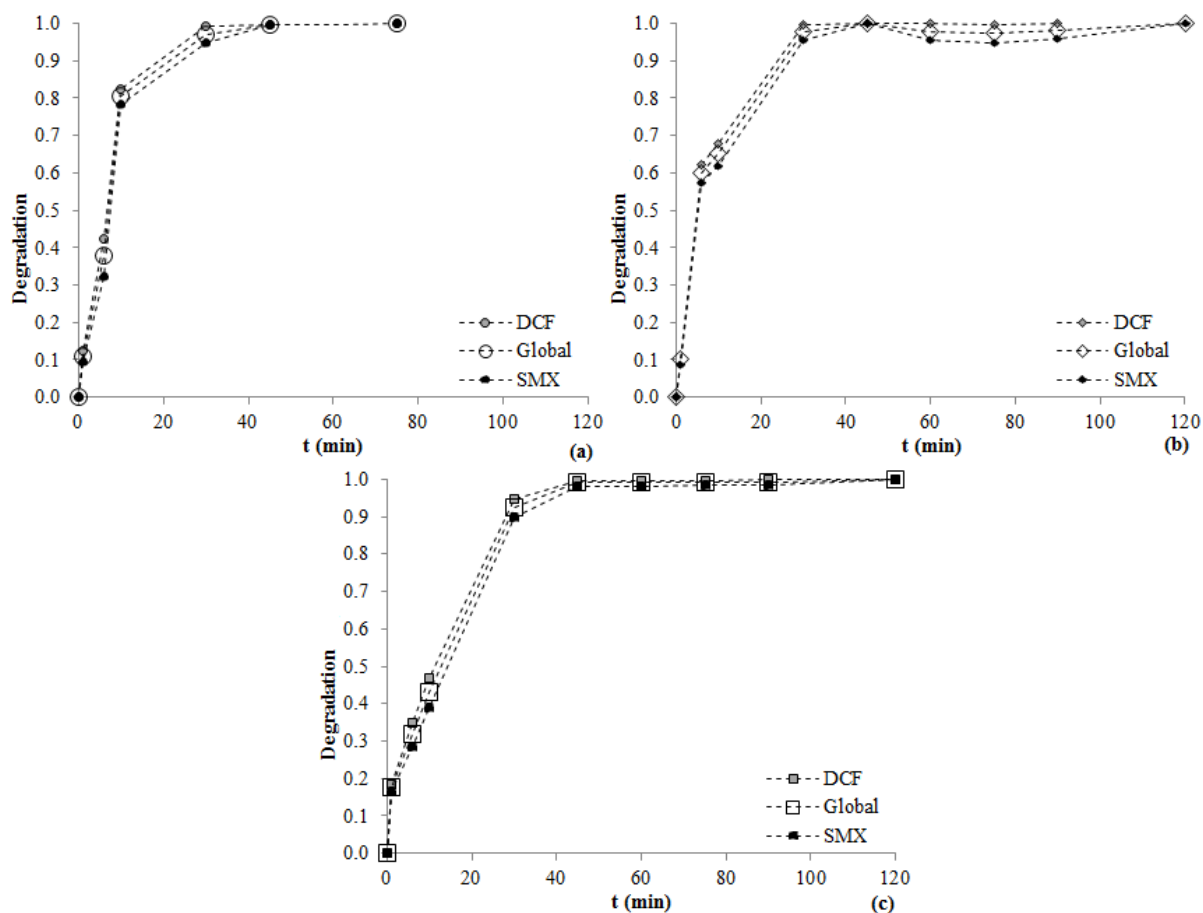
Figure 21 – Degradation evolution of SMX, DCF and Global degradation along the trials of simple Ozonation (a), Ozonation with catalyst Mn-Ce-O (b) and with catalyst N-150 (c).

From this Figure it is clear that the degradation profile of SMX and DCF follows a similar behaviour (and the Global degradation, being a function of those two, also does), even though the DCF is slightly more easily degraded than the SMX. Taking into account this very close behaviour, and to simplify the figures, just Global degradation plots (as a function of the concentration of individual pollutants determined by HPLC) will be presented as long as Ozonation trials are being considered.

The **Figure 22** shows the comparison of the Global degradation of the three trials: simple Ozonation, Ozonation with catalyst Mn-Ce-O and with catalyst N-150.
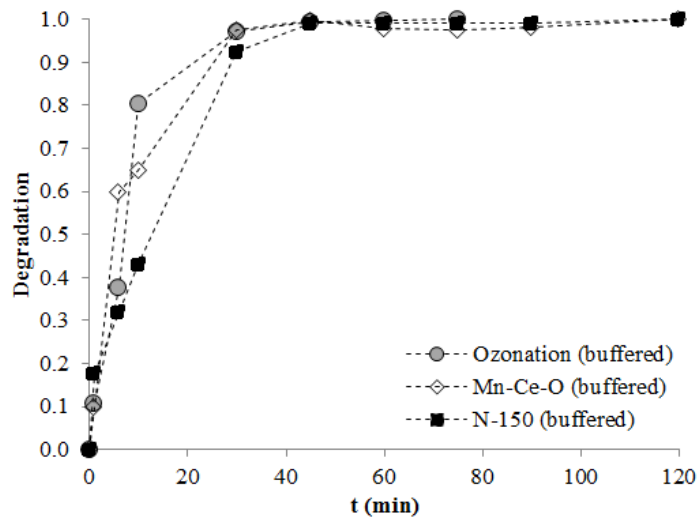
Figure 22 – Global degradation of the three trials: simple Ozonation, Ozonation with catalyst Mn-Ce-O and with catalyst N-150.

It can be observed from this Figure that the presence of the catalyst does not seem fundamental for the effective degradation of the initial pollutants, which is achieved for 50 min. In fact, ozone by itself is very reactive with compounds encompassing high electronic density compounds (please recall SMX and DCF molecular structure on **Figures 2** and **3**). Moreover, at pH 7 some hydroxyl radicals production due to the decomposition of ozone is possible which enhances single Ozonation efficiency. On other hand, at this pH both SMX and DCF are protonated and therefore more reactive than the in the non-ionic forms.

The use of a catalyst may be more important for the abatement of the COD once the accumulation of by-products during the process can reduce the efficiency on the removal of this parameter.

The **Figure 23** shows the evolution of the degradation of the compounds among time for the three trials. The degradation is calculated according to the following:

$$Degradation \ (COD)_t = 1 - \frac{COD_t}{COD_{t=0}} \tag{2.12}.$$
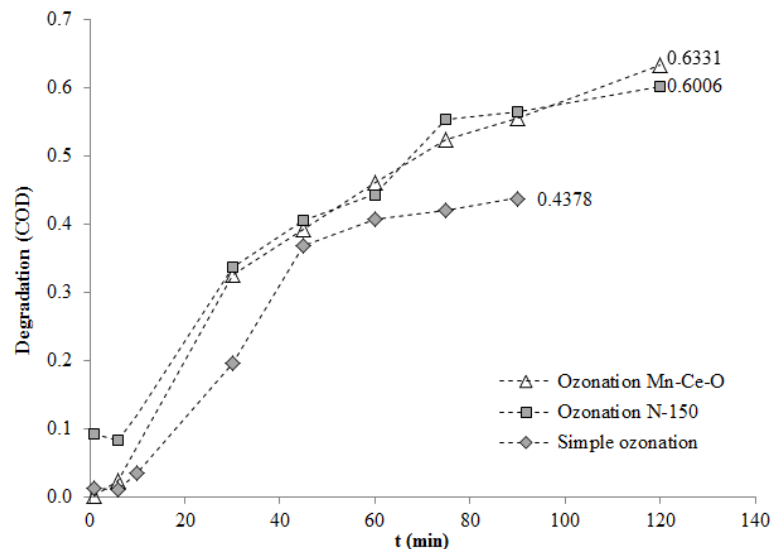
Figure 23 – Evolution of the degradation of the COD among time for the three trials: without catalyst, catalysed by Mn-Ce-O and by N-150.

From the analysis of the data on the **Figure 23** it is clear that the bigger removal of oxygen demand is achieved with the catalyst Mn-Ce-O leading to a a degradation percentage of 63.31% (in comparison with 43.78% for simple Ozonation and 60.06% for Ozonation catalysed by N-150). It seems thus that, even if no significant differences are found for the removal of the initial compounds when comparing single and catalytic Ozonation, the presence of a catalyst improves the abatement of COD. In fact, the oxidation of SMX and DCF leads to low molecular weight intermediates that are more refractory to ozone reactions. Mn-Ce-O and N-150 enhance ozone action over these by-products improving this way the COD abatement.

In order to identify if the treatment improvement attained when the solid materials were used in Ozonation is really due to oxidation of the organic matter or due to the adsorption of the pollutants over the catalysts surface, elemental analysis of the fresh and used catalysts was performed (**Table 17**).

Table 17 – Elemental analysis for the used N-150 and Mn-Ce-O catalysts in comparison to the fresh samples.

Catalyst	Description	% N (w/w)	% C (w/w)	% H (w/w)	% S (w/w)
Mn-Ce-O	Fresh	0.192	1.201	0.626	≤100 ppm
	After 120 min of buffered OZ[*]	0.186	1.501	1.117	≤100 ppm
N-150	Fresh	0.143	1.504	0.958	≤100 ppm
	After 120 min of buffered OZ[**]	0.203	1.215	0.86	≤100 ppm

[*]This catalyst corresponds to the filtered and dried catalyst on the final of the trial O3 (**Table 12**).

[**]This catalyst corresponds to the filtered and dried catalyst on the final of the trial O2 (**Table 12**).

From **Table 17**, it is possible to conclude that only a slight adsorption effect of organic matter is observed for Mn-Ce-O (below 3 mg C L^{-1}). On the other hand a lower amount of C is detected for N-150 after use. It seems that ozone is able to remove some carbonaceous impurities initially present in this catalyst surface. In this context, one can rule out the role of adsorption on the efficiency of catalysed Ozonation.

Liquid samples collected in the end of the catalysed Ozonation trials were under analysis through **Atomic Absorption Spectroscopy** in order to verify the stability of the catalysts regarding the leaching of the active metals to the liquid (**Table 18**).

Table 18 – Results of the Atomic Absorption Spectroscopy applied to liquid samples collected in the end of buffered and catalysed Ozonation trials.

Sample Description	mg Mn L^{-1}	mg Fe L^{-1}
Liquid sample collected after 120 min Ozonation catalysed by Mn-Ce-O (buffered)[*]	2.5	-
Liquid sample collected after 120 min Ozonation catalysed by N-150 (buffered)[**]	1.7	≤ 0.088

[*]This sample corresponds to the filtered liquid on the final of the trial O3 (**Table 12**).

[**] This sample corresponds to the filtered liquid on the final of the trial O2 (**Table 12**).

The results shown on **Table 18** evidence that the catalysts seems to be stable regarding the leaching of active metals to the liquid. In fact, for Mn-Ce-O only 2.5 mg L^{-1} of Mn were detected in solution after 120 min of catalytic Ozonation. This value is very close to the legal threshold on this metal allowed for the discharge of a wastewater (2 mg L^{-1}). Higher stability was still observed for N-150 since only 1.7 mg L^{-1} of Mn and a value below the analytical technique detection limit for Fe were determined after 120 min of treatment. These materials seem to be promising on the removal of emerging contaminants from water.

Buffering effect on catalysts' efficiency

Buffering the solution that undergoes Ozonation is convenient to ensure that the pH is within the conventional range in WWT processes (6.5 − 7.5), which is imposed by the use of microorganisms. Even though the COD removal with the catalyst Mn-Ce-O is quite significant, the percentage of organic matter degradation obtained on the trials with this material and buffering was not as high as expected, taking into consideration previous studies. The same can be said in a smaller extense regarding the catalyst N-150. (Martins and Quinta-Ferreira, 2011) Therefore, the motives that lead to this low efficiency were under investigation.

One possible motive that could justify the low efficiency of the catalyst could be the buffering, since it is done with phosphates (disodium phosphate, monosodium phosphate and phosphoric acid) which can be competing with the pollutant in the active sites of the catalyst. (Hordern, 2010) To access if the buffering had a negative effect on the Ozonation performance, two additional trials were performed with each catalyst in which the solution was not buffered, but its pH was adjusted to 7 in the beginning with an aqueous solution of sodium hydroxide (NaOH).

On both experiments the gas flow was kept constant at the value 0.2 L min^{-1}, the initial ozone concentration, $C_{O3,in}$, was around 10 g m^{-3}, the catalyst was powdered and the reactor was agitated at 300 rpm. The concentration of catalyst was 1 g L^{-1}.

On the **Figure 24** the evolution of the degradation of the oxygen demand among time is presented for the trials with and without buffering using the catalysts Mn-Ce-O and N-150.
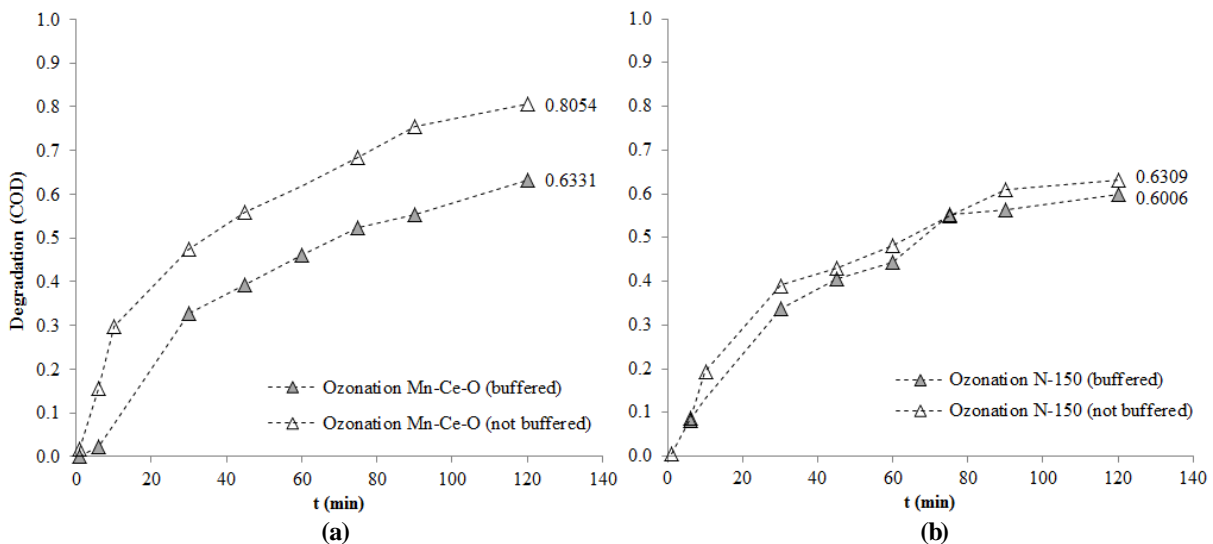
Figure 24 (a) **Evolution of the degradation of the oxygen demand among time with and without buffering when the catalyst Mn-Ce-O is used.** (b) **Evolution of the degradation of the oxygen demand among time with and without buffering when the catalysst N-150 is used.**

On the **Figure 25** is represented the degradation of the parent compounds (determined by HPLC) evolution along time for buffered and not buffered catalysed reactions.
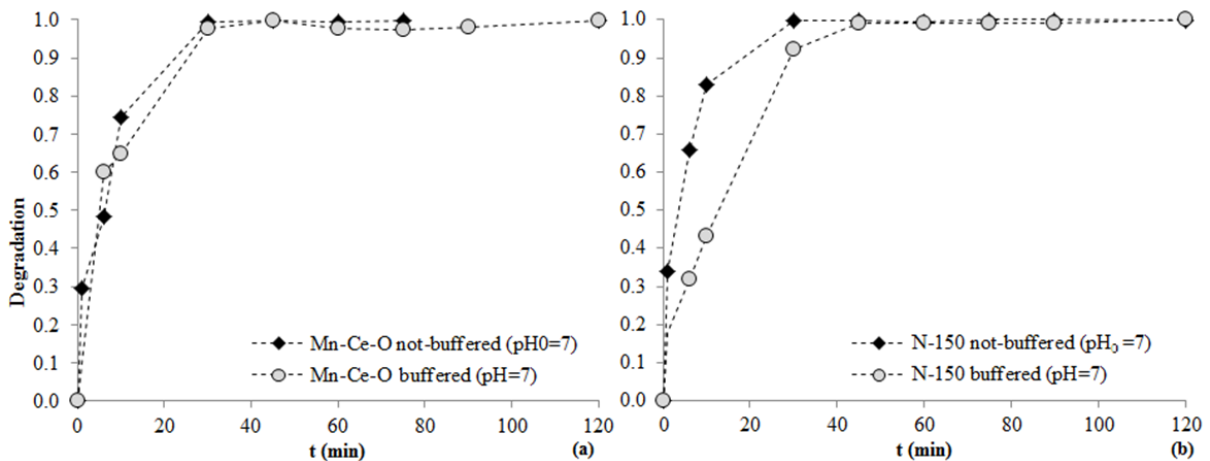
Figure 25 – Degradation evolution for buffered and not buffered catalysed reactions with (a) Mn-Ce-O and (b) N-150.

On the **Figure 26** the evolution of the pH on the not buffered catalysts is shown.
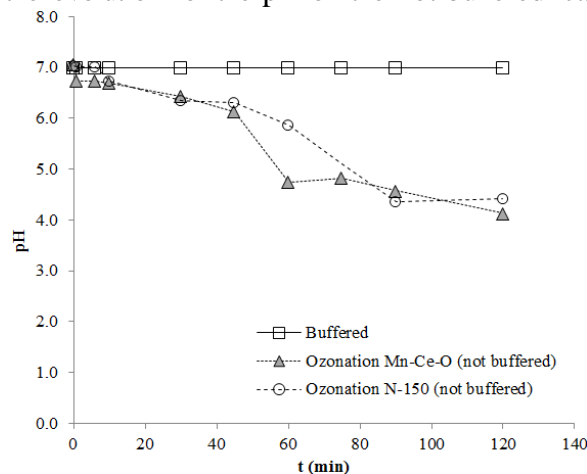
Figure 26 – Evolution of the samples' pH for the not buffered trials in comparison with buffered.

54

From the analysis of all the data, it is possible to conclude that the buffering has a considerable negative effect on the performance of the Mn-Ce-O catalyst. This result is mainly shown by the COD values, since the HPLC shows practically equal results after 50 minutes of reaction.

The **Figure 26** shows that the pH decreases for both trials when it is not buffered. This can be explained by the formation of short chain carboxylic acids and also due to the adsorption of OH^- ions on the surface of the catalyst.

Since the pollutants on the scope of this study have C=C chemical bonds and present high electronic density groups are easily degraded by ozone into organic intermediates. That is why the parent compounds removal is independent of the operating conditions. The subsequent steps of the intermediates mineralization (until CO_2 and H_2O are formed) is tougher, and their efficiency is ruled by the different reaction mechanisms and the aqueous media conditions (Nawrocki and Kasprzyk-Hordem, 2010).

Martins and Quinta-Ferreira (2009) report that the reaction mechanism for the catalyst Mn-Ce-O consists on the ozone adsorption into the catalyst to form reactive oxygen species that will degrade adsorbed organic matter. The fact that the pH is buffered at pH 7 on the Mn-Ce-O catalysed reaction makes the catalyst be negatively charged (due to its point of zero charge, $pH_{zpc} = 4.8$). Since the organic matter is mainly on their negative or neutral form (pK_a of SMX and DCF are 5.81 and 4.18, respectively), there is electrostatic repulsion (or absence of attraction) between the organic matter and the catalyst, which makes the reaction between adsorbed oxygen species and catalyst be limited.

Regarding the catalyst N-150, the difference is not significant. This is explained by the fact that the ozone molecule gets to the catalyst and the hydroxyl radicals are formed regardless the pH of the solution. Therefore, the mineralization occurs with no limitations.

Then, it is important to do further investigation on optimal pH conditions of operation for the catalyst Mn-Ce-O.

pH effect on catalyst Mn-Ce-O

To access the impact of the pH on the efficiency of the catalyst Mn-Ce-O, besides trials with the buffered pH and with the not buffered pH (initially adjusted to 7), another trial was done. In this trial the pH was manually adjusted to 7 along the two hours of the trial. Since the pH with the Ozonation gradually decreases, the pH of samples was measured frequently and the volume of an aqueous solution of NaOH that had to be added in order to maintain it on 7 was calculated and added.

On the **Figure 27** the evolution of the degradation of the pollutants based on COD and HPLC tests is presented for the three trials mentioned above.
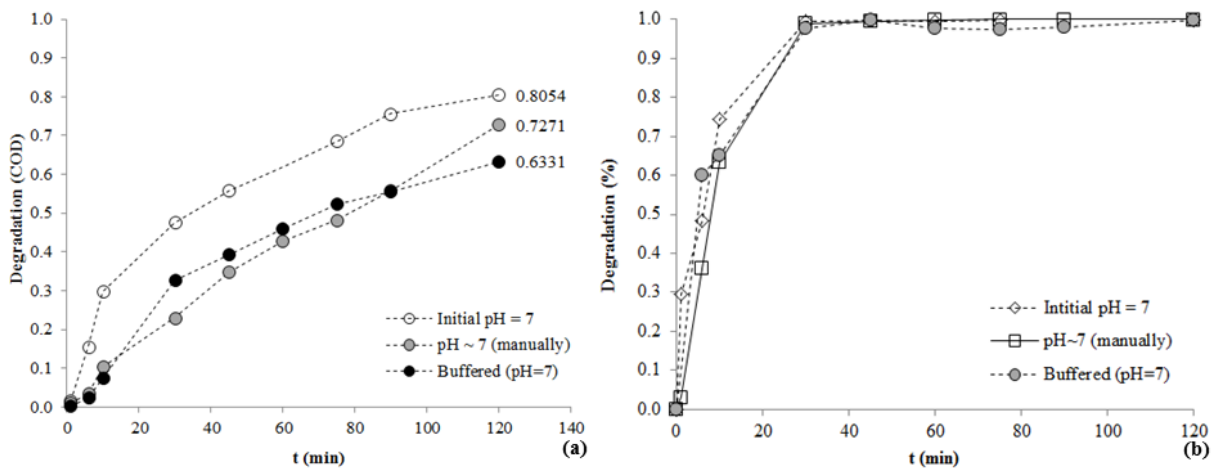
Figure 27 – Evolution of the degradation of the pollutants based on (a) **COD and** (b) **HPLC measurements among time for three catalysed trials with Mn-Ce-O: one buffered at pH=7; another in which the pH was adjusted to 7 initially and another one in which the pH was maintained 7 (by adding NaOH manually) during the trial.**

On the **Figure 28** the evolution of the pH on the not buffered catalysts with and without adjusted pH is shown.
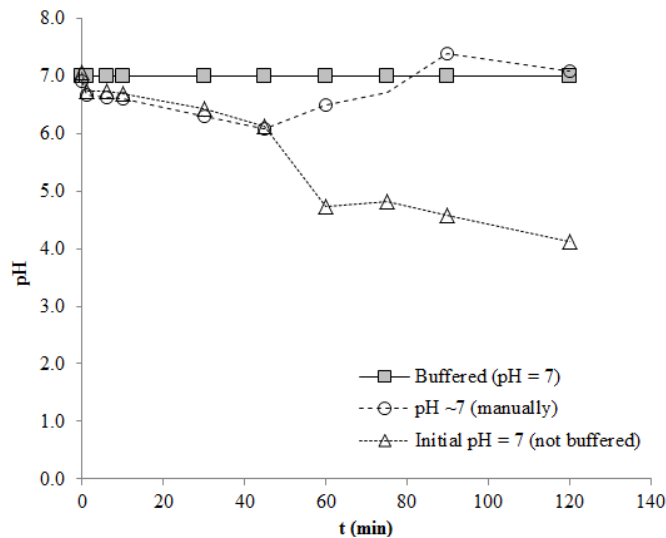
Figure 28 – Evolution of the samples' pH on Mn-Ce-O catalysed Ozonation for the not buffered trials with pH adjusted to 7 initially and manually adjusted to 7 throughout all the trial in comparison with buffered Ozonation.

From the results of the trials performed, it is possible to conclude that the degradation of the pollutants is better achieved if the catalyst Mn-Ce-O is used with the pH being adjusted to 7 on the beginning without further pH correction afterwards. This operating condition leads to a COD removal efficiency of 80.54%.

To explain these results it is necessary to recall the mechanisms through which the Mn-Ce-O catalysed Ozonation occurs. The trial in which the pH is manually adjusted to 7 with NaOH along the reaction is related with the electrostatic repulsion between the pollutants and the catalyst referred before (Nawrocki and Kraspzyk-Hordern, 2010). The fact that the buffered trial (at pH 7) has the worse efficiency can be explained (besides the repulsion between catalyst and pollutants) by the competition between ozone and the phosphates of the

buffer by the active metallic oxide sites of the catalyst (Lewis centers) as indicated by Nawrocki and Kraspzyk-Hordern (2010).

Effect of the presence of Hydrogen peroxide

The hydrogen peroxide (a strong oxidant) was tested in order to optimize the Ozonation conditions. In fact, the interaction between ozone and hydrogen peroxide lead to the production of hydroxyl radicals that may improve the treatment efficiency.

Since the catalyst that showed the best results was Mn-Ce-O, the cumulative use of both the catalyst and hydrogen peroxide was also tested. On this trial the catalyst (1 g L^{-1}) was powdered and the reactor was agitated at 300 rpm.

On both trials the gas flow was kept constant at the value 0.2 L min^{-1}, the pH was buffered to be 7 and the initial ozone concentration, $C_{O3,in}$, was around 10 g m^{-3}. The hydrogen peroxide was administrated to the reactor by 12 injections evenly distributed along time of 8.6 µl of a solution with a concentration of 82.5 g L^{-1}.

To access if the hydrogen peroxide has a positive effect on the efficiency of the Ozonation, firstly two trials are compared: simple buffered Ozonation and buffered Ozonation with peroxide (trials O1 and O7 of **Table 12**, respectively).

On the **Figure 29**, the degradation of the pollutants (accessed by HPLC) and the COD removal efficiency is presented for the two trials that are being compared.

Figure 29 – Comparison between (a) **COD removal and** (b) **degradation of pollutants (HPLC) for the simple buffered Ozonation with and without peroxide.**

It is important to state here that it was expectable that the hydrogen peroxide, being a powerful oxidizer, had a significant positive impact on the efficiency of the Ozonation regarding the degradation of the pollutants. The COD data presented in which this is not fully verified can be explained by the presence of the hydrogen peroxide on the samples. Even though catalase was added, taking into account its sensibility, it is possible that it was deactivated due to the temperature, pH or other adverse conditions. The hydrogen peroxide test strips used could be degraded, therefore not showing the presence of that compound. As it was referred previously, the hydrogen peroxide affects the COD analysis. Therefore, probably

due to the presence of hydrogen peroxide on the analysed samples, the results of the tests performed for the simple Ozonation are not conclusive.

The comparison of the trials of buffered Ozonation catalysed by Mn-Ce-O with and without peroxide (trials O8 and O3 of **Table 12**, respectively) is also apropos. On the **Figure 30** the degradation of the pollutants (accessed by HPLC) and the COD removal efficiency is presented for the two trials that are being compared.
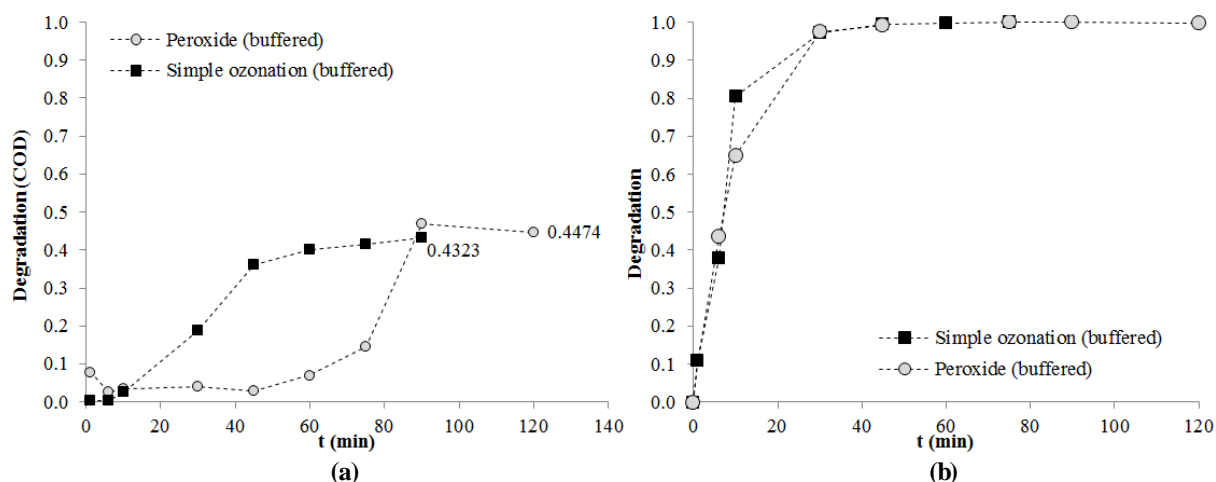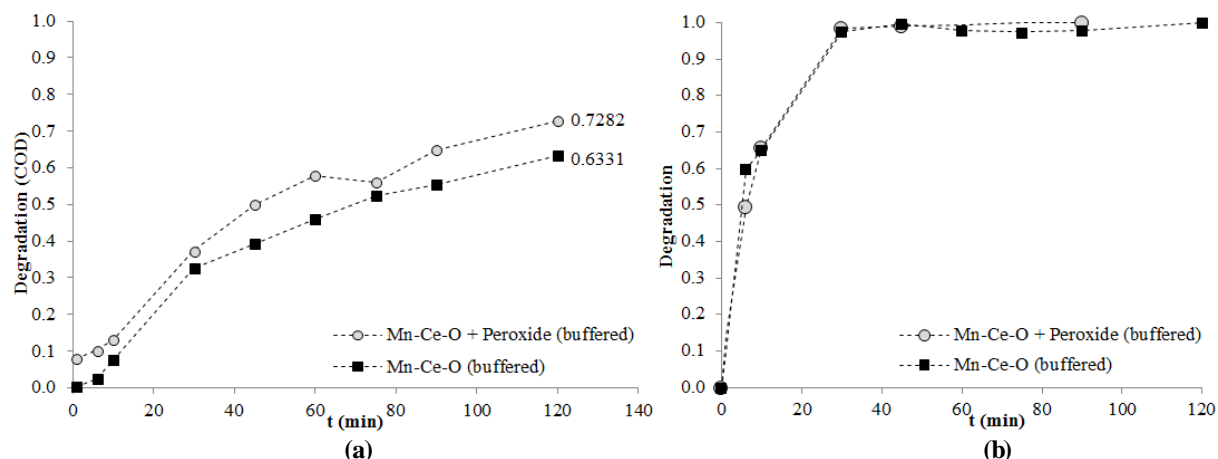

Figure 30 – Comparison between (a) **COD removal and** (b) **degradation of pollutants (HPLC) for the buffered Ozonation catalysed by Mn-Ce-O with and without peroxide.**

This Figure set forth that the presence of hydrogen peroxide can increase the performance of the COD degradation. The hydroxyl radicals formed through the addition of this compound are clearly affecting positively the reaction efficiency.

On the **Figure 31** is the measured evolution of hydrogen peroxide along the catalysed (Mn-Ce-O) trials compared with the theoretical H_2O_2 loaded to the reactor along time.
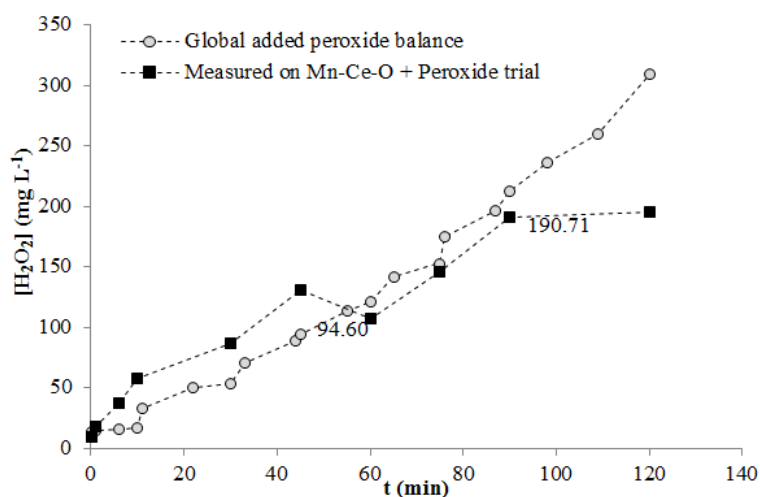
Figure 31 – Hydrogen peroxide concentration along time for Ozonation with catalyst Mn-Ce-O and peroxide determined with metavanadate (Nogueira *et al.***, 2005) and the global added peroxide balance.**

Considering the **Figure 31**, it is possible to say that the hydrogen peroxide is being consumed in the reaction. However, there is a great excess of it along most of the reaction time. It is important to note that H_2O_2 is an unstable chemical; therefore the values presented for the global added peroxide balance are potentially under the ones indicated through the molecule degradation.

Ormad *et al.* (1997) refers that the ideal H_2O_2/O_3 molar ratio should be under 0.5. The calculations of the hydrogen peroxide to add were done taking into account this heuristic. However, the ozone that enters the reactor is not fully dissolved. Therefore, the way the hydrogen peroxide is administered to the reactor should be optimized. One way to do this would be the injection of a greater quantity of hydrogen peroxide in the beginning and avoiding further additions. Moreover, work still must be done to optimize hydrogen peroxide removal from solution before analysing COD.

The elemental analysis was performed for the catalyst Mn-Ce-O collected at the end of the reaction with the hydrogen peroxide. On the **Table 19** the results of this analysis are showed in comparison with the results of the fresh catalyst and the catalyst recovered from the Ozonation reaction catalysed with Mn-Ce-O (without peroxide).

Table 19 – Elemental analysis for the used Mn-Ce-O catalysts in buffered Ozonation trials (with and without peroxide) in comparison to the fresh sample.

Description	% N (w/w)	% C (w/w)	% H (w/w)	% S (w/w)
Fresh	0.192	1.201	0.626	≤100 ppm
After 120 min of buffered OZ[*]	0.186	1.501	1.117	≤100 ppm
After 120 min of buffered OZ with hydrogen peroxide[**]	0.142	1.183	0.714	≤100 ppm

[*]This catalyst corresponds to the filtered and dried catalyst on the final of the trial O3 (**Table 12**).

[**]This catalyst corresponds to the filtered and dried catalyst on the final of the trial O8 (**Table 12**).

From **Table 19** it is possible to conclude that the presence of hydrogen peroxide was able to remove part of the carbonaceous impurities present on Mn-Ce-O. In fact, according to this information, the amount of carbon present on the catalyst is lower after the treatment process when compared with the fresh material.

Liquid samples collected in the end of the catalysed Ozonation with hydrogen peroxide trials were under analysis through **Atomic Absorption Spectroscopy**. On the **Table 20** the results of this analysis are showed in comparison with the results of the same analysis for the liquid sample of Ozonation reaction catalysed with Mn-Ce-O (without peroxide).

Table 20 – Results of the Atomic Absorption Spectroscopy applied to liquid samples collected in the end of buffered and catalysed Ozonation trials.

Sample Description	mg Mn L^{-1}
Liquid sample collected after 120 min Ozonation catalysed by Mn-Ce-O (buffered)[*]	2.5
Liquid sample collected after 120 min Ozonation catalysed by Mn-Ce-O (buffered) with hydrogen peroxide[**]	3.4

[*]This sample corresponds to the filtered liquid on the final of the trial O3 (**Table 12**).

[**] This sample corresponds to the filtered liquid on the final of the trial O8 (**Table 12**).

The results shown on **Table 20** evince that the presence of hydrogen peroxide favoured Mn leaching which increased from 2.5 mg L^{-1} to 3.4 mg L^{-1}.

Effect of Natural water

The effect of Natural water on the Ozonation process was studied towards the optimization of conditions for the real effluent. A solution with 30 mg L^{-1} of SMX and 30 mg L^{-1} of DCF on natural water (filtered water from the river) was prepared and submitted to not buffered Ozonation. It was decided not to buffer because this process would be integrated with the Nanofiltration and the buffering could interfere on the separation.

On the **Figure 32** stands the degradation of pollutants calculated along time based on COD and concentration (HPLC) measurements.
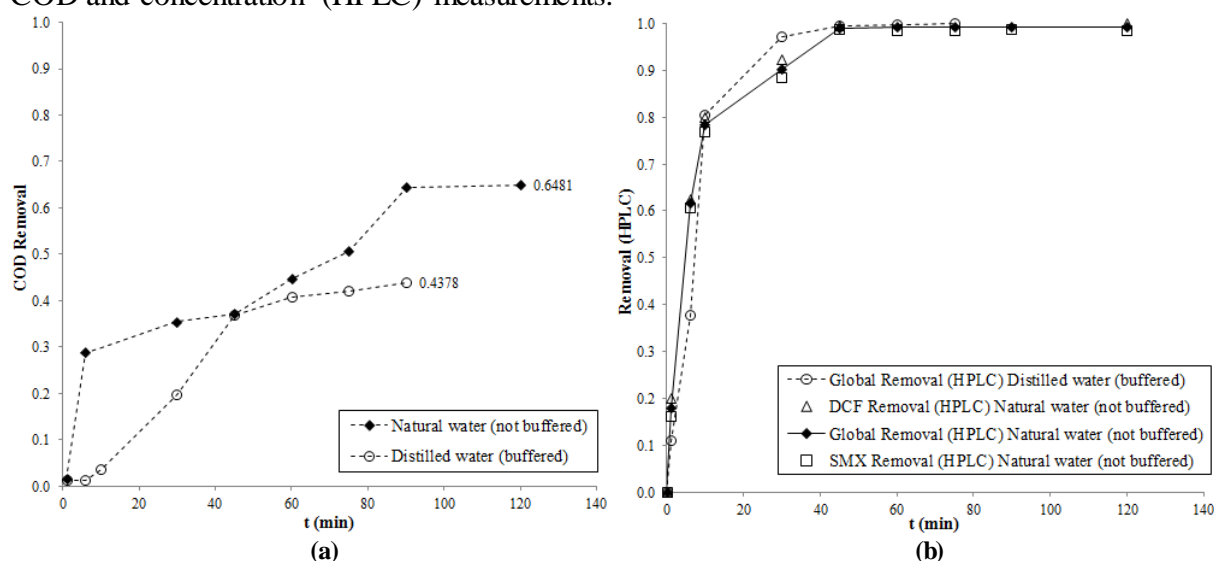
Figure 32 – Pollutants' degradation as a function of reaction time for (a) **COD and** (b) **concentration (HPLC) measurements for the trial with natural water in comparison with the trial with distilled water.**

From the analysis of **Figure 32** it is possible to conclude that the change of the aqueous matrix (from distilled to natural water) does not have a significantly negative impact on the efficiency of the Ozonation process. In fact, even higher COD removal is observed when natural water was applied. This behaviour should be related with the presence of easy degradable compounds in the matrix.

5.3   Process Integration

The main goal of this work is to evaluate the efficiency of the integration of both processes on WWT. It was necessary to firstly optimize individually the two techniques in order to ensure the conditions on the process integration allowed the achievement of better results.

Regarding the Nanofiltration, the optimum conditions determined previously were applied: it was done under a pressure drop (ΔP) of 7 bar and the pH of the feed was adjusted to 7 before the operation (also to approach the pH of a common WWT process).

However, due to the nature of the WWT processes used in the scope of this study, the integration had to be done with different Ozonation conditions than the optimum. Since the powdered catalyst and the phosphates used for buffering the pH could interfere in the Nanofiltration process with which Ozonation was being integrated, it was decided to perform the simple Ozonation without pH adjustment. The gas flow was kept constant at the value 0.2 L min^{-1} and the initial ozone concentration, $C_{O3,in}$, was around 10 g m^{-3}.

To decide which sequence of processes would be the best, two sequences were done: Nanofiltration followed by Ozonation (NF + OZ) and Ozonation followed by Nanofiltration (OZ + NF). On the **Table 21** the results for the two trials are presented.

Table 21 – Retention and removal COD and concentration values for the two trials performed for the Nanofiltration (NF) and Ozonation (OZ) process integration (NF+OZ and OZ-NF).

		COD (mg O$_2$ L^{-1})	COD Retention/ Degradation (%)	[SMX] (mg L^{-1})	SMX Retention / Degrad. (%)	[DCF] (mg L^{-1})	DCF Retention / Degrad. (%)	HPLC Global Retention/ Degrad. (%)
NF+OZ	**Initial**	80.22		38.0814		33.0843		
	(After) NF (ΔP = 7 bar)	67.22	15.65	21.8850	42.53	26.3499	20.36	32.22
	(After) OZ (120 min)	23.43	68.84	0.1136	99.48	0.0083	99.97	99.75
	Final / Overall process	23.43	**70.79%**	0.1136	99.70	0.0083	99.97	**99.83%**
OZ+NF	**Initial**	84.03		23.4587		23.0575		
	After OZ (120 min)	31.88	62.06	0.3368	98.56	0.1631	99.29	98.93
	After NF (ΔP = 7 bar)	29.68	6.91	0.1442	57.18	0.0185	88.63	67.44
	Final / Overall process	31.88	**64.68%**	0.1442	99.39	0.0185	99.92	**99.65%**

From the **Table 21** it is possible to conclude that the best sequence in terms of COD and pollutant removal is Nanofiltration followed by Ozonation. The **Figure 33** evinces the global

results of the two integrated processes regarding the reduction on the pollutant's concentration and the COD removal.
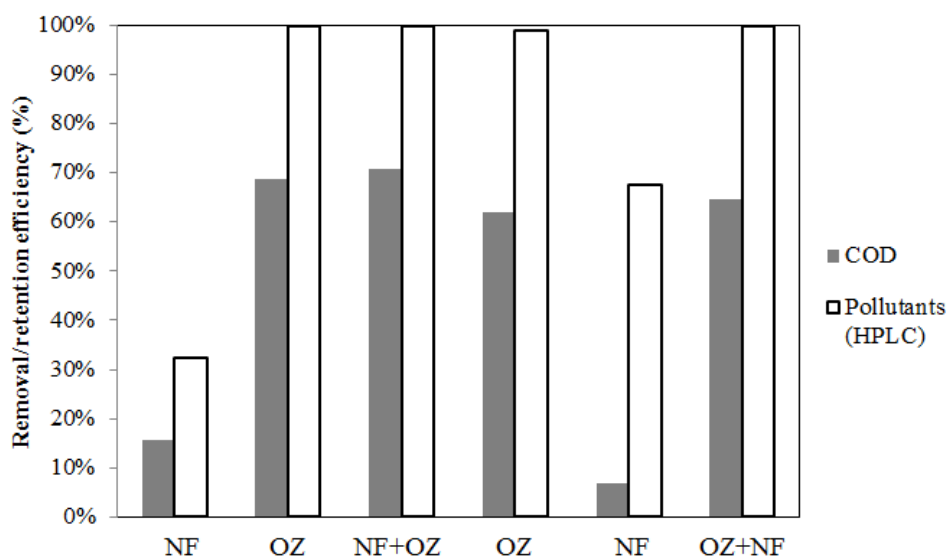

Figure 33 – Comparison between the two integration options regarding COD and reduction of pollutants' concentration (HPLC) and (b) COD removal/ retention.

The toxicity of the product of the two sequences was also studied. On the **Table 22** the results of EC_{20} of the two process final streams in comparison with the filtered water from the river and natural water effluent are presented.

Table 22 – Results of the Luminescent Bacteria to evaluate the toxicity of the natural water, the natural water effluent and the products of the two sequences of the Process Integration.

	EC_{20} (%)
Natural water (filtered water from river Mondego)	26.50
Natural water effluent (30 mg L^{-1} SMX and DCF)	0.34
NF + OZ	8.86
OZ + NF	29.21

The higher the EC_{20}, the more toxic substance it is necessary to add to make the bacteria loose response, so the less toxic the substance is.

From the **Table 22** (where the values for EC_{20} are presented, since the values for EC_{50} were not available for all the samples), it is possible to conclude that the less toxic effluent is the one that accrue from the sequence OZ + NF. As expected, both treatment sequences reduce the toxicity of the Natural water effluent (containing the pollutants). It is noteworthy that the sequence OZ-NF reduces the toxicity beyond the value for the filtered water from the river Mondego.

When comparing the two integration options it is evident that the reaction products concentrations obtained after each sequence should be surely different which will imply a dissimilar toxic character. Dantas *et al.* (2008) reports, for the first 30 min of Ozonation, the formation of intermediates with higher acute toxicity than SMX unreacted solution. For OZ+NF the potentially toxic intermediates formed on Ozonation are partially filtrated on

Nanofiltration, what will reduce their concentration on the final product of this sequence (thus, reducing the toxicity). On the other hand, on the sequence NF+OZ, the Ozonation starts with a smaller concentration of SMX (due to the preceding NF), but the same toxic intermediates can be formed and have toxic concentrations (since no filtration is done afterwards). Another possible explanation for this result is the fact that, with the sequence NF + OZ, the product has still dissolved ozone which is toxic for the bacteria.

From the integration point of view, OZ+NF can bring advantages in what concerns the reduction of the Nanofiltration membrane's fouling. On one hand, the early Ozonation reduces the dissolved solids on the solution, avoiding fouling on the following Nanofiltration. On the other hand, ozone is referred in other membrane processes as a cleansing agent (Kim *et al.*, 2007 and Lim and Bai, 2003).

It is important to point out that the fact that this test indicates low toxicity does not mean that the same sample is not potentially toxic for other organisms. Nevertheless, this is still a trustable and standard test that can be used to assess accurately if the effluent is appropriate for discharge.

Despite the fact that the COD removal is higher for the sequence NF+OZ, the toxicity is significantly higher for this sequence. Moreover, the COD values presented for the end of both processes are under the legal limit for discharge (125 mg O_2 L^{-1}). Therefore, the determinative factor should be the toxicity of the product of the treatment. All things considered, from the process integration, it is possible to conclude that the best sequence is Ozonation followed by Nanofiltration.

6. Conclusions and Future work

6.1 Conclusions

The main objective of this work, since Nanofiltration and Ozonation were already broadly used for the removal of these individual emerging contaminants, was to evaluate the performance of these methods for mixtures of the two components: SMX and DCF.

The Nanofiltration experiments permitted the analysis of the effects that are determinant on this specific membrane separation process. DCF has higher retention due to its higher molecular weight and hydrophobicity (membrane is more hydrophilic with increasing pH). Due to the membrane's negative zeta-potential the species which are negatively charged are rejected by electrostatic repulsion. The change of the aqueous matrix has a significant negative impact on process efficiency perhaps due to the presence of Ca^{2+} ions. Pressure drop of 7 bar and pH = 7 were identified as the best operating conditions for this process. With Nanofiltration it is possible to remove up to 85% of COD and between 90 and 100% of each contaminant. The pollutants were adsorbed on the membrane after 40 hours of operation. The interactions of the pollutants on the rejection mechanisms for the pH range 3 -6 should be further investigated.

The batch Ozonation performed trials confirmed the previously stated fact that the Ozone itself is enough for the SMX and DCF degradation. However, the presence of a catalyst can increase the COD degradation. The Ozonation's optimal conditions determined were the use of the catalyst Mn-Ce-O which is a specific area of 109 m^2 g^{-1} and an average diameter of pore of 0.0179 μm. Due to the reaction mechanism presented by this catalyst, the pH should not be buffered or adjusted. The aqueous matrix did not have influence on the process efficiency.

The process integration was done without the Ozonation catalyst since its separation from the reaction media was difficult. The Ozonation carried on process integration was performed for 120 min on simple mode and with the Natural water effluent. Regarding the Nanofiltration, it was done on pH = 7 and pressure drop of 7 bar. Regarding the toxicity evaluation, the best sequence for Nanofiltration and Ozonation Process integration is Ozonation followed by Nanofiltration.

6.2 Perspectives for forthcoming work

While conducting this research, new ideas emerged involving the three main steps of the investigation: Nanofiltration optimization, Ozonation optimization and Process Integration.

Regarding the rejection of the pollutants on the experiments performed in Nanofiltration, there was a crucial question that needed further investigation to be answered.

Considering the individual behaviour of SMX and DCF in solution, it was expectable that their rejection dropped with the decreasing pH due to the presence of neutral or positively charged species that have opposite charge as the membrane (even though the zeta potential of the membrane increases with pH). However, the observed retentions for SMX and DCF for pH under 6 increase, even though they were expected to decrease. This behaviour could be explained by the competitive behaviour of SMX and DCF on the Nanofiltration process, something that was never investigated before and consists on a good suggestion for future work. Some methodologies to remove of the pollutants adsorbed on the membrane should be investigated.

Regarding the Ozonation, considering the hypothesis that the presence of dissolved ozone can interfere on the bio-toxicity of the effluent, air could be used to purge ozone out of the solution. One interesting step that could be done is the injection of SMX and DCF possible intermediates under the same HPLC conditions in order to categorize unidentified peaks. The product of Ozonation of aqueous solutions containing only SMX and DCF could be analysed (HPLC under the same conditions) to determine which compound originates the intermediate detected on the unidentified HPLC peak. Moreover, the effect of tert-butanol radical scavenger could be tested in order to re-evaluate the Ozonation reaction paths. The way of administration of hydrogen peroxide should be optimized (taking into account the dissolved ozone) to keep the ozone/ hydrogen peroxide proportion favourable to the mineralization reaction occurrence. A Design of Experiments could be developed in order to access which combination of different conditions would be better to optimize the Ozonation process. Other analyses to investigate the catalyst stability should be performed.

On the Process Integration, the main problem was that it was not possible to use the optimal conditions for Ozonation due to the impossibility to remove the powdered catalyst Mn-Ce-O from the liquid (even after centrifugation and filtration), which would affect the Nanofiltration process. Even though at a large scale process this would not be a problem (since pellets of catalyst are normally used), it would be relevant to investigate new techniques to separate the catalyst from the liquid efficiently to explore experimentally the optimization path.

The effects of the pollutants' concentration and the effect of the pollutants' ratio could be accessed for both Nanofiltration and Ozonation in order access which variables are important for the process performance.

Considering the low resolution of the analytical method used for small concentrations of the pollutants, it would be remarkable to try to develop suitable robust methods to quantify very low concentrations of the pollutants in aqueous streams.

Moreover, the computer simulation has major importance to predict the process performance.

The investigation on the scope of the removal of emerging contaminants from water streams is crucial for the improvement of the environment quality around the world, as well as the reduction of the nefarious effects of milieu problems on the nature and society. These treatments are promising for the treatment of drinking water.

7. References

Aguinaco, A.; Beltrán, F. J.; García-Araya, Juan F.; Oropesa, A. (2012) – *Photocatalytic ozonation to remove the pharmaceutical diclofenac from water: Influence of variables*. Chemical Engineering Journal, 189– 190, 275– 282.

Akhtar, J.; Amin, N. S.; Aris, A. (2011) – *Combined adsorption and catalytic ozonation for removal of sulfamethoxazole using Fe_2O_3/CeO_2 loaded activated carbon*. Chemical Engineering Journal, 170, 136–144.

Bellona, C.; Drewes, J. E. (2005) – *The role of membrane surface charge and solute physico-chemical properties in the rejection of organic acids by NF membranes*. Journal of Membrane Science, 249(1-2), 227-234.

Beltrán, F. J.; Aguinaco, A.; Rey, A.; García-Araya, J. F. (2012) – *Kinetic Studies on Black Light Photocatalytic Ozonation of Diclofenac and Sulfamethoxazole in Water*. Industrial and Engineering Chemistry Research, 51, 4533−4544.

Beltrán, F. J. (2004) - *Ozone Reaction Kinetics for Water and Wastewater Systems*. Lewis Publishers, Boca Ratón, Florida.

Beltrán, F. J.; Pocostales, P.; Álvarez, P. M.; López-Piñeiro, F. (2009) – *Catalysts to improve the abatement of sulfamethoxazole and the resulting organic carbon in water during ozonation*. Applied Catalysis B: Environmental, 92, 262–270.

Beltrán, F. J; Aguinaco, A.; García-Araya, J. F. (2009) – *Mechanism and kinetics of sulfamethoxazole photocatalytic ozonation in water*. Water research, 43, 1359–1369.

Bolong, N.; Ismail, A. F.; Salim, M. R.; Matsuura, T. (2009) – *A review of the effects of emerging contaminants in wastewater and options for their removal*. Desalination, 239, 229–246.

Brunauer, S.; Emmett, P. H.; Teller, E. (1938) – *BET Theory*. Journal of the American Chemical Society, 60, 309.

Chang, E.-E.; Chang, Y.-C.; Liang, C.-H.; Huang, C.-P.; Chiang, P.-C. (2012) – *Identifying the rejection mechanism for nanofiltration membranes fouled by humic acid and calcium ions exemplified by acetaminophen, sulfamethoxazole, and triclosan*. Journal of Hazardous Materials, 221– 222, 19– 27.

Cheremisinoff, N. P. (2002) – *Handbook of Water and Wastewater Treatment Technologies (1st Edition)*. Butterworth Heinemann, Boston.

Cheryan, M. (1998) – *Ultrafiltration and Microfiltration Handbbok*. Technomic Publishing Company, Inc., Pennsylvania.

Coelho, A. D.; Sans, C.; Agüera, A.; Gómez, M. J.; Esplugas, S.; Dezotti, M. (2009) – *Effects of ozone pre-treatment on diclofenac: Intermediates, biodegradability and toxicity assessment*. Science of the Total Environment, 407, 3572–3578.

Connell, D.W (1991) – *Extrapolating test results on bioaccumulation between organism groups*. Bioaccumulation in aquatic systems – Contributions to the assessment, R. Nagel and R. Loskill, 133-149. Proceedings of an international workshop, Berlin, 1990. VCH Publishers, Weinheim.

Dantas, R. F.; Contreras, S.; Sans, S.; Esplugas, S. (2008) – *Sulfamethoxazole abatement by means of ozonation*. Journal of Hazardous Materials, 150, 790–794.

Daughton, C. G.; Ternes, T. A. (1999) – *Pharmaceuticals and personal care products in the environment: agents of subtle change?*. Env. Health Perspective 107(6), 907–938.

Frias, C. F.; Gramacho, S. A.; Pineiro, M. (2014) – *Cromatografia Gasosa-Espectrometria de Massas e Derivatização assistida por Micro-ondas na identificação de Isômeros de Glicose: uma prática para o ensino avançado em análise e caracterização de Compostos Orgânicos*. Química Nova, 37, 1, 176-180.

Geraldes, V.; Afonso, M. D. (2008) – *Concentration polarization in a reverse osmosis/nanofiltration plate-and-frame membrane module*. Journal of Membrane Science, 325, 580–591.

Gomes, S.; Cavaco, S. A.; Quina, M. J.; Gando-Ferreira, L. M. (2010) – *Nanofiltration process for separating Cr(III) from acid solutions: Experimental and modelling analysis*. Desalination 254, 80–89.

Gómez-Ramos, M. M.; Mezcua, M.; Agüera, A.; Fernández-Alba, A. R.; Gonzalo, S., Rodríguez, A.; Rosal, R. (2011) – *Chemical and toxicological evolution of the antibiotic sulfamethoxazole under ozone treatment in water solution*. Journal of Hazardous Materials, 192, 18-25.

Gracia-Lor, E.; Sancho, J. V; Serrano, R.; Hernández, F. (2012) – *Occurrence and removal of pharmaceuticals in wastewater treatment plant at the Spanish Mediterranean area of Valencia*. Chemosphere, 87, 453–462.

Heberer, T. (2002) – *Tracking persistent pharmaceutical residues from municipal sewage to drinking water*. Journal of Hydrology, 266, 175-189.

Heberer T., Fuhrmann B, Schmidt-Baumler K, Tsipi D, Koutsouba V, Hiskia A (2001) – *Occurrence of pharmaceutical residues in sewage, river, ground and drinking water in Greece and Berlin (Germany)*.

Joss A.; Zabczynski S.; Göbel A.; Hoffmann B.; Löffler D.; McArdell C. S. (2006) – *Biological degradation of pharmaceuticals in municipal wastewater treatment: proposing a classification scheme*. Water Res, 40, 1686–96.

Kestin, J; Sokolov, M; Wakeham, W. A. (1987) – *Viscosity of Liquid Water in the Range – 8ºC to 150ºC*. Journal of Physical Chemistry, 7, 3.

Kim, J.-O.; Jung, J.-T., Yeom, I.-T.; Aoh, G.-H. (2007) – *Effect of fouling reduction by ozone backwashing in a microfiltration system with advanced new membrane material*. Desalination, 202, 1–3, 361–368.

Lim, A. L.; Bai, B. (2003) – *Membrane fouling and cleaning in microfiltration of activated sludge wastewater*. Journal of Membrane Sicence, 216, 1–2, 279–290.

Madureira, T. M.; Barreiro, J. C.; Rocha, M. J.; Rocha, E.; Cass, Q. B.; Tiritan, M. E. (2010) – *Spatiotemporal distribution of pharmaceuticals in the Douro River estuary (Portugal)*. Science of the Total Environment, 408, 5513–5520.

Martins, R. C.; Quinta-Ferreira, R. M. (2009) – *Catalytic ozonation of phenolic acids over a Mn–Ce–O catalyst*. Applied Catalysis B: Environmental, 90, 268–277.

Martins, R. C.; Quinta-Ferreira R. M. (2011) – *Phenolic wastewaters depuration and biodegradability enhancement by ozone over active catalysts*. Desalination, 270, 1–3, 90–97.

Miller, G. L. (1959) – *Use of Dinitrosalicylic Acid Reagent for Determination of Reducing Sugar*. Analytical Chemistry, 31(3), 426-428.

Mulder, M. (1996) – *Basic Principles of Membrane Technology (2nd Edition)*. Dordrecht: Kluwer Academic Publishers.

Nikolaou, A.; Meric, S.; Fatta, D. (2007) – *Occurrence patterns of pharmaceuticals in water and wastewater environments*. Analytical and Bio-analytical Chemistry, 387, 1225–1234.

Nguyen, L. N.; Hai, F. I.; Kang, J.; Price, W. E.; Nghiem, L. D. (2013) – *Removal of emerging trace organic contaminants by MBR-based hybrid treatment processes*. International Biodeterioration & Biodegradation, 85, 474-482.

Nawrocki, J.; Kasprzyk-Hordern, B. (2010) – *The efficiency and mechanisms of catalytic ozonation*. Applied Catalysis B: Environmental, 99, 27–42.

Nghiem, L. D. (2005) – *Removal of emerging trace organic contaminants by nanofiltration and reverse osmosis*. University of Wollongong.

Nghiem, L. D.; Schäfer, A. I; Elimelech, M. (2005) – *Pharmaceutical Retention Mechanisms by Nanofiltration Membranes*. Environmental Science & Technology, 39 (19), 7698–7705.

Nghiem, L. D.; Hawkes, S. (2007) - *Effects of membrane fouling on the nanofiltration of pharmaceutically active compounds (PhACs): Mechanisms and role of membrane pore size*. Separation and Purification Technology, 57, 182–190.

Nogueira, R.F.P., Oliveira, M.C., Paterlini, W.C. (2005) – *Simple and fast spectrophotometric determination of H2O2 in photo-Fenton reactions using metavanadate*. Talanta, 66, 86-91.

Ormad, P.; Cortes, S. L.; Puig, A.; Ovelleiro, J. L. (1997) – *Degradation of organochlorine compounds by O_3 and O_3/H_2O_2*. Water Res., 31, 2387–2391.

Pocostales, P.; Álvares, P.; Beltrán, F. J. (2011) – *Catalytic ozonation promoted by alumina-based catalysts for the removal of some pharmaceutical compounds from water*. Chemical Engineering Journal, 168, 1289–1295.

Quintanilla, V. A. Y. (2010) – *Rejection of Emerging Organic Contaminants by Nanofiltration and Reverse Osmosis Membranes: Effects of Fouling, Modelling and Water Reuse*. CRC Press/ Balkena.

Radjenović, J.; Petrović, M.; F. Ventura, D. Barceló (2008) – *Rejection of pharmaceuticals in nanofiltration and reverse osmosis membrane drinking water treatment*. Water research, 42, 3601–3610.

Richardson, S. D.; Ternes, T. A. (2005) – *Water Analysis: Emerging Contaminants and Current Issues*. Analytical Chemistry, 77, 3807 – 3838.

Sari, S.; Özdemir, G.; Yangin-Gomec, C.; Zengin, G. E.; Topuz, E.; Aydin, E.; Pehlivanoglu-Mantas, E.; Tas, D. O. (2014) – *Seasonal variation of diclofenac concentration and its relation with wastewater characteristics at two municipal wastewater treatment plants in Turkey*. Journal of Hazardous Materials, http://dx.doi.org/10.1016/j.jhazmat.2014.03.15.

Sawyer, S. N.; McCarty, P. N.; Parkin, G. F. (2003) - *Chemistry for Environmental Engineering and Science* (5th ed.). New York: McGraw-Hill.

Seifirtová, M.; Pena, A.; Lino, C. M.; Solich, P. (2007) – *Occurrence of fluoroquinolones residues in hospital and municipal wastewaters from Coimbra*. IX International Symposium on Analytical Methodology in the Environmental Field, Poster 121, 270-272.

Simon, A.; Nghiem, L. D.; Le-Clech, P.; Khan, S. J.; Drewes, J. E. (2009) – *Effects of membrane degradation on the removal of pharmaceutically active compounds (PhACs) by NF/RO filtration processes*. Journal of Membrane Science 340, 16–25.

Schäfer, A. I.; Fane, A. G.; Waite, T. D. (2005) – *Nanofiltration - Principles and Applications*. Elsevier, Oxford.

Snyder, S.; Wert, E. C.; Lei, H. D.; Westerhoff, P.; Yoon, Y. (2007) – *Removal of EDCs and Pharmaceuticals in Drinking and Reuse Treatment Processes*. American Water Works Association Research Foundation (AWWARF) and IWA Publishing.

Srinivasan, P.; Sarmah, A. K.; A, Manley-Harris, M.; Wilkins, A. L. (2010) – *Sorption of sulfamethoxazole, sulfachloropyridazine and sulfamethazine onto six New Zealand dairy farm soils.* World Congress of Soil Science, Soil Solutions for a Changing World.

Sutzkover, I. (2000) – *Simple technique for measuring the concentration polarization level in a reverse osmosis system.* Desalination, 131, 117-127.

Tran N. H.; Urase T.; Kusakabe O. (2009) – *The characteristics of enriched nitrifier culture in the deg-radation of selected pharmaceutically active compounds*. Journal of Hazard Mater, 171, 1051–1057.

Vogna, D.; Marotta, R.; Napolitano, A.; Andreozzi, R.; d'Ischia, M. (2004) – *Advanced oxidation of the pharmaceutical drug diclofenac with UV/H_2O_2 and ozone*. Water Research, 38, 414–422.

Vergili, I. (2013) – *Application of nanofiltration for the removal of carbamazepine, diclofenac and ibuprofen from drinking water sources*. Journal of Environmental Management, 127, 177-187.

Verliefde, A. R. D.; Cornelissen, E. R.; Heijman, S. G. J.; Verberk, J. Q. J. C.; Amy, G. L.; Van der Bruggen, B.; Van Dijk, J. C. (2008) – *The role of electrostatic interactions on the rejection of organic solutes in aqueous solutions with nanofiltration*. Journal of Membrane Science, 322, 52–66.

Webgraphy

Active Pharmaceutical Ingredients Database. Available on http://api-data.com/ on 11 October 2013.

Entidade Reguladora dos Serviços de Águas e Resíduos. Avaliable on http://www.ersar.pt/ on 8 September 2011.

Sterlitech Corporation, Flat Sheet Membranes Specifications. Available on www.sterlitech.com/flat-sheet-membranes-specifications.html in August 2013.

Appendices

Appendix I – Experiments to evaluate membrane fouling.

Table I.1 – Experiments performed on the Nanofiltration equipment with the aim of the analysis of the membrane fouling.

Conditions	Studied variables	Code
Distilled water ΔP= 5, 10, 18 bar After N2B	J_v (m^3 m^{-2} s^{-1}) vs ΔP	N4A1
Distilled water ΔP= 5, 10, 18 bar After N3	J_v (m^3 m^{-2} s^{-1}) vs ΔP	N4A2
Distilled water ΔP= 5, 10, 18 bar After N5A	J_v (m^3 m^{-2} s^{-1}) vs ΔP	N4B1
Distilled water ΔP= 5, 10, 18 bar After N5B	J_v (m^3 m^{-2} s^{-1}) vs ΔP	N4B2
Distilled water ΔP= 10 bar New membrane	J_v (m^3 m^{-2} s^{-1}) vs t	N4C1
Distilled water ΔP= 10 bar New membrane after N4D1	J_v (m^3 m^{-2} s^{-1}) vs t	N4C2
SMX 30 mg L^{-1} + DCF 30 mg L^{-1} ΔP= 5, 10, 18 bar New membrane after N4C1	J_v (m^3 m^{-2} s^{-1}) vs t	N4D1

Appendix II – Variables measured in Ozonation.

Table II.1 – Variables measured for each Ozonation experiment done before process integration.

Code	$C_{O3,in}$ (g m^{-3})	$C_{O3,out}$ among time (g m^{-3})	pH among time	Initial pH	COD among time	HPLC among time	[H$_2$O$_2$] among time (g L^{-1})
O1	•	•		•	•	•	
O2	•	•		•	•	•	
O3	•	•		•	•	•	
O4	•	•	•	•	•	•	
O5	•	•	•	•	•	•	
O6	•	•	•	•	.•	•	
O7	•	•		•	•	•	•
O8	•	•		•	•	•	•

Appendix III – Further information on analytical techniques for liquid samples

COD – Calibration curve

A calibration curve was prepared by the determination of the absorbance corresponding to samples with known COD that were under this procedure (**Figure III.1**). The mean absorbance value for the blanc was subtracted to the mean absorbance values for each two

vials and that result was considered in the calibration curve to obtain the COD value in milligrams of oxygen per litter of solution (mg O_2 L^{-1}).
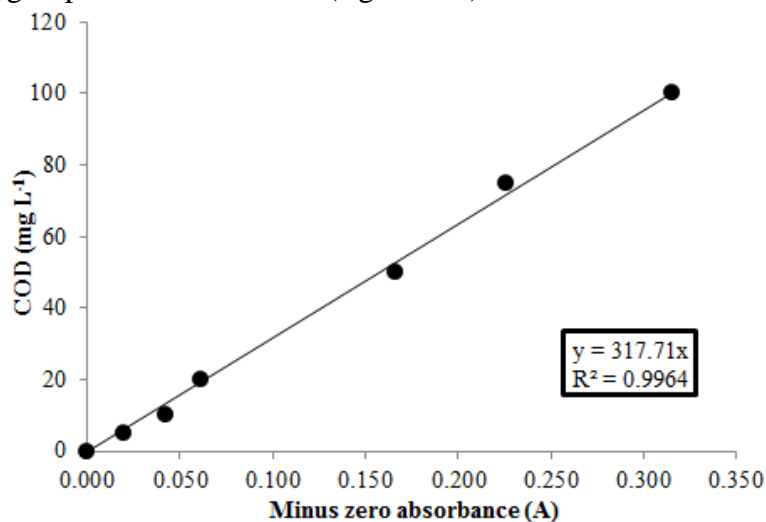

Figure III.1 – COD calibration curve.

HPLC – Eluent optimization

One example of a liquid eluent that is commonly used in HPLC analysis is a mixture of ethanol and water 50:50. This mobile phase was tested for different detection wavelengths, different retention times and different temperatures of the column, but the compounds on the scope of this study (mainly SMX and DCF) could not be detected.

The literature study unveiled that a mobile phase of acetonitrile and water at a 40:60 volume ratio, acidified at pH 3 by the addition of phosphoric acid would be efficient detecting SMX. Using this eluent, the UV detector was settled for a 270 nm wavelength (Dantas *et al.*, 2008). This solution was tested for different retention times and temperatures of the column. After optimization, it was decided that the retention time used would be 30 minutes and the temperature set-point would be 50ºC. These conditions allowed one to have two peaks that later were matched to SMX and to DCF (by analysing solutions containing these compounds separately).

HPLC – Calibration curve

The **Figure III.2** shows the calibration curve obtained by HPLC analysis of solutions with known concentrations of SMX and DCF. The regressions relate the area of the peak (found with the automatic peak detection of Borwin software) with the concentration of the compound of interest (SMX or DCF).
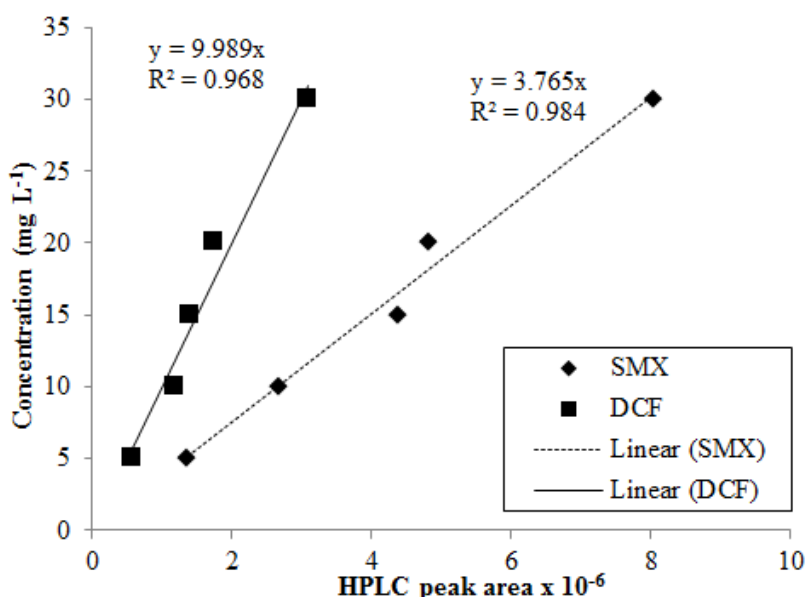
Figure III.2 – HPLC calibration curve for SMX and DCF.

Even though the correlation coefficients (R^2) for these regressions are not very satisfactory (they should be closer to one), these results are comprehensible due to the high sensibility of the HPLC equipment.

On the **Figure III.3** is shown the result of a HPLC analysis of the solution prepared with distilled water, 30 mg L^{-1} of SMX and 30 mg L^{-1} of DCF.
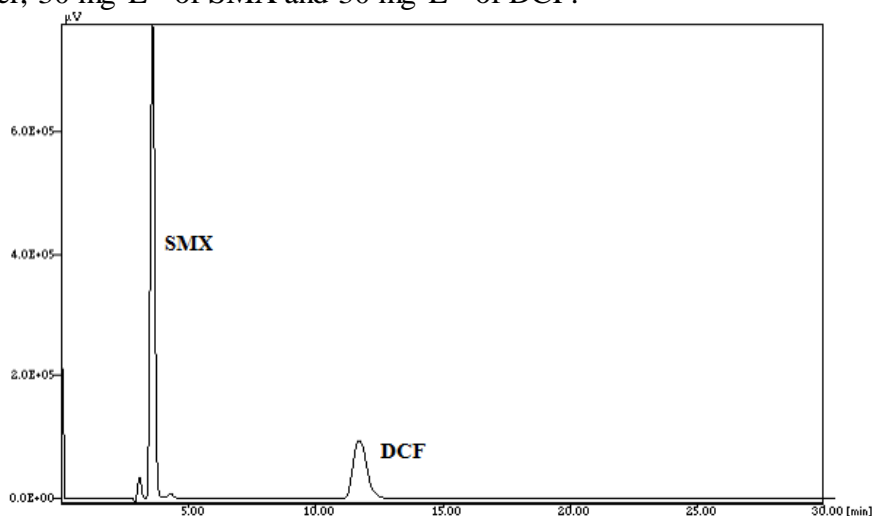

Figure III.3 – Graphic of the HPLC signal (at 270 nm using water and acetonitrile (60:40) as eluent and with a column temperature of 50ºC) for a solution prepared with distilled water, 30 mg L^{-1} of SMX and 30 mg L^{-1} of DCF.

On this signal graphic that was obtained after the optimization of the conditions of the HPLC analysis, it is possible to detect the presence of both contaminants: SMX is the bigger an narrower peak on the left with a retention time of approximately 3.5 min and DCF is the smaller and flatter peak on the right with a retention time of approximately 11.5 min. Ideally, the DCF peak should be narrower, but, despite all the optimization efforts, it was not possible to make the two peaks simultaneously ideal.

Spectroscopy UV-Vis – Analysis performed as an attempt to detect xylose

The direct analysis of the sample both on UV and visible spectrum was not effective. DNS and DNS modified methodsuse the dinitrosalicylic acid as a chemical reductor of the sugar. This sugar reduction origins 3-amino-5-nitrosalicylic acid which results in a change in the amount of light absorbed at a wavelength of 540 nm. The absorbance is directly proportional to the amount of reducing sugar (Miller, 1959).